



UNIVERSITY OF TRENTO

Doctoral School in Structural Engineering
Modelling, Preservation and Control
of Materials and Structures

Christian Baldessari

In-plane behaviour of differently refurbished timber floors

April 2010

Ph.D student: Eng. Christian Baldessari

**COMPORTAMENTO NEL PIANO
DI SOLAI LIGNEI
DIVERSAMENTE RINFORZATI**

**IN-PLANE BEHAVIOUR OF DIFFERENTLY
REFURBISHED TIMBER FLOORS**

Tutor: Prof. Eng. Maurizio Piazza

2010

UNIVERSITY OF TRENTO

**Doctoral School in Structural Engineering: Modelling, Preservation
and Control of Materials and Structures**

22° Cycle

Final exam: 19.04.2010

Examination Commission:

prof. Enzo Siviero, University IUAV of Venice

prof. Mario Como, University of Rome Tor Vergata

prof. Gianmarco De Felice, University of Rome 3

prof. Roberto Crocetti, SP Technical Research Institute of Sweden

A mia moglie Elena

ACKNOWLEDGEMENTS

Al termine di questi tre anni molte sono le persone che voglio ringraziare per avermi permesso di realizzare questo ulteriore importante passo della mia vita.

Per primi sicuramente i miei genitori e la mia sorellina che hanno creduto nelle mie capacità e mi hanno sostenuto nei momenti in cui la tentazione di abbandonare l'impresa era tanta.

Mia moglie Elena che con la sua perseveranza è riuscita nel difficile compito di farmi terminare in tempo la tesi.

Il prof. Maurizio Piazza che mi ha accompagnato in questo percorso di formazione dandomi preziosi consigli nell'interpretazione dei risultati sperimentali e nelle scelte relative alla modellazione numerica.

I tecnici di laboratorio Marco, Luca, Tiziano, Ivan e Alfredo con i quali ho potuto realizzare le prove sperimentali.

I compagni d'avventura Andrea, Ermanno, Mauro e Cristiano che hanno condiviso con me l'esperienza del Dottorato.

Gli studenti che ho incontrato e con i quali ho avuto la fortuna di collaborare.

Infine Colui che mi ha accompagnato in questo cammino e che mi ha dato la forza di raggiungere questo importante traguardo della mia vita.

A tutti voi un sentito Grazie.

Christian Baldessari

Trento, aprile 2010

SUMMARY

1. THE ROLE OF FLOORS IN SEISMIC BEHAVIOUR OF BUILDINGS.....	13
1.1 <i>Introduction</i>	13
1.2 The role of the floor in the transfer of seismic action.....	16
2. EXPERIMENTATION, MODELLING AND ANALYSIS	19
2.1 The types of floor analysed.....	19
2.1.1 Dimensions of test specimens	21
2.1.2 Floor with simple timber boards.....	22
2.1.3 Floor reinforced with timber boards	23
2.1.4 Floor reinforced with steel plates	24
2.1.5 Floor reinforced with FRP strips	25
2.1.6 Floor reinforced with three plywood layers	27
2.1.7 Floor reinforced with concrete slab.....	28
2.2 Experimental tests	29
2.2.1 Test set-up for specimens 5x4 m.....	31
2.2.2 Instrumentation for specimens 5x4 m.....	38
2.2.3 Test set-up for specimens 2x1 m.....	40
2.2.4 Instrumentation for specimens 2x1 m.....	42
2.2.5 Test protocol	43
2.2.6 Stiffness calculation	46
2.3 Modelling and numerical analysis	50
2.3.1 Introduction	50
2.3.2 General features of the FEM model.....	51
2.3.3 The numerical model features	53
2.4 Floor strength verifications.....	54
3. FLOOR WITH SIMPLE TIMBER BOARDS.....	59
3.1 Introduction	59
3.2 Specimen construction features	60

3.2.1	Floor dimension 2x1 m	60
3.2.2	Floor dimension 5x4 m	62
3.2.3	Summary of construction features and materials	63
3.3	Floor stiffness.....	64
3.4	Numerical model features	67
3.5	Strength verifications	69
3.5.1	Shear verification	69
3.5.2	Tension verification.....	70
3.5.3	Compression verification	73
3.5.4	Shear and tension verification of floor-wall connections.....	73
4.	FLOOR REINFORCED WITH TIMBER BOARDS	75
4.1	Introduction	75
4.2	Specimen construction features	76
4.2.1	Floor dimensions 2x1 m.....	76
4.2.2	Floor dimensions 5x4 m.....	77
4.2.3	Summary of construction features and materials	78
4.3	Floor stiffness.....	80
4.4	Numerical model features	83
4.5	Strength verification	85
4.5.1	Shear verification	85
4.5.2	Tension verification.....	85
4.5.3	Compression verification	87
4.5.4	Shear and tension verification of floor-wall connections.....	87
5.	FLOOR REINFORCED WITH STEEL PLATES.....	89
5.1	Introduction	89
5.2	Specimen construction features	90
5.2.1	Floor dimension 2x1 m	90
5.2.2	Floor dimension 5x4 m	91
5.2.3	Summary of construction features and materials	93
5.3	Floor stiffness.....	94
5.4	Numerical model features.....	97
5.5	Strength verification	99

5.5.1	Shear verification	99
5.5.2	Tension verification	100
5.5.3	Compression verification	102
5.5.4	Shear and tension verification of floor-wall connections...	102
6.	FLOOR REINFORCED WITH FRP STRIPS.....	103
6.1	Introduction	103
6.2	Specimen construction features	104
6.2.1	Floor dimension 2x1 m	104
6.2.2	Floor dimension 5x4 m	106
6.2.3	Summary of construction features and materials	107
6.3	Floor stiffness.....	108
6.4	Numerical model features.....	111
6.5	Strength verification	112
7.	FLOOR REINFORCED WITH PLYWOOD PANELS	113
7.1	Introduction	113
7.2	Specimen construction features	114
7.2.1	Floor dimension 2x1 m	114
7.2.2	Floor dimension 5x4 m	115
7.2.3	Summary of construction features and materials	116
7.3	Floor stiffness.....	118
7.4	Numerical model features.....	121
7.5	Strength verification	123
7.5.1	Shear, tension and compression verification.....	123
7.5.2	Shear and tension verification of floor-wall connections...	124
8.	FLOOR REINFORCED WITH CONCRETE SLAB	125
8.1	Introduction	125
8.2	Specimen construction features	126
8.2.1	Floor dimension 2x1 m	126
8.2.2	Floor dimension 5x4 m	127
8.2.3	Summary of construction features and materials	129
8.3	Floor stiffness.....	130
8.4	Numerical model features.....	133

8.5	Strength verification	135
8.5.1	Shear verification	135
8.5.2	Tension verification	137
8.5.3	Compression verification	138
8.5.4	Shear and tension verification of floor-wall connections...	139
9.	THE NUMERICAL EXAMPLE	141
9.1	Introduction	141
9.2	The geometry	142
9.3	The model	143
9.4	Analysis.....	145
9.5	Results	148
9.5.1	Floor with simple timber boards.....	149
9.5.2	Floor reinforced with timber boards	156
9.5.3	Floor reinforced with steel plates	163
9.5.4	Floor reinforced with FRP strips	170
9.5.5	Floor reinforced with plywood panels	177
9.5.6	Floor reinforced with concrete slab.....	184
10.	REINFORCEMENT COMPARISON.....	191
10.1	Introduction	191
10.2	Experimental tests and modelling.....	191
10.2.1	The load-displacement curves.....	191
10.2.2	Stiffness	199
10.2.3	Stresses	202
10.3	Numerical example	204
10.3.1	Tie-beam contribution	204
10.3.2	Comparison between different reinforcement – walls...208	
10.3.3	Comparison between different reinforcement – floors..213	
11.	CONCLUSIONS AND FUTURE DEVELOPMENTS	217
11.1	Conclusions	217
11.2	Future developments	221
	BIBLIOGRAPHY	223

SUMMARY

This work analyses the behaviour of in-plane timber floors which are differently refurbished. The task is to ascertain the stiffness of the different solutions and to study the influence on the global behaviour of the building. The first type analysed is a floor with simple boards to which different reinforcing techniques have been applied. These are double boards, steel plates, diagonally set FRP strips, glued plywood panels and concrete slabs. For each of these types of reinforcement experimental displacement control tests were carried out. They were monotonic and cyclic tests of specimens with dimensions 2x1 m and 5x4 m, with and without perimeter tie-beams. The same tests were numerically reproduced and a numeric model of simple implementation was created able to simulate non-linear behaviour of floor and tie-beam. On the end, the floor model was used in order to analyse a traditional building.

Experimental analysis and numeric modelling confirmed the need to guarantee efficient floor-masonry connections and showed the notable contribution offered by perimeter tie-beam in terms of in-plane floor stiffness. The comparison between different techniques of reinforcement showed the inadequacy of simple boards to stand up to seismic action.

SOMMARIO

Il presente lavoro analizza il comportamento nel piano di solai lignei diversamente rinforzati con l'obiettivo di determinare la rigidezza delle diverse soluzioni e di studiarne l'influenza nel comportamento globale dell'edificio. La tipologia di partenza è il solaio monordito con semplice tavolato al quale sono state applicate differenti tecniche di rinforzo: secondo tavolato, bandelle metalliche o fasce di FRP a posa diagonale, pannelli di compensato incollati, getto di una soletta di calcestruzzo. Per ciascuna di queste tipologie di rinforzo sono state effettuate prove sperimentali, in controllo di spostamento, di tipo monotono e ciclico, su campioni di dimensione 2x1 m e 5x4 m, in presenza e in assenza di cordolo-tirante perimetrale. Le stesse prove sono state quindi riprodotte numericamente ed è stato elaborato un modello numerico di semplice implementazione in grado di simulare il comportamento non lineare del solaio e del cordolo-tirante. Infine il modello del solaio è stato utilizzato nell'analisi di un edificio tipo.

Le analisi sperimentali e la modellazione numerica hanno confermato la necessità di garantire efficaci connessioni solaio-muratura e hanno mostrato il notevole contributo offerto dal cordolo-tirante perimetrale in termini di rigidezza nel piano del solaio. La comparazione tra le diverse tecniche di rinforzo ha mostrato inoltre l'inadeguatezza del semplice tavolato a resistere alle azioni sismiche.

1. THE ROLE OF FLOORS IN SEISMIC BEHAVIOUR OF BUILDINGS

1.1 *Introduction*

Construction solutions which characterise masonry built historic buildings almost always aim to ensure resistance to vertical loads with a device counteracting possible horizontal push brought on by vaults or arches.

If you exclude some special cases, it can be said that masonry structures are rarely planned to stand up to different actions from the vertical. Due to this, such constructions are intrinsically vulnerable to horizontal action brought on by seismic activity.

This is due in small part to strength properties of masonry substance. Construction flaws do not allow for counteraction as regards seismic activity and above all there is almost total absence of connecting elements between masonry walls and then between these and ceilings.

Moreover, the excessive deforming quality of floors and covers reduces the chance of splitting up the horizontal action on the perimeter walls almost to nil so robbing the building of a valid strength system.

During seismic actions these shortcomings determine the formation of non counteracted kinematic chains destined to create collapse due to loss of equilibrium.

The macro-elements that make up the kinematic chain are parts of a unitary structure and can have various forms. They are pinpointed starting out from characteristic elements of building vulnerability, such as the lack of floor-masonry connections, differing masonry texture, the presence of cracking scenarios and damage produced by past earthquakes.

La Fig. 1 represents the main mechanisms linked to collapse in which in-plane floor deformability and floor-masonry link are determining factors for its development.

Proceeding in clockwise direction, the first mechanism and the fourth are the overturning of the whole wall due to the lack of link between floors and orthogonal walls in seismic action.

The second mechanism is vertical wall instability and is manifested through the formation of three cylindrical horizontal rifts, because of the push of the intermediate floor not anchored to the wall.

The third is rupture and flexure of the wall with the formation of a vertical rift in the central zone due to the presence of pushing elements or to excessive deformability of the floor.

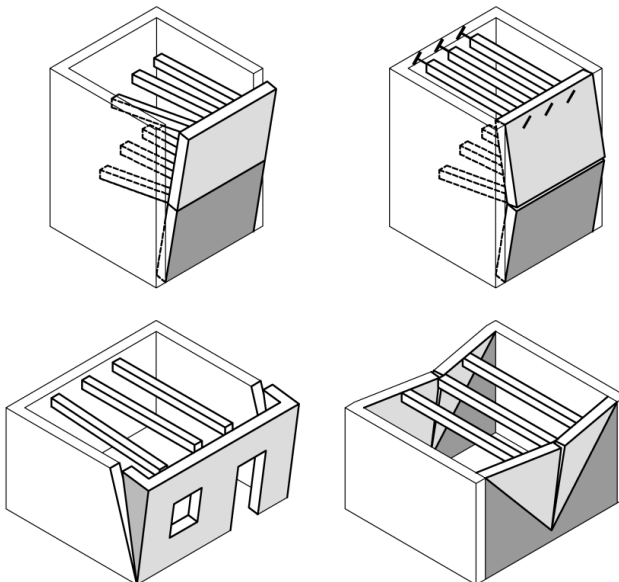


Fig. 1 Collapse mechanisms

Therefore, it is necessary to ensure an efficient link between walls and floors which must, moreover, guarantee sufficient in-plane stiffness so as to avoid excessive deformations which would, in any case, mean overturning the perimeter walls due to lack of equilibrium.

During the last 30 years, different intervention techniques have been employed. Above all the concrete slab on the existing flooring with prior insertion of opportune connectors so as to complete a section made up of wood-concrete, able to increase both in-plane stiffness as well as load carrying capacity of the floor (Piazza e Turrini, 1983 – Ronca et al., 1991 – Giuriani, 2002 – Giuriani, 2006 – Piazza e Ballerini, 2006). Following on from such technique, solutions have been developed to efficiently link the concrete slab to the perimeter walls with distributed pin components (Felicetti et al., 1997 – Gattesco e Del Piccolo, 1997). The negative points in this technique are increase in weight introduced with the concrete slab which augments seismic actions on the bracing walls and then the small chance of reversibility.

So, techniques have been developed using two or more components which include laying timber panels, plates or steel sheets over the existing boards solidified with pressure fixture metal pins in calibrated holes to load carrying floor beams (Giuriani et al., 2002 – Giuriani, 2004 – Modena et al., 2004 – Gattesco e Macorini, 2006 – Gattesco et al., 2007 – Brignola et al., 2008). These techniques, alternatively to the concrete slab, increase the in-plane floor stiffness and at the same time they increment carrying capacity including wood-wood or wood-steel composed sections.

1.2 The role of the floor in the transfer of seismic action

The role of the floors, and especially their stiffness and their perimeter wall link, is of primary importance in allowing the building to resist seismic action.

With vertical loads only, even the simple support of the floors on masonry is sufficient to guarantee equilibrium. Seismic action, instead, induces horizontal inertia forces on masonry which are transmitted to floors. These have to be able to transfer such forces to bracing walls.

There is, therefore, the repeatedly underlined need to guarantee link between floors and masonry so ensuring efficient passage to transfer inertia forces.

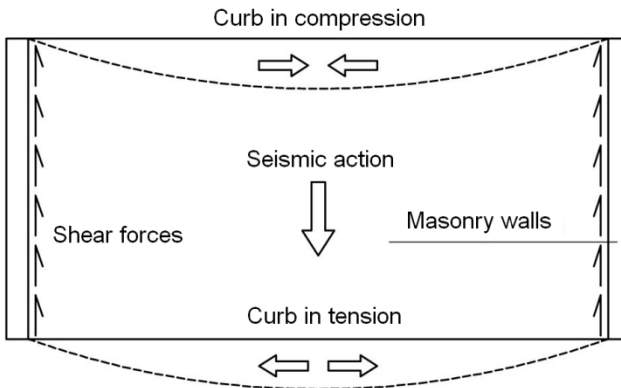


Fig. 2 Floor stress with horizontal seismic action

Fig. 2 represents the floor scheme with vertical bearing frame subject to lateral seismic force direct, in this case, from high to low. The seismic action induces a compression state in the high part of the floor and traction in the low part. Shear seismic action is also present at the floor sides representing the forces which the floor transmits to the resisting walls.

The behaviour just described is typical of so-called stiff floors but is also representative of floors which present a certain deformability due to in-plane behaviour.

To guarantee distribution of forces as in Fig. 2 it is necessary to place connecting elements between floor and shear walls, which are able to transmit shear actions deriving from the seismic action.

What is more, to avoid overturning orthogonal walls during seismic action a tension floor-walls link is needed.

Proceeding with analysis of Fig. 2, the compressing action is easily counteracted by the boards or by the layout which makes up the deck.

Instead, to resist the tension action, there must be a purpose made resisting component, previously excluding the possibility of completing a concrete breach curb in the masonry.

This type of operation means doing continuous shear in the walls which further weaken the existing masonry texture. The great difference of stiffness between masonry and concrete curb induces, in the presence of earthquake, the detachment of the curb from the punching wall.

The adopted solution, valid both for floors and roof, is the tie-beam in metal profile – steel plate or L shape- proposed by Doglioni (Doglioni F., 2000, 164). It consists of laying a metal profile along the floor perimeter – steel plate or L shape – linked to the floor plotting by softening screws, threaded bars or “c” welding steel plates. The profile heads are anchored in the exterior wall corners or in the floor-wall node, with threaded bars 20 to 30 mm diameter allowing for a tightening limit if a bolt fixing end is used.

Fig. 3 is an example of the tie-beam application in the wall-floor node. The advantages of this solution are many. These metal profiles have the function of traditional free ties at floor level and impede out of plane mechanisms regarding the opposing facings or corners.

To this, however, we add the advantage of greater connection numbers to floor and masonry guaranteeing more widespread division of seismic action and so avoiding concentrating only on opposing heads.

Moreover, the presence of many anchor points along the way also allows for the use in the case of non rectilinear walls where opposition of a free tie would be problematic.

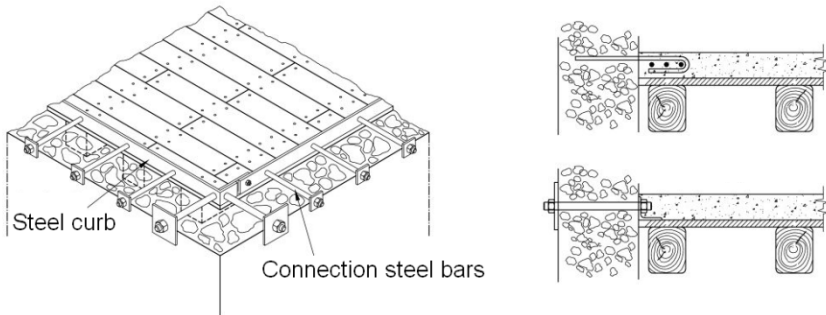


Fig. 3 Application of tie-beam

Anchoring almost continuously along floor to masonry is completed with threaded bars of small diameter linked to the profile by welding or bolts which go through the thickness of the walls and are blocked on to the external face by key drop fixing end with bolts or cemented internally in the masonry itself.

These elements impede unthreading of beams and separation of external perimeter masonry, counteracting out of plane wall turnover.

2. EXPERIMENTATION, MODELLING AND ANALYSIS

2.1 The types of floor analysed

Types of floor chosen are interlinked as regards technical viewpoints in widespread use nowadays for seismic improvement, both for the environment of ordinary civil building housing construction as well as for buildings of historic-artistic worth.

The work carried out has the purpose of studying and comparing some possible stiffening operations for in-plane timber floors and then determining the contribution offered regarding seismic improvement for existing buildings.

Initially, work carried out has, on the one hand, been involved with test set-up planning, while on the other hand it has analysed the peculiarities of each type of intervention, planning and defining the effective workings for completion of test specimens.

Analysis types cover the possibilities of intervening on existing floors in quite an exhaustive way. The departure solution is the simple timber floor reinforced with a second layer at 45° compared to the first, then with metal plates or diagonally laid FRP strips and then there is glued plywood panels, followed by reinforced concrete slabs.

The last solutions, in particular, allow both for increased in-plane stiffness as well as floor load bearing ability creating a mixed wood-wood structure in the case of plywood and wood-concrete in the last case.

Carrying out these operations is meant to be wholly in accordance with criteria of architectural restoration.

The objective, dictated mainly by good sense, is to answer strongly felt needs, above all, in works of great artistic-historic relevance, but also for modest buildings tied to the traditions of a people. We must alter structures minimally and so tend to be intervening minimally, looking for compatibility, with the chance to reverse, respecting authenticity, preserving materials, controlling the visual impact. The types analysed, delineated in the following way, are represented in Fig. 4.

- Floor with simple timber boards (Fig. 4a)
- Floor reinforced with timber boards (Fig. 4b)
- Floor reinforced with steel plates (Fig. 4c)
- Floor reinforced with FRP strips (Fig. 4c)
- Floor reinforced with plywood panels (Fig. 4d)
- Floor reinforced with concrete slab (Fig. 4e)

Tests have been carried out on all types of floor with and without tie-beams with the aim of evaluating their efficiency. In the following paragraphs the types of interventions proposed will be described as well as specimen features which have been worked on.

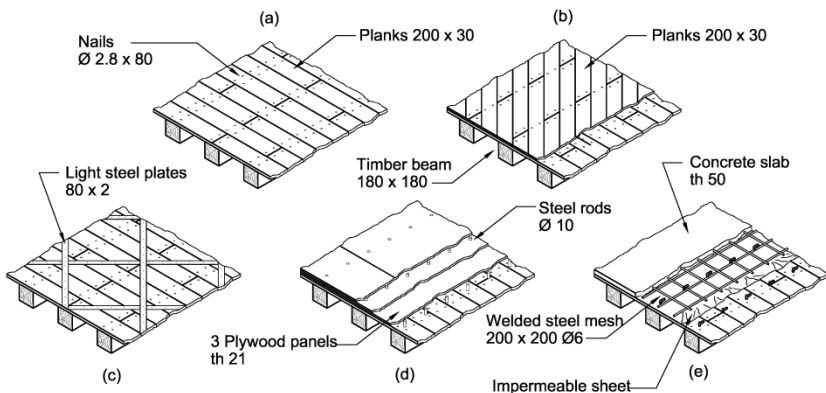


Fig. 4 Type of floor

2.1.1 Dimensions of test specimens

As regards specimen dimensions it was decided to carry out the experimental campaign using two configurations, with plan dimensions of 2x1 m and 5x4 m. In all the subject test specimens the direction of bearing frame is parallel to the floor short side with span of 50 cm.

Tests carried out on the 2x1 m floor were conducted with the aim of determining the initial floor stiffness. Such stiffness values have, in fact, allowed for calibrated load parameters for cyclic tests carried out on 5x4 m dimension floors.

The dimensions were chosen because they represent real floor dimensions in common housing. The second reason is related to the length-width relationship, choosing between 1 and 2, within the limits of possibility offered by the test laboratory, with the aim of amplifying effects of seismic activity and so having the chance to more easily study the contribution offered by the perimeter tie-beam stiffness.

With regards to the test campaign foreseen on floor dimension 2x1 m, the reasons for choosing this sort of configuration are due to the need for having a set of specimens available representative of the six kinds of analysed floor, with the scope of determining initial floor stiffness.

The chosen configuration is, moreover, the consequence of some experimental requirements such as the need for symmetric specimens and the chance to punctually apply the load.

2.1.2 Floor with simple timber boards

The first type of floor analysed is simply timber boards made up of 20 cm width boards and 3 cm thickness nailed orthogonally to bearing beams which are laid on span of 50 cm.

This type is found most often in historic buildings and represents the starting point for seismic improvement operations. In particular it highlights notable in-plane deformation possibilities due mainly to limited strength offered by board-beams connections. There are many intervention techniques which can be adopted but it is especially indispensable to guarantee efficient link-up between floor and masonry so avoiding out of plane turnover of perimeter walls. Experimental tests have analysed such solutions with perimeter tie-beam. This operation allows, in fact, for increase in-plane stiffness but is not, however, sufficient to guarantee structural safety for this particular type of floor.



Fig. 5 Floor with timber boards

2.1.3 Floor reinforced with timber boards

Here we are dealing with the first kind of proposal which allows for increase in floor stiffness. This solution consists of laying a second timber level, placed at an angle of 45° to the first.

The second layer may be completed using common planks or with ones of greater width. The link between the two layers may be completed in different ways. In the first place it can be done by nailing the two together. Alternatively the stiffened link can be further augmented using connectors made up of threaded bars subsequently injected with epoxy adhesive. In this case, before connector insertion, the big boards may be placed on the floor and temporarily fixed with screws. The chosen solution includes the use of self threading screws to solidify the second board to the first.



Fig. 6 Floor reinforced with timber boards

2.1.4 Floor reinforced with steel plates

This kind of operation means laying holed strips in steel on a simple timber board placed at an oblique angle to the floor at 45° compared to the floor bearing frame. This requires components available on the market made of rolls which are lain on the floor and linked to the board with nails or screws.

The advantages of using this material are many and various. Further load is not added to structure. The operation can be measured and so can span steel plates according to seismic action, being easily completed as well as reversible. Moreover, the reinforcement is not aesthetically invasive and brings good increase in structure ductility.

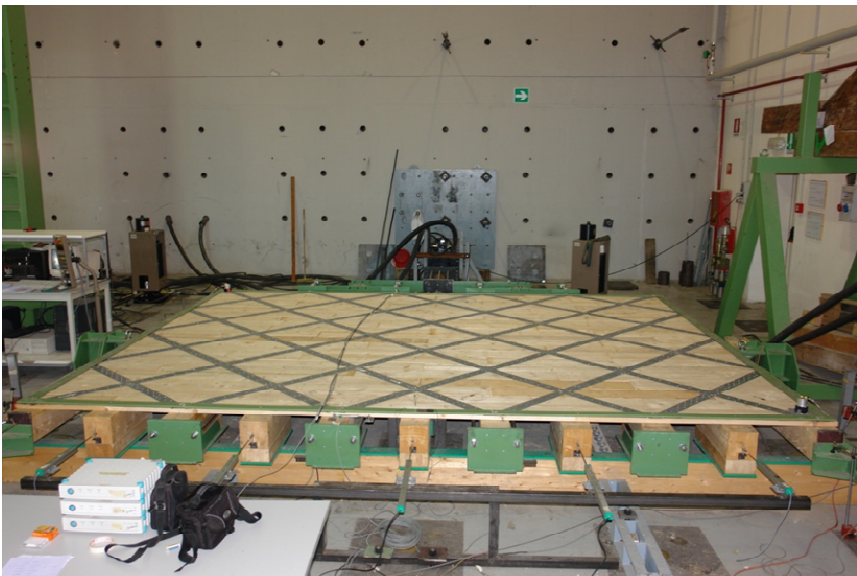


Fig. 7 Floor reinforced with steel plates

2.1.5 Floor reinforced with FRP strips

Fibre Reinforced Polymer materials, known by the English acronym FRP, are materials made up of high strength long fibres immersed in a polymer matrix. The fibres are the resistant part of the material, having a greater axial strength while the polymer matrix has the job of protecting the fibre from wear, ensuring alignment and guaranteeing uniform spread of forces on the fibres.

The application of this building technology, such as FRP, begun at the end of the 1980s and following a vast study phase and experimentation in different countries, has been amply affirmed as technique for structural refurbishment for concrete and masonry works. In the case of timber floors they can be used in the same ways as strips in steel, laying the FRP strips orthogonally one to another with an angle of 45° compared to the floor bearing frame.

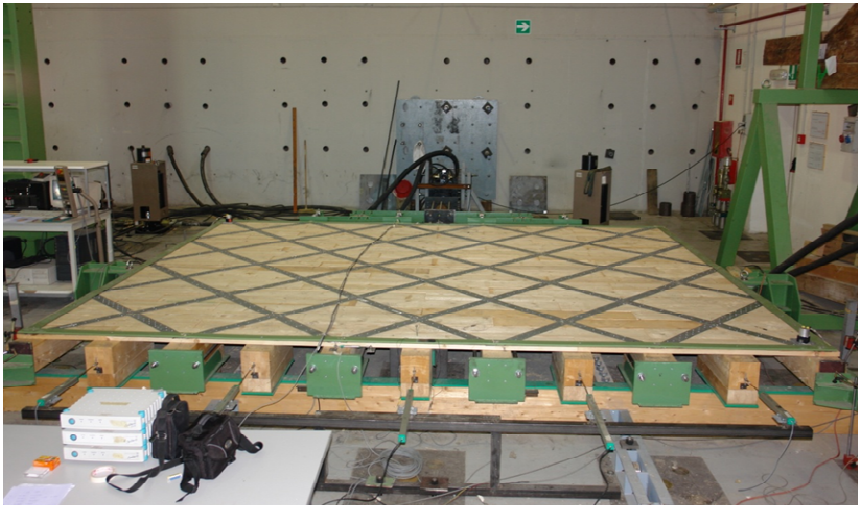


Fig. 8 Floor reinforced with FRP strips

The connection to the lower strata is achieved by laying a layer of epoxy resin on to a well prepared sub strata so guaranteeing fixing.

The advantages of using this material are analogous to those shown in the preceding paragraph related to utilising steel plates.

The main disadvantages of this technique involve intrinsic material cost which allow only for use in special circumstances where alternative operation techniques cannot be possible.

Such technique requires, moreover, specialised labour for the right kind of material laying. Then there is the operation efficiency strongly influenced by the type of reinforcement installation.

2.1.6 Floor reinforced with three plywood layers

This kind of operation includes laying three staggered plywood layers on top of the existing boards of each with a thickness of 21 mm for a total of 63 mm. The three layers of plywood are glued within using polyurethane glue and are rendered solid to the existing structure with nails and by means of final insertion of connectors made of threaded bars glued with epoxy resin. The bars are inserted a flush to the upper plywood layer with the aim of uniform plane for subsequent laying of the upper finish. This technique allows for the increase of in-plane floor stiffness and at the same time for completion of a section wood-wood which raises the load bearing capacity of the floor.

Laying three plywood layers one on top of the other permits the use of panels of contained size but staggered joint are needed to achieve a homogeneously resistant package.

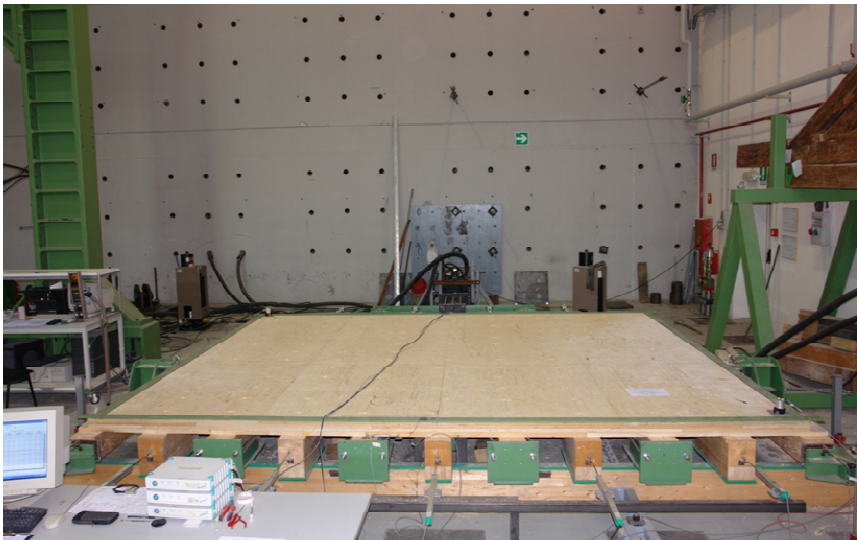


Fig. 9 Floor reinforced with three staggered layers of plywood

2.1.7 Floor reinforced with concrete slab

The last type of option proposed consists of the concrete slab over the existing boards. A floor is then completed made up of wood-concrete by means of laying L shape steel template connectors along bearing beams needed to solidify the new slab to the existing floor structure.

The operation also allows for incrementing in-plane floor stiffness and resistance to vertical loads. This solution includes tie-beam immersed in slabs made up of the right reinforced bars placed along the whole floor perimeter.



Fig. 10 Floor with concrete slabs above existing boards

2.2 Experimental tests

Using test apparatus is the fruit of hard analysis and verification work achieving a test set-up capable of allowing research regarding in-plane floor behaviour. The notable specimen dimension has brought to light many issues of a practical nature which have been confronted with numerical simulation of entire test set-up utilising SAP2000 numerical solver.

Tests were carried out on specimens with dimensions of 5x4 m and 2x1 m to also allow for determining floor behaviour with varying plan sizes.

The main features of the test set-up described in the following refer to specimen dimension, ground constraining and in-plane floor load system.

Dimensions of specimen 5x4 m are to be as close as possible to real floor plan sizes in historic buildings. Experimental tests have favoured such choices and have highlighted the absolute importance of using samples of large sizes. Reduced size specimens are comparable to constituent components, the specimen in itself negatively conditioning the test being axis length equal to 100-160 cm

It is, moreover, worth noting the ground constraining system for the sample. Such constrain should be able to simulate floor anchoring to perimeter bracing walls. Since the ultimate aim of the test campaign is to determine the in-plane stiffness it was decided not to introduce further complex aspects deriving from floor masonry connections which would be difficult to interpret in the phase of result processing. So it was considered important to guarantee full freedom regarding in-plane floor deformation and this was achieved by pinpointing a sole ground constrain shifting displacement, positioned in the bracing wall mid span. In this way the floor was allowed to deform transversally and so it was possible to determine its real in-plane stiffness.

As far as the load system is concerned, also in this case the intent was to get as close as possible to real conditions regarding seismic actions, being the load uniformly spread in the plane, depending on own weight and linear loads deriving from inert forces which act upon walls orthogonally to seismic activity. Such activity can, therefore, be translated into a linear uniform load which acts on in-plane floor.

At this point the aim is to define a configuration of load faithful to uniform spread, the whole test set-up being numericalallly modelled, including the load system. The floor was defined with a plate equivalent and subsequently loaded in-plane with 4 different configurations. The first, for reference, is with load uniformly spread while the subsequent ones foresee an isostatic load agent system on the bearing beams.

Being 11 beams per test floor, the load considered configurations include respective loading of 11, 6 and 4 beams. The following table shows the displacement mid span entity to the floor and the percentage deviation from the uniform load condition.

Table 1 Comparison central node displacement

Load	Displacement	Difference	
	[mm]	[mm]	[%]
uniform	25,65	-	-
11 beam	23,86	1,79	7,0
6 beam	23,38	2,27	8,8
4 beam	23,54	2,11	8,2

Given the minimum differences, the adopted solution foresees loading the heads of 4 floor beams with an isostatic system.

2.2.1 Test set-up for specimens 5x4 m

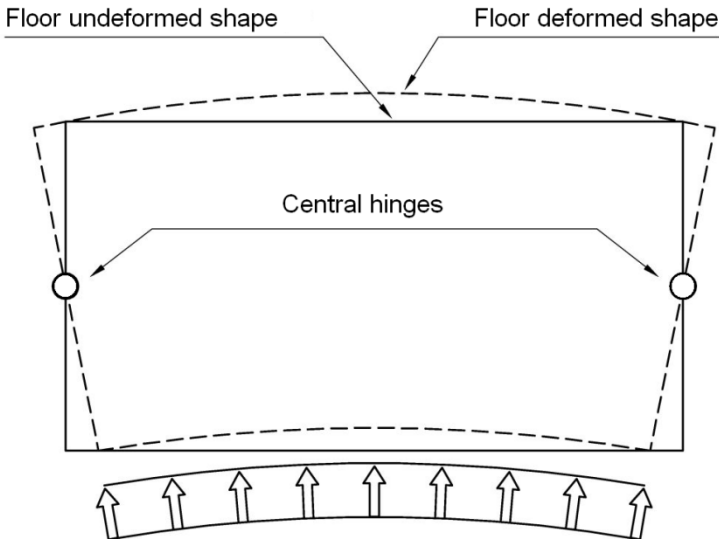


Fig. 11 Deformed configuration of floor with lateral uniform load

Bearing in mind the need to research in-plane floor specimen stiffness, the static scheme adopted is simple floor support bound to ground by means of two hinges placed in the mid span of sides of lesser length.

Such binding allows rotation of side around a point, ensures symmetrical floor behaviour and deformation according to intrinsic stiffness features, as in scheme Fig. 11. It represents floor deformation in seismic action, in correspondence to the beam head of a uniformly spread linear load.

Such load is applied utilising an isostatic system with four points represented in Fig. 12. The MTS electro-hydraulic actuator, is able to maximally push to 100 t and pull to 60 t. One end is anchored to the counteracting laboratory wall by means of a holed plate, the other to the beam system which allows the application of in-plane floor seismic action. We are talking about an isostatic system with 4 points made up of

a main beam HEB 240 of 2.3 m length and two secondary beams HEB 240 of 1.3 m. The main load beam is directly connected to the jack head which loads it at the mid span point. The seismic action is then transferred to the secondary beam mid span by means of two hinges. To complete the link two holed plates have been welded at the ends of the main beam in correspondence with the mid span of the secondary ones. The anchorage is completed with insertion of a calibrated bolt in the holes created in such plate. The constrain selected allows for reciprocal rotation of bearing beams following on from floor deformation, so as to ensure steady contact with floor beam head guaranteeing the condition of chosen load.

To augment the shear strength, in correspondence to the ends, to the centre point of the main beam and those secondary, stiffening steel plates have been welded.

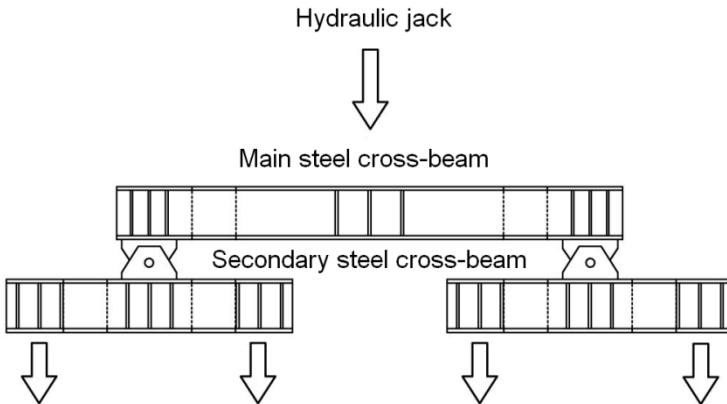


Fig. 12 Isostatic load system

The seismic compression is transferred to the head of the 4 loaded floor beams by means of two cylindrical rolls of 50 mm diameter with vertical axis. The rolls transfer the load to the timber beams through a further

steel plate, solid to support carrying floor beams, so as to avoid embedment of the wood.

Such system means leaning the ends of the floor carrying beams on purpose made steel skids in which two holes are set needed for anchoring the two M24 threaded bars. The bars, which are placed at the sides of the floor carrying beams, are attached to the secondary load beams through the end skid by means of two stretchers. The secondary beams are represented in Fig. 13.



Fig. 13 Load system secondary beams

This system permits the application of compression forces to the floor beams nearest to the actuator directly through the vertical cylinders while the tension forces are transmitted to the floor by means of stretchers and the threaded bars at the ends of the floor beams farther away from the actuator, still in the form of compression action.

In Fig. 14 is shown the whole load system.

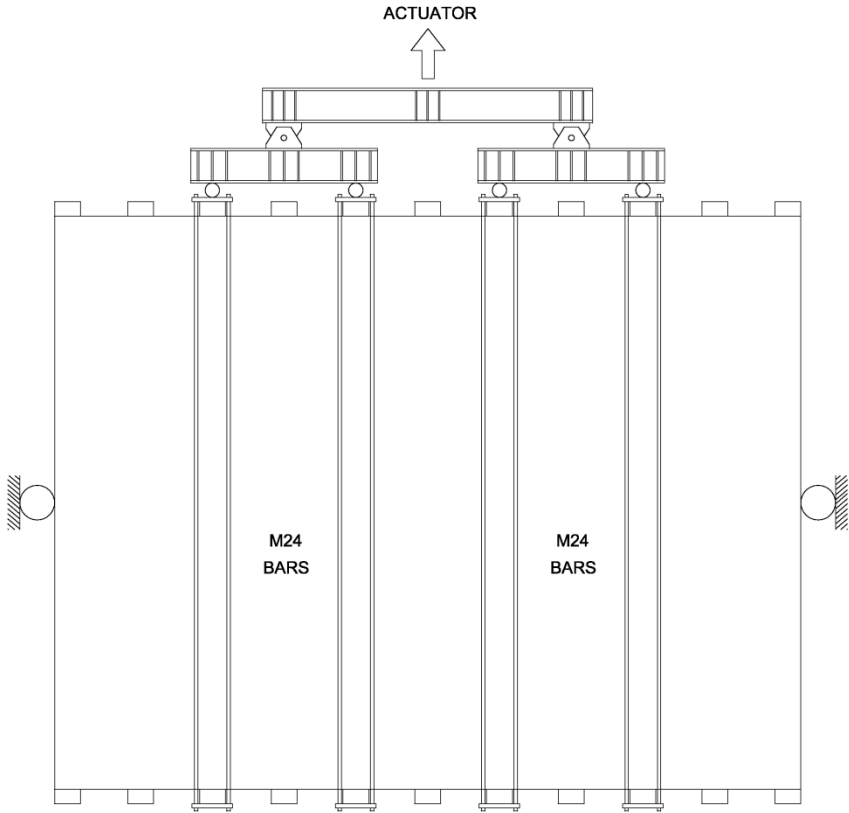


Fig. 14 Test set-up scheme

Each skid supporting the floor beams includes placing a timber thickness internally on which the beam is supported so as to align the floor with the ground constrains. In Fig. 15 an axonometry is shown for the connection of the head plate with the M24 bars.

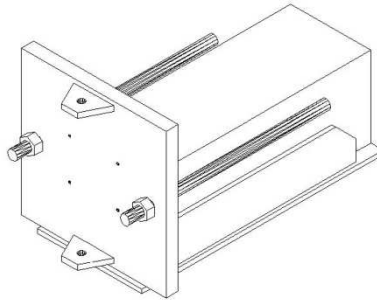


Fig. 15 Head plate



Fig. 16 Detail polyzene plate

The floor includes a scheme for vertical loads in simple bearing with constrains placed at 3,6 m span. We are talking about two timber thickness beams placed transversally to the test specimen, blocked on the ground by means of purpose made steel components bound to each other with two timber beams that perform the function of bracing system. The thickness beams are withdrawn 30 cm compared to external floor shape to guarantee head support for beams for any position reached in deformed configuration.

On all of the surfaces which rub one against the other, purpose made polyzene plates were placed with 10 mm thickness to reduce frictions during the relative rubbing between the contact surfaces. Fig. 16 shows a detail of such plates. The metal plates set between timber elements and sheets of polyzene have the job of avoiding timber beam crush in orthogonal direction to the grain.



Fig. 17 Global view of lateral tubular support

The test specimen transfers ground action applied through two end tubular beams in steel on which end floor beams rest. At the mid span of the steel tubular beams two holed plates are welded in which the bolt is placed which transfers the shear seismic action to the base plate anchored to the ground.

Fig. 17 shows a global view of the support component for lateral beams and their connection to the base plate which transfers the action to the ground. In Fig. 18 an axonometry is represented of the whole test set-up.

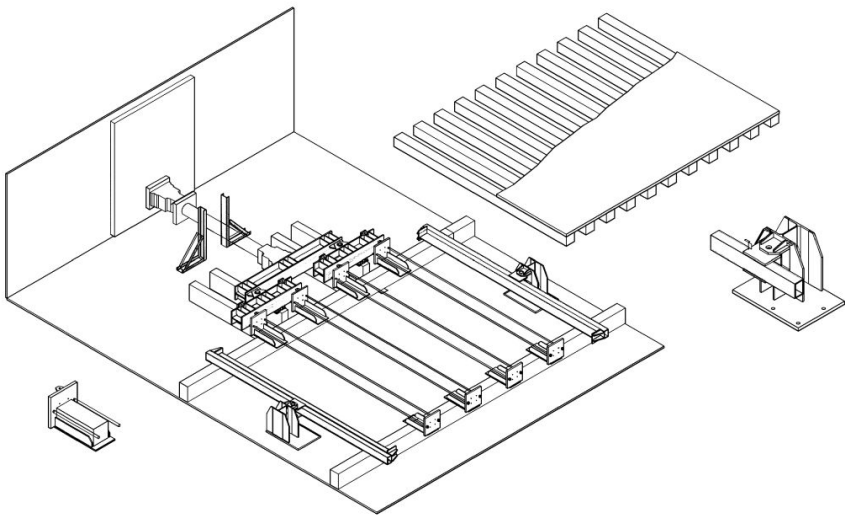


Fig. 18 Axonometry of test set-up

The experimental tests on the 5x4 m floor have the aim of evaluating strength and in-plane timber floor stiffness when planned seismic action is brought to bear. Six samples have been totally analysed, differing in reinforcement type especially for their in-plane stiffness, with the scope of understanding which is their contribution, in terms of stiffness and strength, of single reinforcement systems as well as with tie-beam placed along the perimeter of each floor.

For each type of floor with dimensions of 5x4 m, two different tests were carried out. One monotonic test without tie-beam was done as well as a cyclic test with tie-beam.

The only exception is the floor reinforced with concrete slab for which only the cyclic test was done given the impossibility of applying it to subsequent tie-beam immersed in concrete slab substance.

The loading steps for the cyclic tests were calibrated on the basis of results obtained from monotonic tests carried out on floors of 2x1 m dimension.

2.2.2 Instrumentation for specimens 5x4 m

The instrumentation utilised includes a series of displacement transducers and strain gauges to monitor displacements in mid span on the head of non loaded beams, the transversal displacement in correspondence to the floor corners as well as the deformation of the board and the tie-beam following the application of a seismic force. In Fig. 19 the exact position of the instrumentation can be made out.

For all the monotonic tests the steel strain gauges were not used since the tie-beam orthogonal to the load was applied only in the cyclic test.

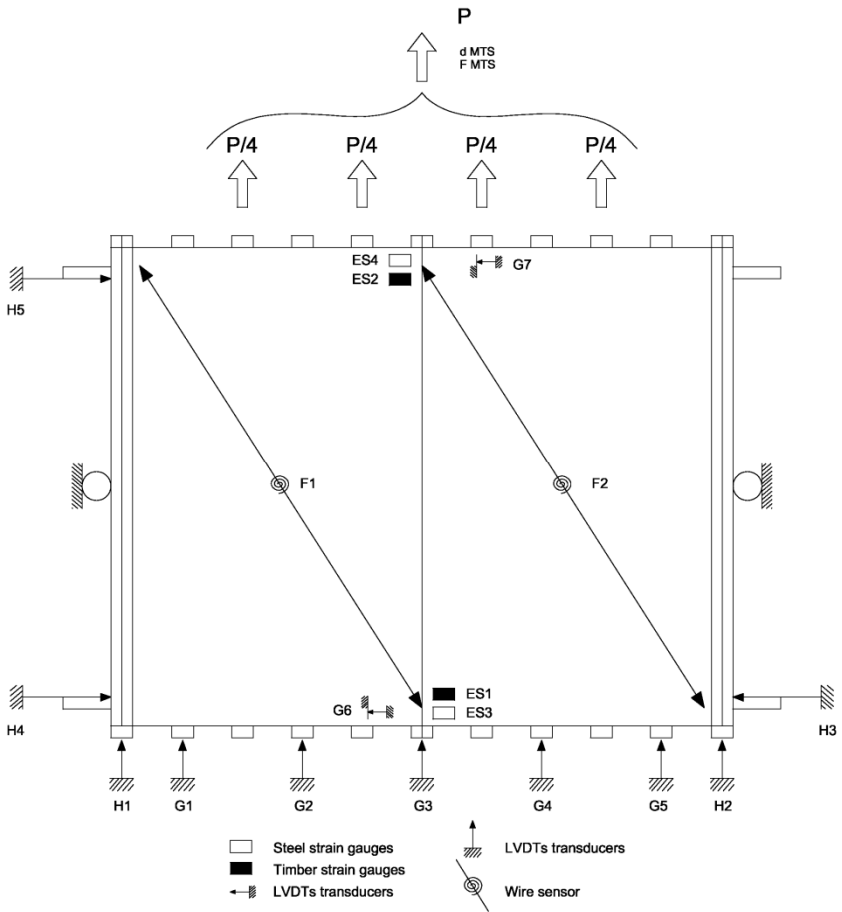


Fig. 19 Floor instrumentation 5x4 m

The following table shows the type of instruments used with scale base values, the precision and the description of measurements made.

Table 2 Floor instrumentation 5x4 m

Type		Full scale	Precision	Description
LVDTs transducers	G6	50 mm	0,025 mm	floor-beam connections deformation
	G7			
LVDTs transducers	G1	300 mm	0,15 mm	beam displacement
	G5			
LVDTs transducers	G2	500 mm	0,25 mm	beam displacement
	G3			
	G4			
LVDTs transducers	H1	40 mm	0,04 mm	rigid floor displacement
	H2			
LVDTs transducers	H3	100 mm	0,1 mm	lateral floor displacement
	H4			
	H5			
Wire sensor	F1	500 mm	0,5 mm	shear floor displacement
	F2			
Steel strain gauges	ES1	-	10 $\mu\text{m}/\text{m}$	boards deformation
	ES2			
Timber strain gauges	ES3	-	10 $\mu\text{m}/\text{m}$	tie-beam deformation
	ES4			

2.2.3 Test set-up for specimens 2x1 m

The tests on floors of 2x1 m dimension have the aim of determining the value of specimen stiffness needed for the calibration of cyclic tests on floors of 5x4 m dimension in accordance with description in EN 12512:2006, to which reference is made. Only monotonic tests are carried out on these given that the test apparatus is simpler than described for floors of dimension 5x4 m. For these tests, punctual seismic action was applied to the floor.

Initially, loading the central floor beam was foreseen but during the phase of testing it was preferred to directly load the deck, in that, after

reaching the last strength of connection deck nails, the central beam tended to unthread. Fig. 20 describes the test set-up scheme.

Regarding the vertical loads, a scheme of steady support is provided for and, in fact, the central floor beams rest on the thickness beams for the whole length. Transversal and longitudinal blocking of such elements is achieved by means of a purpose made UPN 100 profile anchored to the ground. The floor support along the border beams and the earth connection of the whole test apparatus is guaranteed because of the same tubular elements described previously for floors of 5x4 m dimensions as also use of polyzene sheets.

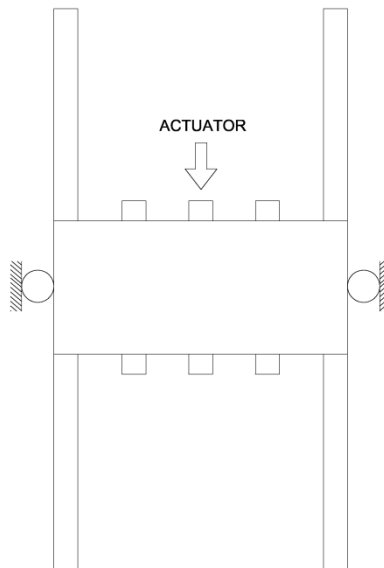


Fig. 20 Floor test Set-up 2x1 m

2.2.4 Instrumentation for specimens 2x1 m

As with floors of great dimensions, also in this case the instrumentation includes displacement transducers as well as strain gauges. The only difference is the absence of steel strain gauges for monotonic tests because their carried out without tie-beam orthogonally to the load direction.

In Fig. 21 the exact position of the instrumentation can be seen. Table 3 shows type, description and position of the various instruments.

Table 3 Floor instrumentation 2x1 m

Type		Full scale	Precision	Description
LVDTs transducers	G6_P	50 mm	0,025 mm	floor-beam connections deformation
	G7_P			
LVDTs transducers	G2_P	300 mm	0,15 mm	beam displacement
	G3_P			
	G4_P			
LVDTs transducers	H1_P	40 mm	0,04 mm	rigid floor displacement
	H2_P			
LVDTs transducers	H3_P	40 mm	0,04 mm	lateral floor displacement
	H4_P			
	H5_P			
Wire sensor	F1	500 mm	0,5 mm	shear floor displacement
	F2			
Timber strain gauges	ES3	-	10 $\mu\text{m/m}$	tie-beam deformation
	ES4			

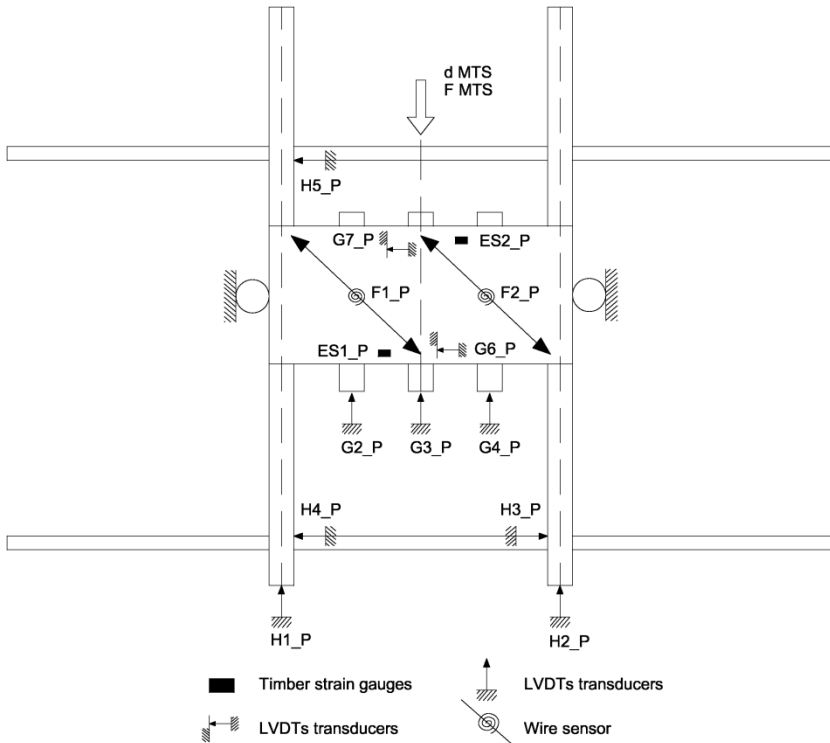


Fig. 21 Floor instrumentation 2x1 m

2.2.5 Test protocol

For each type of floor, monotonic tests have been carried out on specimens of 2x1 m dimension as well as monotonic and cyclic tests on specimens of 5x4 m dimension.

The monotonic test is conducted in displacement control and Fig. 22 represents the load curve of specimen.

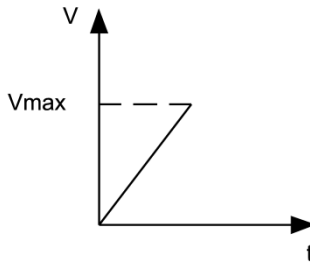


Fig. 22 Test protocol of monotonic tests

According to the type of sample the maximum displacement reached was equal to $1,4 \div 15$ mm with a speed of load variable in the interval of $0,05 \div 0,1$ mm/s.

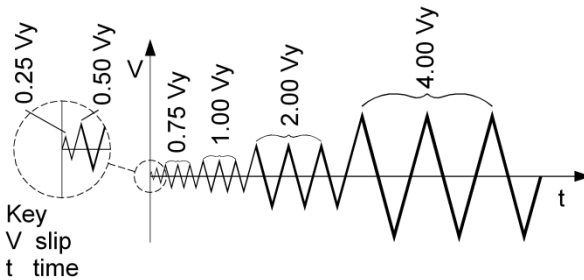


Fig. 23 Test protocol of cyclic tests

The pseudo static cyclic tests followed record documented in Fig. 23 of EN 12512:2006.

To be able to carry out such tests it is necessary to determine the yield displacement of specimen. To do this the procedure described in EN 12512:2006 was applied to estimated monotonic tests carried out on sample dimension 2×1 m. Fig. 24 is an example of yield displacement calculation in the case of simple board floor.

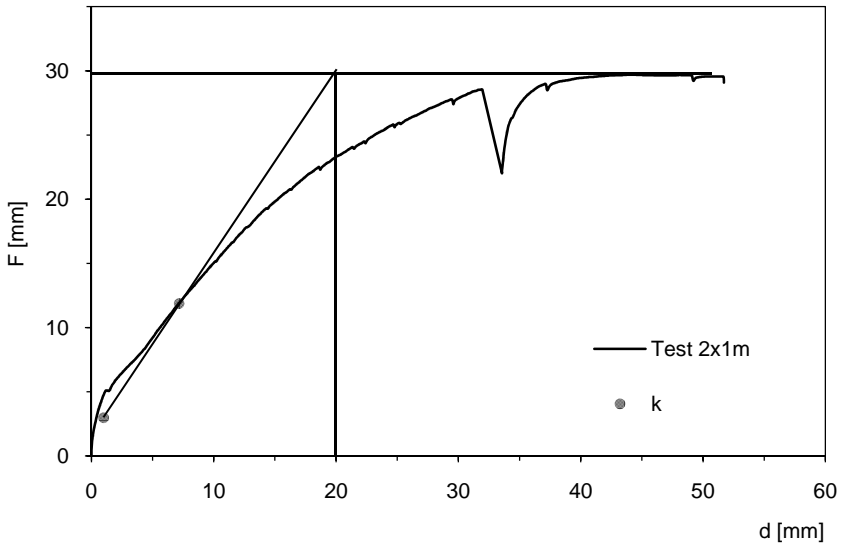


Fig. 24 Procedure calculating yield displacement

During the cyclic tests the speed is steadily maintained for each cycle. To determine the load-displacement curve it is necessary to use the complete application procedure regarding load, illustrated in Fig. 23. As far as the characteristic parameters of the cyclic tests are concerned, the yield displacement is made up of $6,5 \div 30$ mm, intervals, the yield load in the interval $23,5 \div 125$ kN, the actuator displacement in the interval $0,25V_y \div 6V_y$, the speed of variable load between $0,05 \div 2$ mm/s.

2.2.6 *Stiffness calculation*

In this chapter the procedure used for obtaining force-displacement curves from experimental data will be explained in detail on the basis of which each floor stiffness is calculated.

Graphs inserted in the report show, in fact, the discontinuities due to refining of instruments or present us with zero points not coinciding with the cartesian axis zero. It was also necessary to opportunely shift test curve position or reconstruct the curve of the same monotonic so as to obtain the force-displacement graph of an “ideal” monotonic test without imperfections.

Once curves were obtained, the floor stiffness was calculated applying EN 12512:2006.

In the case of floors with small dimensions (2x1 m), starting out from load-displacement curves obtained from experimental data, envelopes were obtained with the aim of having continuity curves, as regular as possible, eliminating unevenness. This operation was essential and in calculating stiffness it is necessary to use a most regular load-displacement curve.

As already explained in the final considerations of the various reports, all the irregularities present are due to data purification. All the temporary intervals have, in fact, been erased where the actuator was blocked during tests for viewing the specimen.

The final floor displacement was, moreover, clarified by rigid displacement of specimen, revealed by purpose made transducers placed in correspondence to floor border beams.

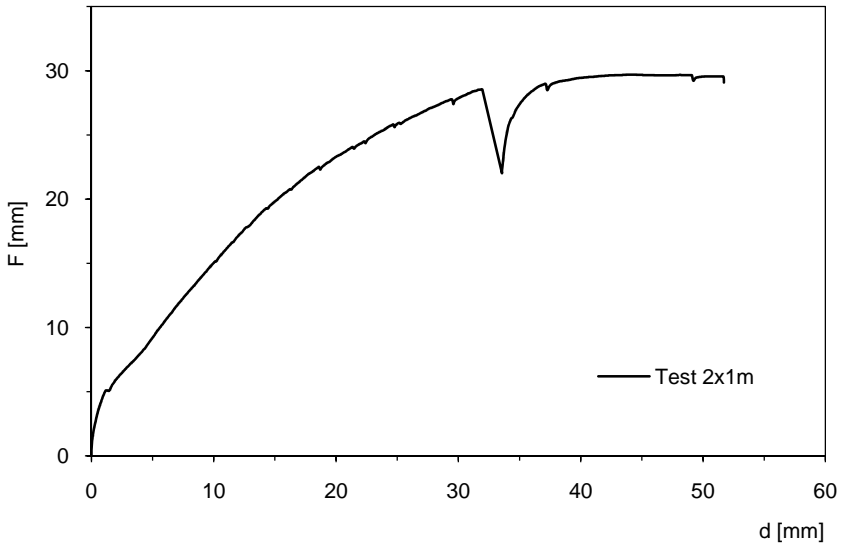


Fig. 25 Curve ascertained from experimental data

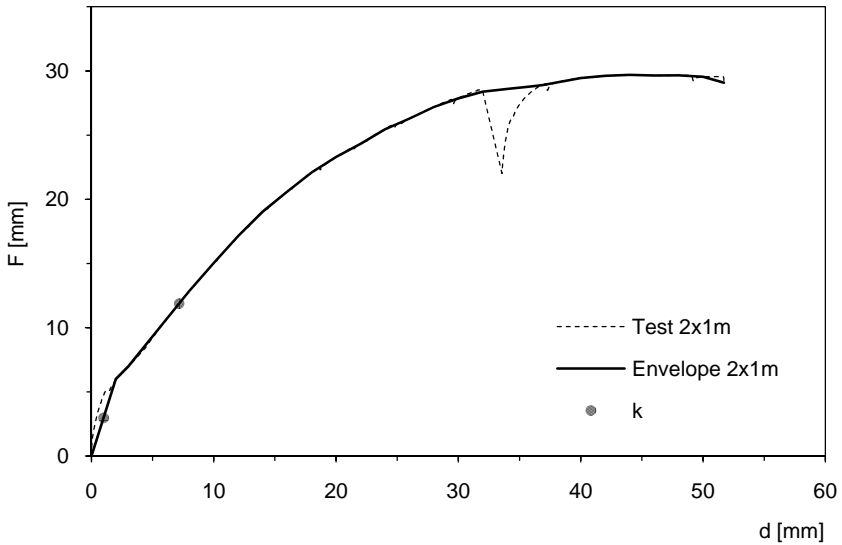


Fig. 26 Re-worked curve for calculating stiffness

Fig. 25 and Fig. 26 give an example of force-displacement graphs obtained directly from acquired data and those re-worked for subsequent calculation of stiffness.

For floors of greater dimension (5x4 m), with tie-beam, the load-displacement curve was obtained from cyclic tests. To determine the interpolating curve, the first cycle of each load step was used, since, in the two subsequent cycles, deterioration in stiffness was noted.

Before isolating the single branches of interest, it is necessary to opportunistically shift each load cycle graph position to coincide the last point of a cycle with the first of the subsequent one. This is the point at which a value of nil force generally corresponds and a displacement of transducer G3 next to the zero.

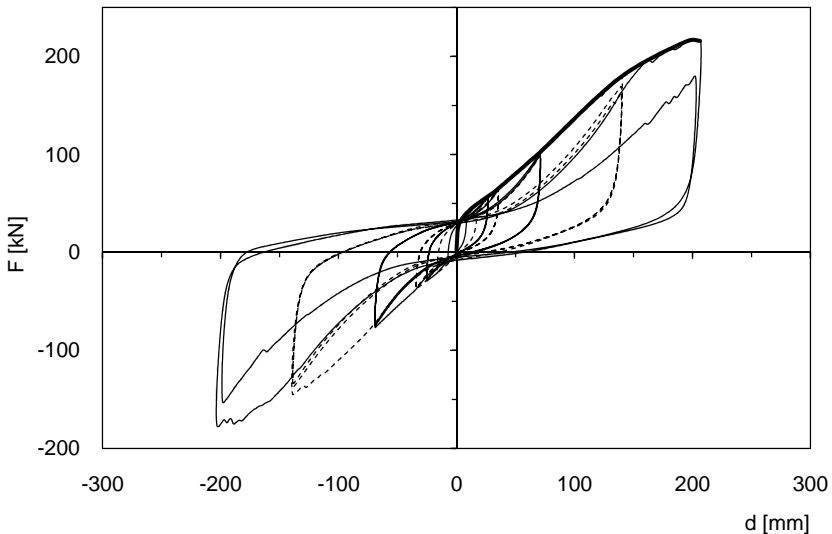


Fig. 27 Cyclic graph comparison with interpolating curve

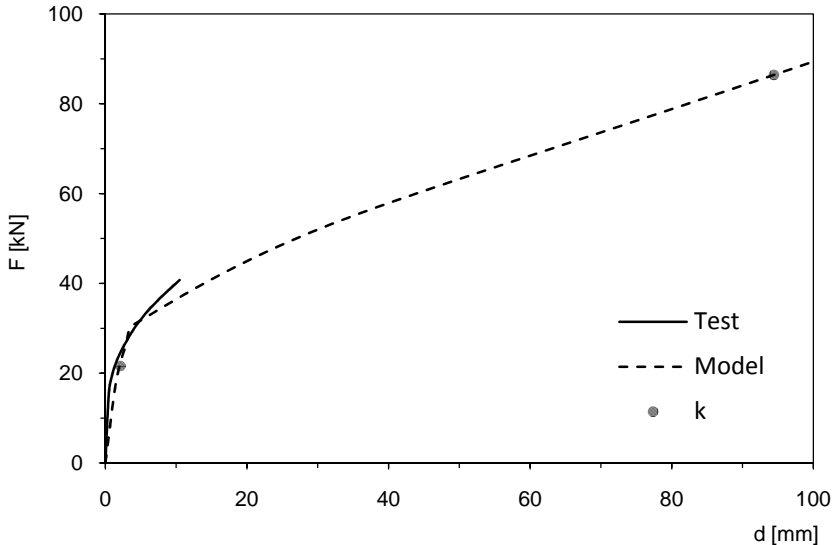


Fig. 28 Load-displacement curve 5x4 m floor without tie-beam

For each floor type the following chapters document the load-displacement curve of cyclic tests and their curve in the case of tie-beam and the monotonic test without perimeter tie-beam. Fig. 27 and Fig. 28 show the load-displacement curves related to cyclic test and to the monotonic one without tie-beam for floor with simple boards.

The stiffness of single floors is calculated using the procedure described in EN 12512:2006. In working through it was chosen to always consider F_{\max} equal to maximum load registered during test. Stiffness is calculated using the following formula

$$k = \Delta F / \Delta v \quad (1)$$

where k is the stiffness, ΔF and Δv represent the increase of force and respective increment of displacement obtained in correspondence with 10% and 40% of the maximum force applied to the specimen.

In the following paragraphs the stiffness for each type of floor will be calculated starting from the load-displacement curve obtained from experimental tests and numerical analysis.

In the case of simple boards, Table 4 documents the stiffness values obtained starting from the experimental tests and numerical analysis both for samples of 2x1 m dimension and for those of 5x4 m. In the following chapters, stiffness documented in the following table is determining for each type of floor.

Table 4 Floor stiffness with simple boards

Floor type	0,1 F _{max}	d _{0,1Fmax}	0,4 F _{max}	d _{0,4Fmax}	k
	[kN]	[mm]	[kN]	[mm]	[kN/mm]
Test 2x1m - no reinf.	2,97	0,99	11,88	7,17	1,44
Test 5x4m - reinf.	21,61	0,94	86,43	55,92	1,18
Model 2x1m - no reinf.	2,91	0,40	11,63	1,60	7,26
Model 5x4m - reinf.	21,61	1,16	86,43	44,82	1,48
Model 5x4m - no reinf.	21,61	2,12	86,43	94,44	0,70

2.3 Modelling and numerical analysis

2.3.1 Introduction

In this chapter the numerical model features are described adopted to simulate floor behaviour with differing types of reinforcement for in-plane actions.

For such numerical analysis the SAP2000 calculation code was used, version 11.0.8. The aim is to supply the engineers with a method of simple analysis which is fast and representative of real floor features,

without having to prolong in representing single structure components, but only changing few input parameters as regards floor dimension and reinforcement type.

2.3.2 General features of the FEM model

Floor modelling was carried out starting from a base model with rectangular shape. The right and left hand sides are made up of frame components which define the floor beams. The upper, lower and diagonal sides are made up of link components. The dimensions of such base module are the floor beam span function which we intend to model. The whole floor model is obtained by approaching base modules one to another until reaching real dimensions of floors examined

The idea at the basis of such modelling is assigning the opportunely scaled characteristic load-displacement curve of the experimental tests to the axial type link element, solely working with geometric features of the numerical model.

Such modelling, in fact, does not have the effect of real floor dimensions in examination since link components reproduce the load-displacement curve imposed, independently from the length.

This allowed us to define the load-displacement curve to assign link elements using simple geometric considerations enunciated in the following.

The link elements used have an elastic-plastic behaviour and are the "MultiLinear Plastic" type. Links with elastic behaviour were also used of the "Hook" type to model the perimeter tie-beam.

The constraining system is faithful to the one at the experimental test site and foresees supports at the ends of each bearing beam to complete the scheme of simple support for vertical loads and then two ground hinges

in the lateral beam mid span to allow the free deformation of in-plane floor.

As regards the load system, the horizontal forces were uniformly applied on the whole floor and applied on each of the four nodes which define the base model.

The adopted model allows for modelling in an exhaustive manner regarding the floor behaviour subject both to vertical and horizontal load.

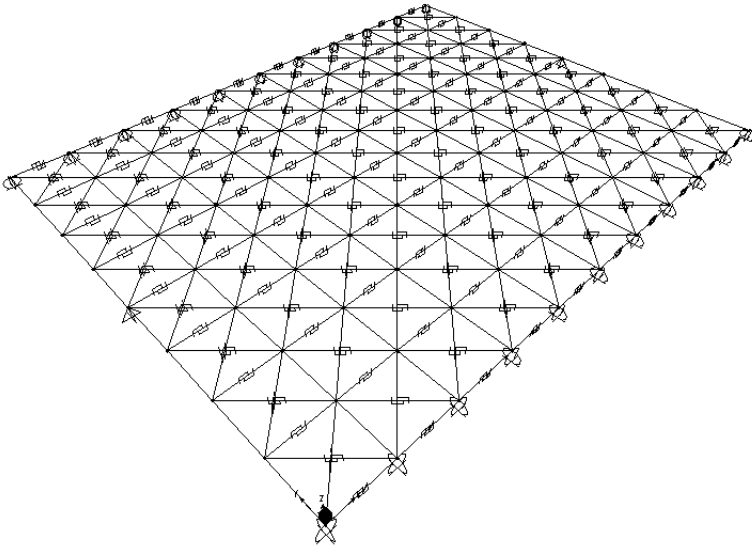


Fig. 29 Three dimensional view of floor model

Fig. 29 represents the numerical floor model. Base modules can be seen that make up the floor and in particular the diagonal link elements.

2.3.3 The numerical model features

For each type of analysed floor it is necessary to define the load-displacement curve to assign link elements that make up the model. As mentioned in the previous paragraph, such curve can be obtained by simple geometric considerations.

Remembering that the link elements used are the axial type, they are able to transfer force only in their developing direction. Hypothesising to fix end floor beams to lateral displacement, the force and displacement on each link element are unequivocally determined regarding the total F force applied to the floor, of the total relative displacement d , of the angle α of inclination of link elements and their number.

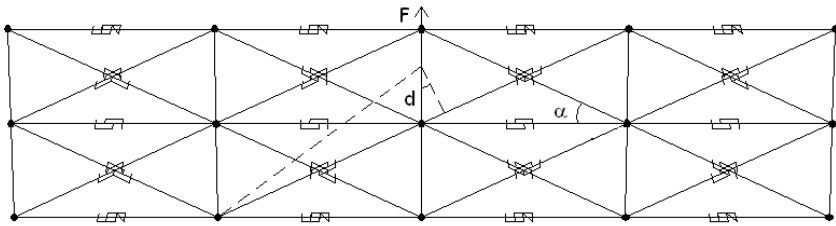


Fig. 30 Numerical model features

In particular, with reference to Fig. 30 we determine the force F^* on element link and the displacement d^* of element link using the following expressions:

$$F^* = F / (\sin \alpha \cdot 2n_f) \quad (2)$$

$$d^* = d \cdot \sin \alpha / (n_d / 2) \quad (3)$$

In the preceding expressions n_f is the number of diagonal links included between two beams in the direction of the horizontal force while n_d is the number of base modules which form half floor in orthogonal direction to

the horizontal force. This value is halved to bring into consideration the floor not being bound laterally but free to rotate on the plane.

Referring to Fig. 30 the two parameters are respectively worth $n_f=4$, $n_d=2$. This figure represents the floor model of 2x1 m dimension with $\alpha=45^\circ$.

In the case of the floor dimension 5x4 m, as represented in Fig. 29 the characteristic parameters are equal to $n_f=16$, $n_d=5$.

With the aim of modelling the perimeter tie-beam, a link element was used with elastic linear behaviour of the "Hook" type for which it is necessary to merely define elastic stiffness.

Being the tie-beam completed with metal elements in steel Fe430 with yield tension at $\sigma = 430$ MPa, yield deformation $\varepsilon = 2\%$, section $A = 75 \times 5$ mm and connected in correspondence to each beam with span $L = 500$ mm, the stiffness can be determined as the following

$$k = F/\Delta L = \sigma \cdot A/(\varepsilon \cdot L) = 161,25 \text{ kN/mm} \quad (4)$$

2.4 Floor strength verifications

In this paragraph the safety verifications are described regarding in-plane, in terms of strength and differing types of floor. Such verifications are needed in planning intervention of reinforcement and complete the picture of operation choice having already determined stiffness and the maximum displacement of each floor.

With this information it is, in fact, possible to choose the reinforcement technique most adapted regarding stability verification for local collapse mechanisms of the perimeter wall.

Different resistant reinforcement techniques, in fact, determine different tension states in the floor. So, in each of the following chapters, dedicated to the six types of analysed reinforcement, there is a paragraph dedicated to such strength verifications.

In the following, seismic activity is described which acts upon the floor, showing actions to which it is subject, describing a procedure of pre-dimensioning of elements of reinforcement such as the perimeter tie-beam and floor-masonry connections.

Note the geometry of the building to be analysed, noting the masses of perimeter walls and of the floors. With those, using the formula (7.3.6) hereunder mentioned from the D.M. 14/01/08 and subsequent modifications, it is possible to determine the horizontal force that acts at the level of each floor.

$$F_i = F_h \cdot z_i \cdot W_i / \sum_j z_j W_j \quad (5)$$

In the preceding equation, W_i is the weight of single levels including floors and perimeter walls. F_h represents the total shear force at the base of the building, as regards the first period of vibration of structure T_1 estimated with (7.3.5) of D.M. 14/01/08 and subsequent modifications.

To pre-dimension the perimeter tie-beam and the floor-masonry connections we can schematically see the floor as a beam in simple support with a uniform load f , equal to the seismic action present at the level of the considered deck, hypothesising in the first approximation the floor infinitely stiff on its own plane.

With these hypotheses we can determine the maximum moment at the mid span and the shear on the supports according to the scheme documented in Fig. 31. Concentrating the resisting elements of tension and compression at the level of the curbs it is possible to define an arm of the internal couple Z and with this, calculate the tension force, determining the area of steel necessary.

Finally, noting the shear action q , we determine the span and diameter of floor-masonry connectors. It is important to underline that such verifications must be carried out both in direction x and y .

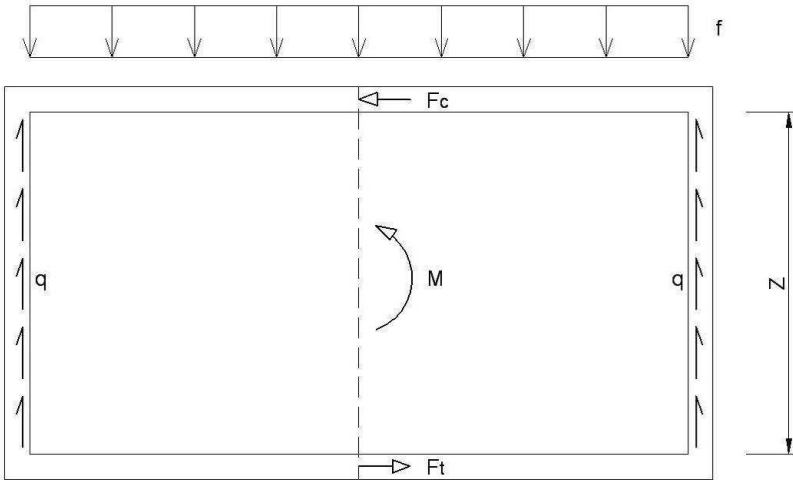


Fig. 31 Internal and external force acting upon floor

The tension force F_t and compression F_c which the perimeter tie-beam is subject to can be determined by means of the following equation, placing L the length of the floor on which the seismic action f acts.

$$F_t = F_c = f \cdot L / Z \quad (6)$$

The numerical model of floor defined in this chapter and loaded according to that previously shown allows us to ascertain tension, compression and shear action on the deck in the zones highlighted in Fig. 32.

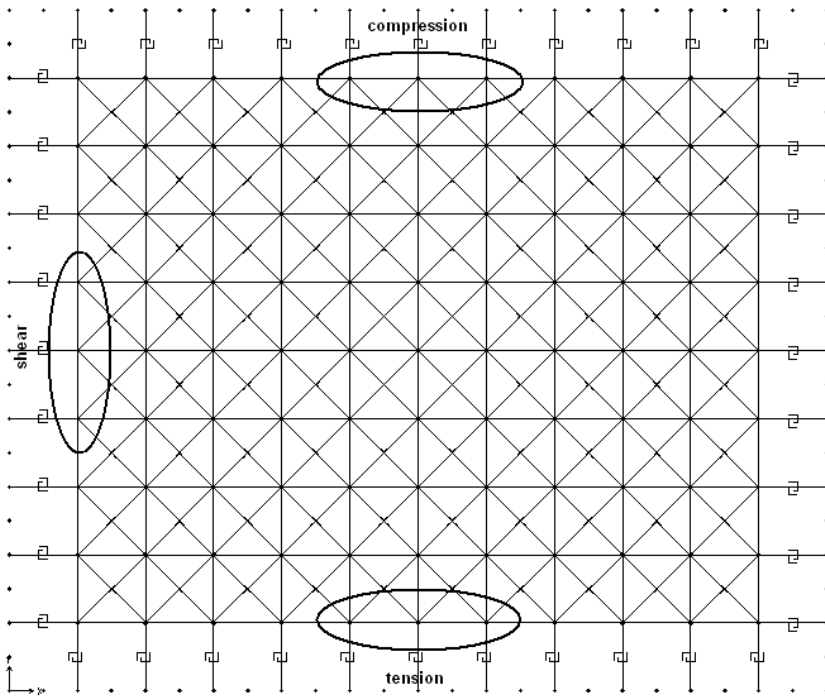


Fig. 32 Detail of the zones of floor subject to verification

For each type of floor considered the following chapters will describe strength verifications related to the floors.

As will be shown in detail in Chapter 9, the floor-masonry connections are modelled, analogously to those carried out for floors, with link elements from elastic-plastic behaviour of the “Multi Linear Plastic” kind. The tension and shear verifications on such connections will be carried out on the basis of actions obtained from numerical analysis.

3. FLOOR WITH SIMPLE TIMBER BOARDS

3.1 Introduction

The floor with simple timber boards represents the first solution as regards the experimental test campaign and one mostly present in the consolidation operations for the existing building patrimony.



Fig. 33 Floor with simple timber boards

3.2 Specimen construction features

3.2.1 Floor dimension 2x1 m

The following Fig. 34 documents, as titled, a plan view of the floor under consideration:

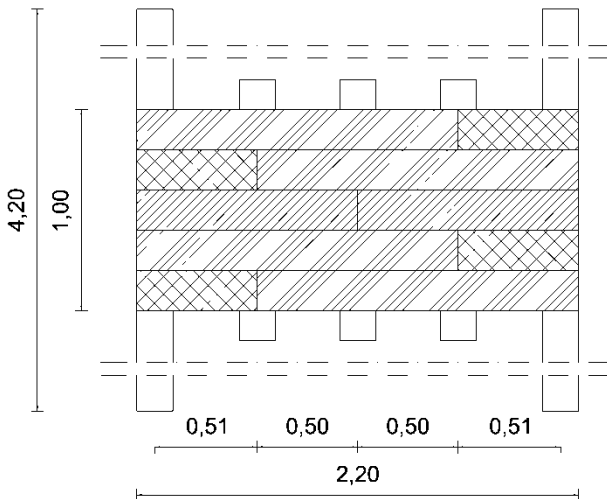


Fig. 34 Floor with simple timber boards

The bearing beams are in GL24c of second category and have transversal sections equal to $180 \times 180 \text{ mm}^2$. The floor bearing frame is made up in total of 5 beams, three central beams of length equal to 1.30 m and two lateral of 4.20 m length. The lateral beams are longer to be able to use the load and ground constraining system planned for the 5x4 m floors.

The span between the beams is 51 cm between the border beam and the first internal beam and 50 cm between the internal beams.

The floor under test has a rectangular plan form of dimensions equal to $2,20 \times 1,00 \text{ m}^2$ and a total thickness of 21 cm. The planks which make up the deck are in class C22, having a transversal section of $20 \times 3 \text{ cm}^2$ and are of variable lengths according to position. The plank laying is staggered joints. The specimen was completed using the following planks: 4 planks $160 \times 20 \times 3 \text{ cm}$, 2 planks $120 \times 20 \times 3 \text{ cm}$, 4 planks $60 \times 20 \times 3 \text{ cm}$.

The following Fig. 35 illustrates the detail relative to the deck plank connection to the carrying beams.

The planks are connected to the floor beams with nails. 4 nails $2,8 \times 80 \text{ mm}$ were used in correspondence to each beam.

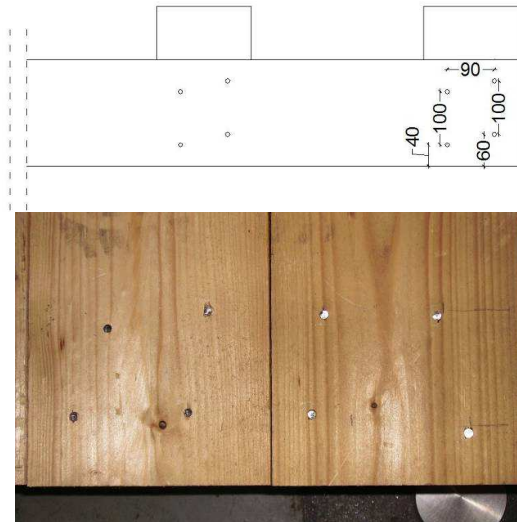


Fig. 35 Nailing detail

3.2.2 Floor dimension 5x4 m

The following Fig. 36 represents a plan view of the floor in question:

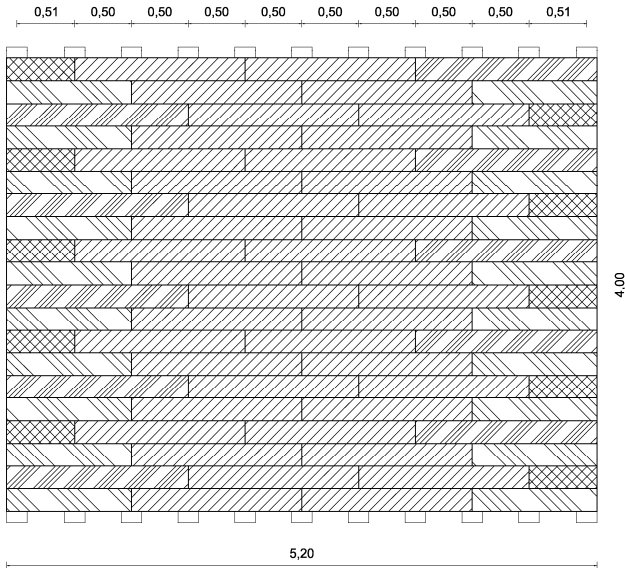


Fig. 36 Floor with simple timber boards

The bearing beams are completed with GL24c of second category and have transversal sections of $180 \times 180 \text{ mm}^2$. The floor bearing frame is made up of 11 beams in total length 4.20 m. The span between the beams is 51 cm between the edge beam and the first internal beams and 50 cm between the other beams and the internal beams. The floor subject to test has a rectangular shape in plan of $5 \times 4 \text{ m}^2$ dimensions and total thickness of 21 cm. The planks which make up the structure are class C22 having a transversal section of $20 \times 3 \text{ cm}^2$ and are variable length depending on position. Laying of planks is with staggered joints.

The specimen was completed with the following planks, 10 planks 160x20x3 cm, 40 planks 150x20x3 cm, 20 planks 110x20x3 cm, 10 planks 60x20x3 cm. The planks used for this structure type have sections of 20x3 cm². As far as tie-beam is concerned, this is made up of section steel plate 75x5 mm², length 5200 mm, connected to the floor beams with screws \varnothing 10x160 mm.

3.2.3 Summary of construction features and materials

Table 5 Floor characteristics with simple boards

Beam		Simple boards	
n.	11	n.	80
Material	GL24c	Material	C22
E	11,6 GPa	E	10 GPa
Section	18x18 cm ²	Section	20x3 cm ²
Span	50 cm	Length	60-160 cm
Floor dim.	5,2x4,2 m ²	Total area	5,2x4,2 m ²
Boards connections		4 nails \varnothing 2,8x80 mm / beam	
Tie-beam reinforcement			
Parallel to load	Element dim.	80x5x3860 mm	
	Material	Fe430	
	E	210 GPa	
	Position	external beam	
	Connections	screws \varnothing 10x160 / 30 cm	
	Test	monotonic and cyclic test	
Orthogonal to load	Element dim.	75x5x5200 mm	
	Material	Fe430	
	E	210 GPa	
	Position	end of floor	
	Connections	screws \varnothing 10x160 / beam	
	Test	cyclic test	

3.3 Floor stiffness

The following figures represent the load-displacement curves coming out of experimental tests. Cases of floors with dimensions of 2x1 m and 5x4 m are especially represented. The latter with and without perimeter tie-beam.

Curves have been obtained from the experiments and from them the envelopes and then experimental stiffness. Stiffness determined from the load-displacement curves has also been documented in Table 6 for completing the picture obtained from numerical analysis.

The stiffness has been determined using procedure described in the EN12512:2006 with reference to load and displacement values relative to 10% and 40% of the maximum force registered. In the following figures the featured points used for determining such stiffness are highlighted.

Table 6 Rigidezze solaio con semplice tavolato

Floor type	0,1 F_{max}	$d_{0,1Fmax}$	0,4 F_{max}	$d_{0,4Fmax}$	k
	[kN]	[mm]	[kN]	[mm]	[kN/mm]
Test 2x1m - no reinf.	2,97	0,99	11,88	7,17	1,44
Test 5x4m - reinf.	21,61	0,94	86,43	55,92	1,18
Model 2x1m - no reinf.	2,91	0,40	11,63	1,60	7,26
Model 5x4m - reinf.	21,61	1,16	86,43	44,82	1,48
Model 5x4m - no reinf.	21,61	2,12	86,43	94,44	0,70

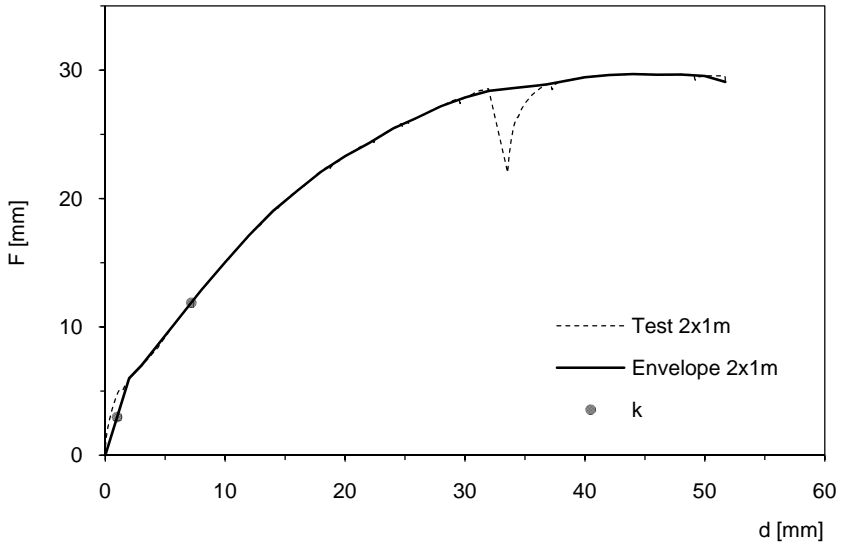


Fig. 37 Load-displacement curve of floor 2x1m

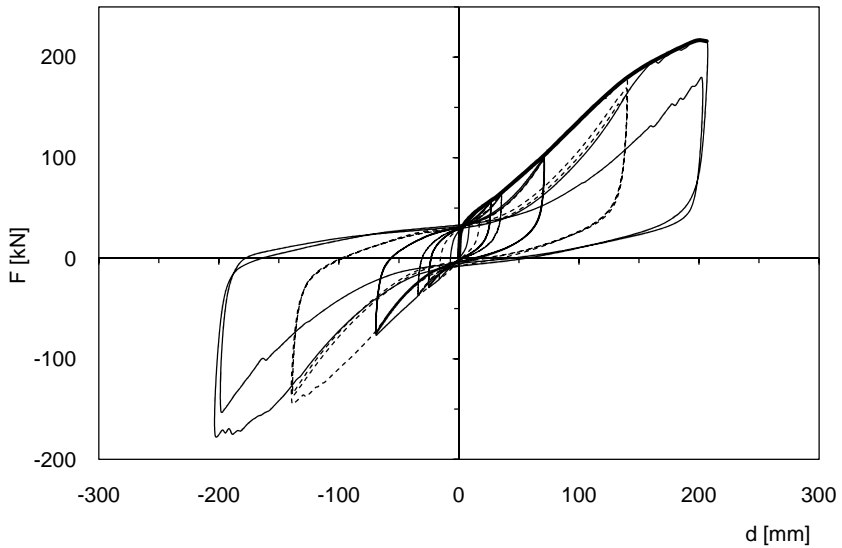


Fig. 38 Load-displacement curve of floor 5x4m with tie-beam

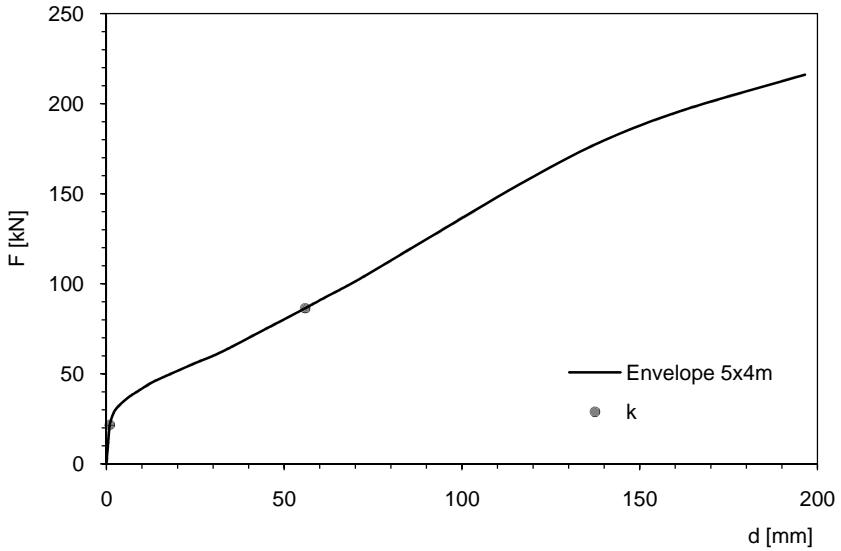


Fig. 39 Envelope load-displacement curve of floor 5x4m with tie-beam

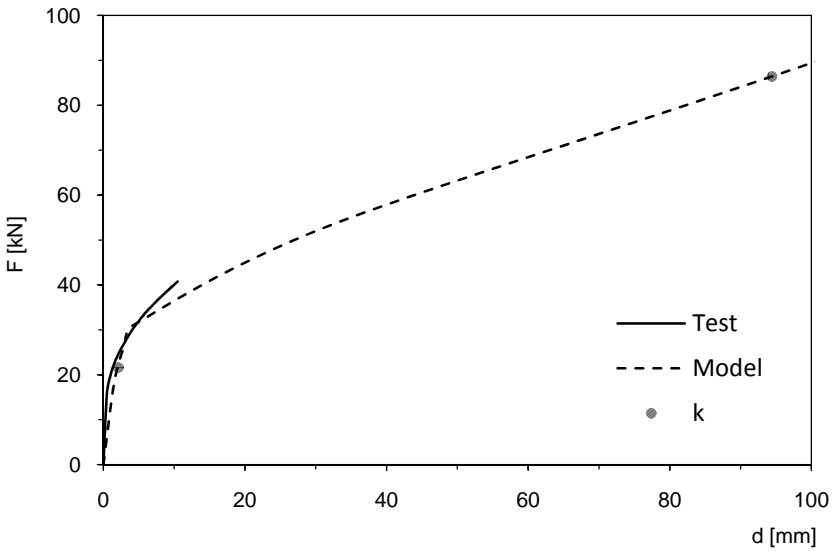


Fig. 40 Load-displacement curve of floor 5x4m without tie-beam

3.4 Numerical model features

To define floor model it is necessary to determinate the force-displacement characteristic curve of link elements as described in paragraph 2.3.3.

In particular in Table 7 the load-displacement curves are documented related to experimental tests carried out on floors with dimensions of 5x4 m. In Fig. 41 is shown the assigned curve to link elements in the floor modelling case of 2x1 m; the model is the same of Fig. 30 and the characteristic parameters are $n_f=4$ e $n_d=2$.

Table 7 Load-displacement curve experimental test and link element

Test		Link	
d [mm]	F [kN]	d [mm]	F [kN]
-46,13	-365,20	-32,62	-64,56
-23,02	-255,32	-16,28	-45,13
-10,96	-180,16	-7,75	-31,85
-3,58	-104,44	-2,53	-18,46
-0,96	-64,68	-0,68	-11,43
-0,56	-42,88	-0,40	-7,58
-0,15	-20,84	-0,10	-3,68
0,00	0,00	0,00	0,00
0,15	20,84	0,10	3,68
0,56	42,88	0,40	7,58
0,96	64,68	0,68	11,43
3,58	104,44	2,53	18,46
10,96	180,16	7,75	31,85
23,02	255,32	16,28	45,13
46,13	365,20	32,62	64,56

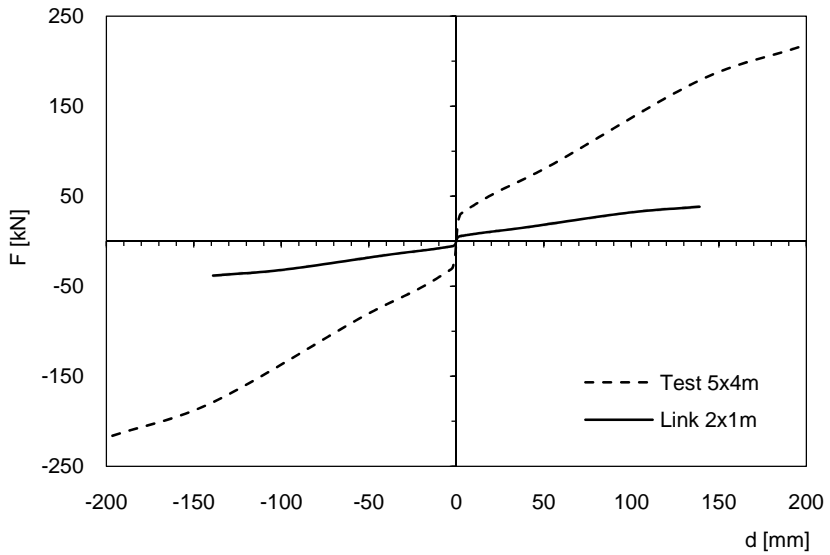


Fig. 41 Load-displacement curve of test and link element

3.5 Strength verifications

3.5.1 Shear verification

Fig. 42 represents the board-beam connection scheme. Noting from the analysis the F force, equal to the shearing stress of the single board, and the connection geometry, it is possible to determine with moments equilibrium the force F'_{sd} which act on single connection elements.

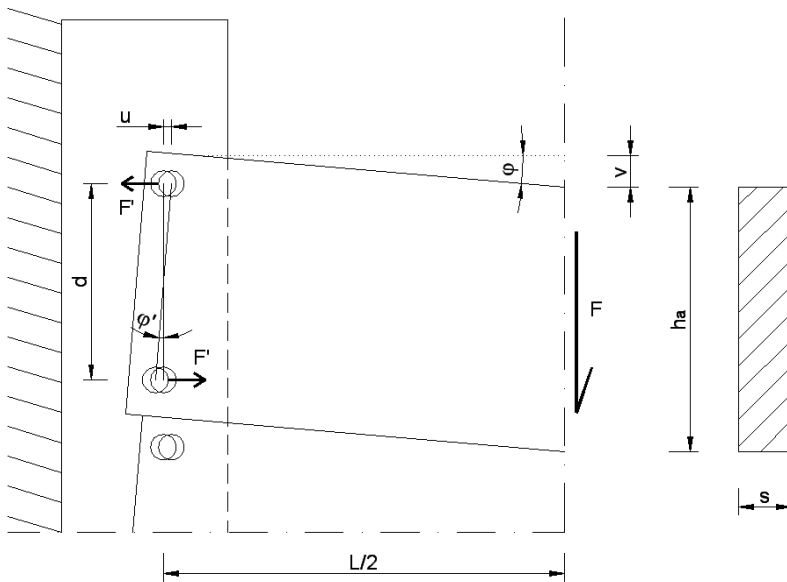


Fig. 42 Shearing stress of board-beam connection

The load-carrying capacity for each shear plane in the timber connections with metal fasteners can be determined starting out from characteristic load-carrying capacity $F_{v,Rk}$ defined at point 8.2.2, formula

(8.6) Eurocode 5. The norm proposes the theory of Johansen which includes six types of union break and from them chooses the most limiting condition based on characteristic embedment strength in the timber member $f_{h,k}$ and on the characteristic fastener yield moment $M_{y,k}$. The connection verification concludes checking the respect of minimum values of span and distance from edges and ends given in table 8.2 and Fig. 8.7 Eurocode 5.

In the end it is necessary to shear check the boards which make up the floor structure. To do this, noting from analysis the tangential tension τ_d , is sufficient to verify the following equation dealt with in Eurocode 5.

$$\tau_d \leq f_{v,d} \quad (7)$$

In (7) $f_{v,d}$ is design shear strength defined in the EN 338.

3.5.2 Tension verification

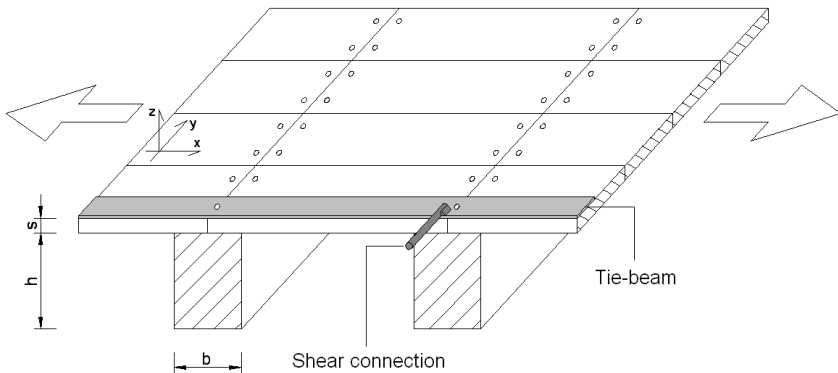


Fig. 43 Detail of tension zone of floor

There are two verifications to be done. The first regards the strength elements that make up the deck, the boards, while the second regards the tie-beams and its connection elements to the floor.

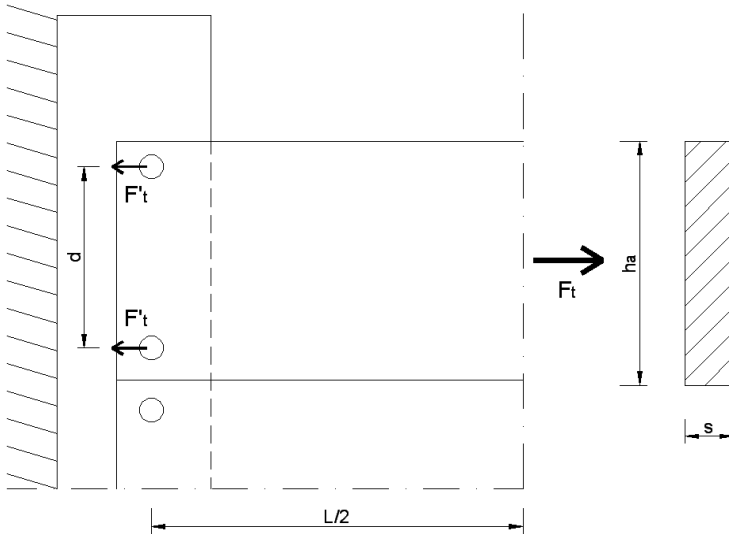


Fig. 44 Tension stress of board-beam connection

With reference to Fig. 44, noting the tension stress, it is necessary to check the boards using formula (6.1) of Eurocode 5.

$$\sigma_{t,0,d} \leq f_{t,0,d} \quad (8)$$

To ensure efficient connection of boards to main beams, the connections will have to respect the following equation where F'_t is the shear stress.

$$F'_t = F_{V,Sd} \leq F_{V,Rd} \quad (9)$$

The second verification regards the tie-beam. It is stressed to the forces illustrated in Fig. 45.

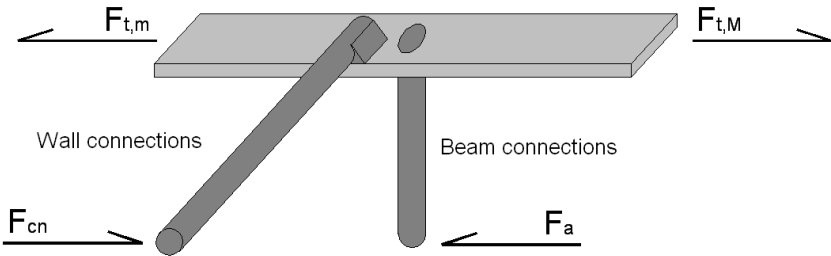


Fig. 45 Forces of tie-beam in tension stress

Force F_a transmitted from the floor to the tie-beam induces a tension stress which is transmitted to the perimeter walls by means of a floor-masonry connection, of intensity F_{cn} .

Tension verifications will have to be done of tie-beam and shear verification of the floor-tie-beam and floor-wall connection.

The tension check is the following equation.

$$N_{Sd} \leq N_{t,Rd} \quad (10)$$

In the preceding formula N_{Sd} is the maximum tension stress in the element while $N_{t,Rd}$ is defined in Eurocode 3

The check of connection with the main beam is carried out with (9).

3.5.3 Compression verification

This check consists of verifying that the compression parallel strength of the boards is greater than the stress obtained by analysis, using the formula (6.2) of Eurocode 5.

$$\sigma_{c,0,d} \leq f_{c,0,d} \quad (11)$$

In the end it is necessary to verify in compression the steel plate that makes up the tie-beam, using the formula of Eurocode 3.

$$N_{Sd} \leq N_{c,Rd} \quad (12)$$

3.5.4 Shear and tension verification of floor-wall connections

The load capacity of the floor-wall connections can be determined from experimental tests. Noting the strength, the safety verifications are the following.

$$N_{Sd} \leq N_{t,Rd} \quad (13)$$

$$F_{V,Sd} \leq F_{V,Rd} \quad (14)$$

4. FLOOR REINFORCED WITH TIMBER BOARDS

4.1 Introduction

The first hypothesis of structural reinforcement is given by the positioning on the existing layer a second one with an inclination of 45° compared to the first.

Such positioning at 45° benefits stiffening effect as regards the second layer independently from the direction in which seismic action comes into force.



Fig. 46 Floor reinforced with timber boards

4.2 Specimen construction features

4.2.1 Floor dimensions 2x1 m

In the case of floors of reduced dimensions, a second layer made up of panels with dimensions of 110x100x2.1 cm was placed over the existing boards. Fig. 47 documents a plan view of floor.

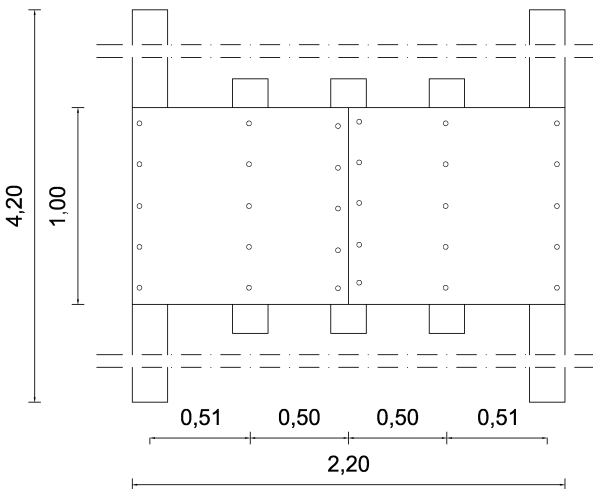


Fig. 47 Plan view of reinforcement layer with second strata

The features of the first timber boards and the bearing beams are the same to those described in the course of the preceding chapter. The upper layer of reinforcement is connected as illustrated the following Fig. 48 to the first boards using connectors made up of threaded bars $\phi 10$, length 150 mm injected with epoxy resin in the beam at span of 30 cm.

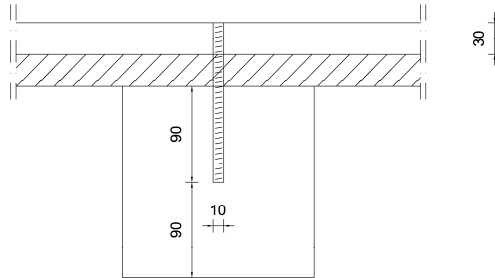


Fig. 48 Section view of connection between two layers

As noted from the preceding figure the connectors are inserted flush to the upper layer of the second one. In the first phase the upper planks are provisional fixing with screws to the lower ones.

4.2.2 Floor dimensions 5x4 m

This type of sample, as the following Fig. 49 illustrates, includes laying a second layer to 45° compared to the first. The planks have 20x3 cm² sections and variable length. Connection is done using screws of ø6x90 mm. Two screws are used for every intersection of plank-beam.

4.2.3 Summary of construction features and materials

Table 8 Floor characteristics reinforced with timber beams

Beam		Simple boards	
n.	11	n.	80
Material	GL24c	Material	C22
E	11,6 GPa	E	10 GPa
Section	18x18 cm ²	Section	20x3 cm ²
Span	50 cm	Length	60-160 cm
Floor dim.	5,2x4,2 m ²	Total area	5,2x4,2 m ²
Boards connections		4 nails ø2,8x80 mm / beam	
Floor reinforcement - second boards			
n.	64		
Material	C22		
E	10 GPa		
Section	20x3 cm ²		
Length	50-290 cm		
Laying	45°		
Total area	5,2x4,2 m ²		
Connections	2 screws ø6x90 mm / board / beam		
Tie-beam reinforcement			
Parallel to load	Element dim.	80x5x3860 mm	
	Material	Fe430	
	E	210 GPa	
	Position	external beam	
	Connections	screws ø10x160 / 30 cm	
Orthogonal to load	Test	monotonic and cyclic test	
	Element dim.	75x5x5200 mm	
	Material	Fe430	
	E	210 GPa	
	Position	end of floor	
	Connections	screws ø10x160 / beam	
	Test	cyclic test	

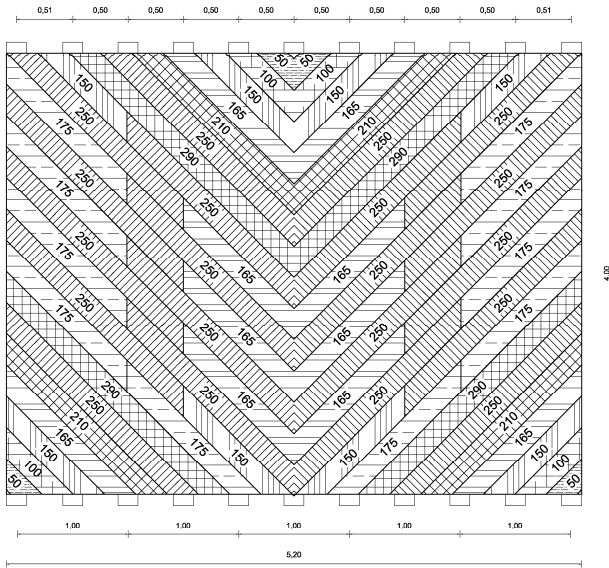


Fig. 49 Detail relative to type of elements used for upper layer of reinforcement

4.3 Floor stiffness

The following figures represent the load-displacement curves coming out of experimental tests. Cases of floors with dimensions of 2x1 m and 5x4 m are especially represented. The latter with and without perimeter tie-beam.

Curves have been obtained from the experiments and from them the envelopes and then experimental stiffness. Stiffness determined from the load-displacement curves has also been documented in Table 9 for completing the picture obtained from numerical analysis.

The stiffness has been determined using procedure described in the EN12512:2006 with reference to load and displacement values relative to 10% and 40% of the maximum force registered. In the following figures the featured points used for determining such stiffness are highlighted.

Table 9 Floor stiffness reinforced with timber boards

Floor type	0,1 F_{max}	$d_{0,1Fmax}$	0,4 F_{max}	$d_{0,4Fmax}$	k
	[kN]	[mm]	[kN]	[mm]	[kN/mm]
Test 2x1m - no reinf.	7,20	0,77	28,82	4,88	5,25
Test 5x4m - reinf.	36,52	0,44	146,08	7,22	16,16
Model 2x1m - no reinf.	6,74	0,16	26,96	0,82	30,72
Model 5x4m - reinf.	36,52	0,49	146,08	6,53	18,15
Model 5x4m - no reinf.	36,52	0,84	146,08	12,93	9,06

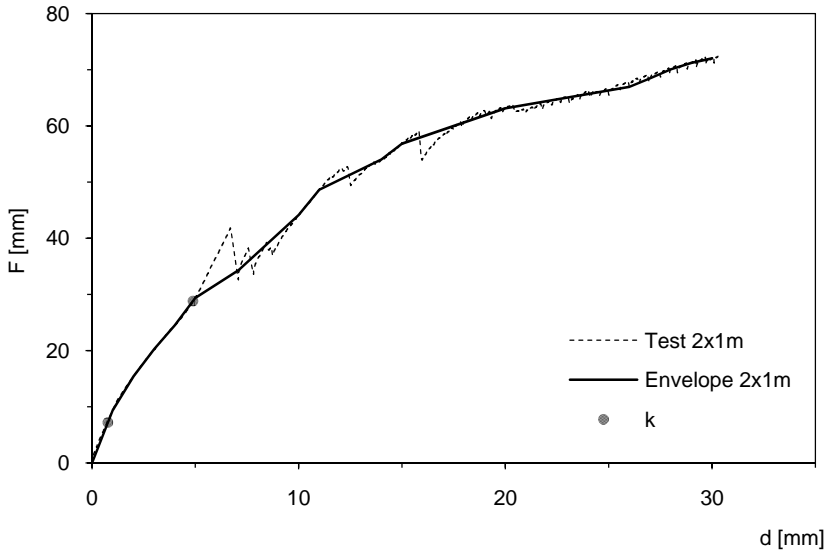


Fig. 50 Load-displacement curve of floor 2x1m

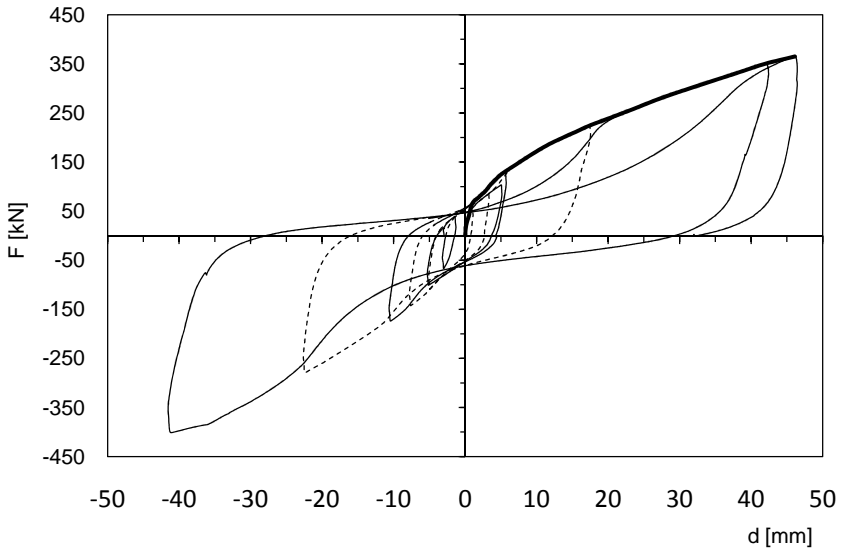


Fig. 51 Load-displacement curve of floor 5x4m with tie-beam

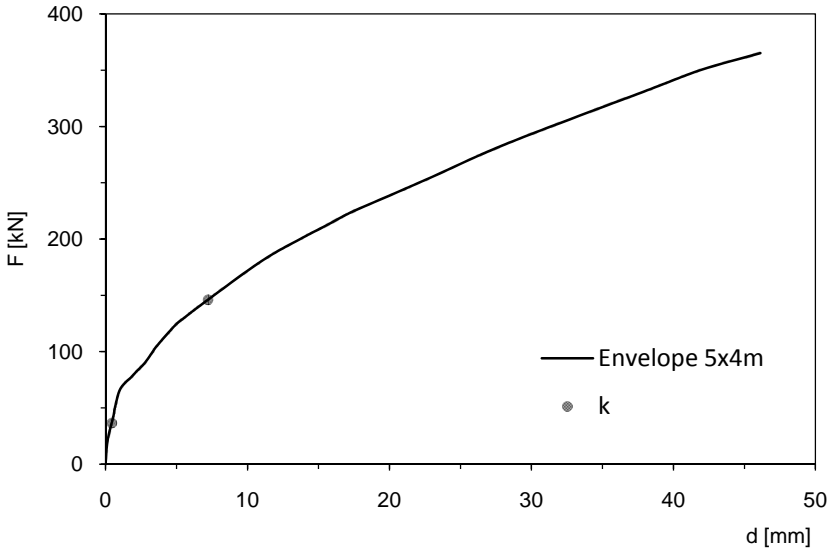


Fig. 52 Envelope load-displacement curve of floor 5x4m with tie-beam

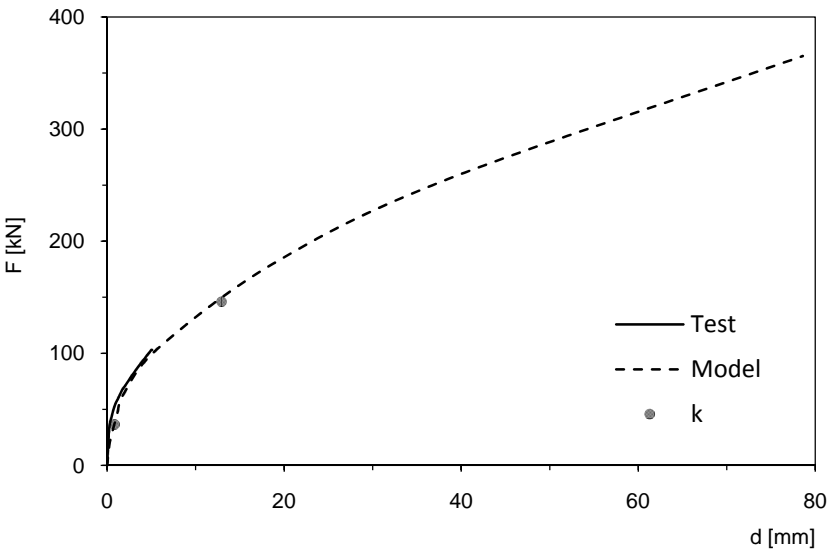


Fig. 53 Load-displacement curve of floor 5x4m without tie-beam

4.4 Numerical model features

To define floor model it is necessary to determinate the force-displacement characteristic curve of link elements as described in paragraph 2.3.3.

In particular in Table 10 the load-displacement curves are documented related to experimental tests carried out on floors with dimensions of 5x4 m. In Fig. 54 is shown the assigned curve to link elements in the floor modelling case of 2x1 m; the model is the same of Fig. 30 and the characteristic parameters are $n_f=4$ e $n_d=2$.

Table 10 Load-displacement curve experimental test and link element

Test		Link	
d [mm]	F [kN]	d [mm]	F [kN]
-196,48	-216,08	-138,93	-38,20
-138,60	-178,37	-98,00	-31,53
-55,66	-86,15	-39,36	-15,23
-21,80	-53,22	-15,41	-9,41
-2,91	-31,05	-2,06	-5,49
-1,69	-26,72	-1,20	-4,72
-0,73	-18,20	-0,52	-3,22
0,00	0,00	0,00	0,00
0,73	18,20	0,52	3,22
1,69	26,72	1,20	4,72
2,91	31,05	2,06	5,49
21,80	53,22	15,41	9,41
55,66	86,15	39,36	15,23
138,60	178,37	98,00	31,53
196,48	216,08	138,93	38,20

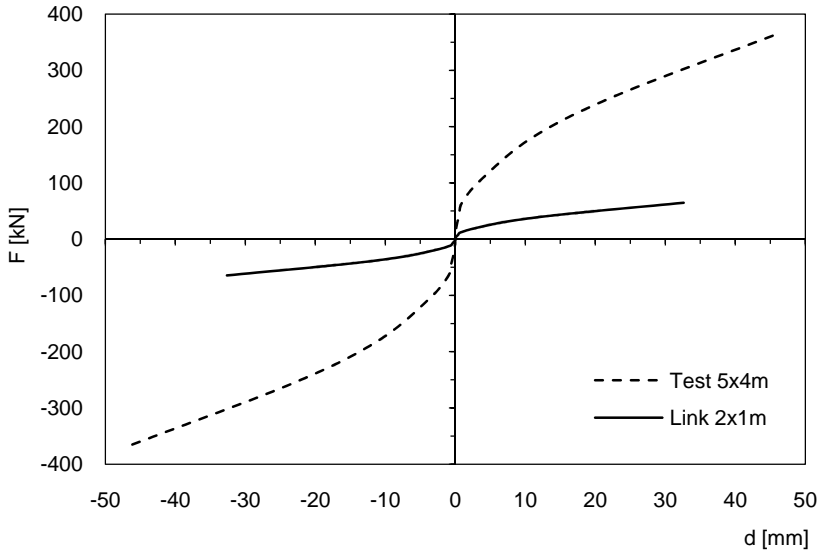


Fig. 54 Load-displacement curve of test and link element

4.5 Strength verification

In the case of double boards the two layers constitute one element. The connections between first and second layer are not verified.

4.5.1 Shear verification

Noting from analysis the shear stress τ_d , is sufficient to verify the following equation from Eurocode 5.

$$\tau_d \leq f_{v,d} \quad (15)$$

In (15), $f_{v,d}$ is the shear strength defined in EN 338.

4.5.2 Tension verification

Even after considering the two layers as a single one, when there is tension stress, we consider, favouring safety, that only the layer with the grain parallel to tension can offer strength so overlooking the second one.

The first check concerns the first layer and its connections with main beams. The second is done on tie-beam and on its deck connections.

Regarding the tie-beam, we prefer, with this type of floor, to use an L profile which facilitates connection of second layer to the tie. In Fig. 55 the detail of connection between L profile and two layers is shown.

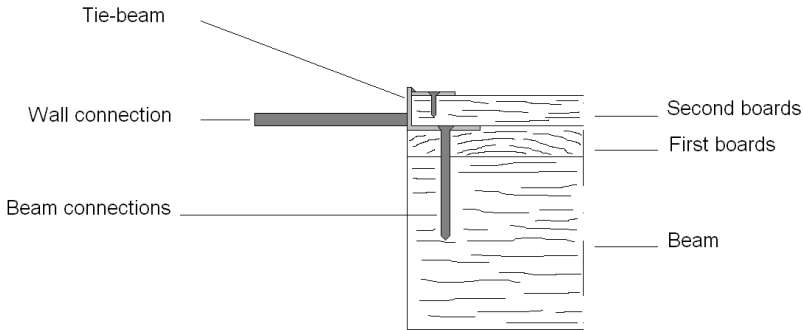


Fig. 55 Detail of tie-beam with L profile

Verifications to be done are the same described for the floor with simple boards. Referring to Fig. 44 we will have to check the boards using the following equation

$$\sigma_{t,0,d} \leq f_{t,0,d} \quad (16)$$

Moreover, it will be necessary to verify connections between layer and main beams determining the strength capacity of fasteners as indicated in Eurocode 5.

$$F'_t = F_{V,Sd} \leq F_{V,Rd} \quad (17)$$

The check on tie-beam will instead be the following.

$$N_{Sd} \leq N_{t,Rd} \quad (18)$$

In the preceding formula N_{Sd} is the maximum tension in the element while $N_{t,Rd}$ is defined in Eurocode 3.

The check of connection with the main beam is carried out with (17).

4.5.3 Compression verification

For this check we do not consider layer presence having grain direction orthogonal to action. The boards with grain parallel to the seismic action must respect the following equation.

$$\sigma_{c,0,d} \leq f_{c,0,d} \quad (19)$$

As regards the tie-beam the check is the following.

$$N_{Sd} \leq N_{c,Rd} \quad (20)$$

4.5.4 Shear and tension verification of floor-wall connections

The load capacity of the floor-wall connections can be determined from experimental tests. Noting the strength, the safety verifications are the following.

$$N_{Sd} \leq N_{t,Rd} \quad (21)$$

$$F_{V,Sd} \leq F_{V,Rd} \quad (22)$$

5. FLOOR REINFORCED WITH STEEL PLATES

5.1 Introduction

The second structural reinforcement hypothesis was completed with the laying of holed steel strips placed at 45° over the existing timber boards. These strips are supplied in rolls and can be cut to size. They are fixed to the boards with screws or nails. On top of this reinforcement another layer can be laid so as to obtain a coplanar surface for laying the finish.



Fig. 56 Floor reinforced with steel plates

5.2 Specimen construction features

5.2.1 Floor dimension 2x1 m

The reinforcement proposed includes laying diagonal strips made up of steel holed strips, placed according to angles of 45 degrees compared to the floor bearing frame direction. The following Fig. 57 documents a plan view of the floor subject to test.

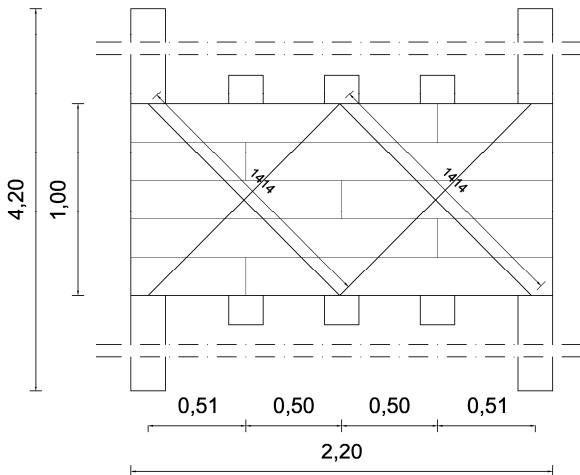


Fig. 57 Floor reinforced with metal plates

The metal strips, as can be noted in Fig. 58, are connected to the lower level using screws $\varnothing 4 \times 40$ mm inserted in the holes strips. The same Fig. 58 shows the overlapping of two metal strips.

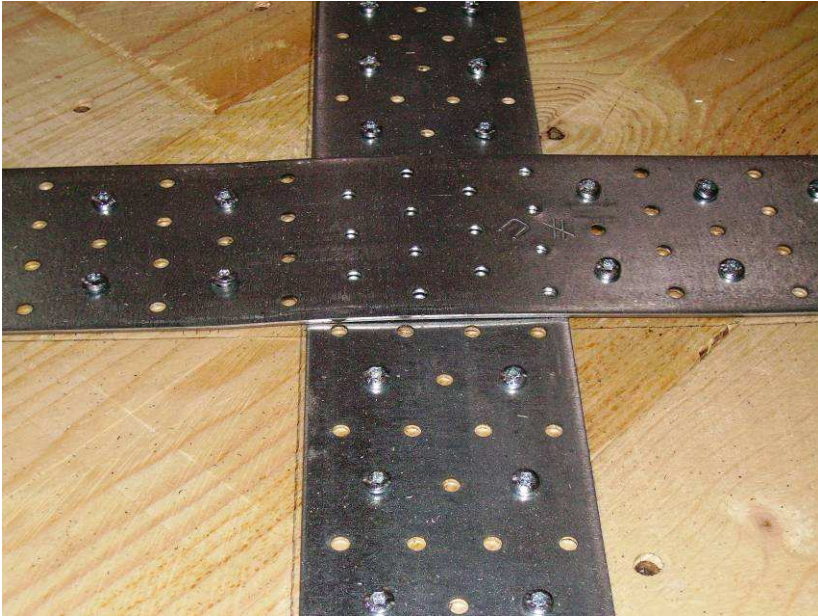


Fig. 58 Detail of strip metal-layer connection

Also in this case it is possible to use an upper timber layer to protect the reinforcement. A second layer for closing allows to limit instability of steel plates when they are subject to compression stress. Experimental tests do not include a second protective layer allowing instability in the metal strips.

5.2.2 Floor dimension 5x4 m

Above the first timber boards metal strips are placed with variable lengths, anchored to the surface with timber screws. In particular, 4 strips of 1550 mm, 4 strips of 2950 mm, 4 strips of 4350 mm and 4 strips of 5550 mm were used.

Fig. 59 shows reinforcement position.

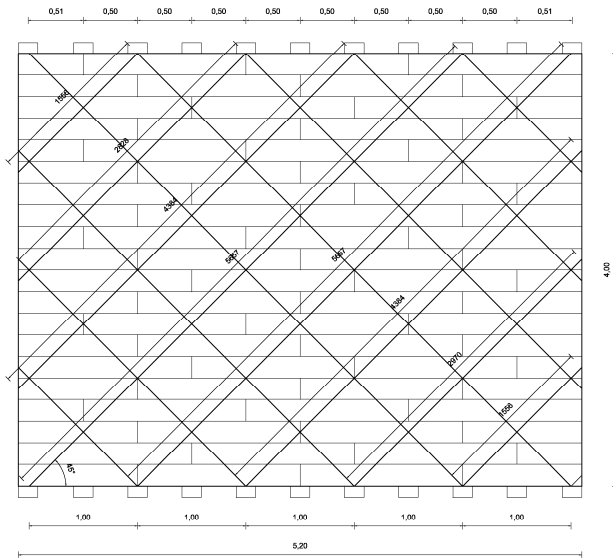


Fig. 59 Detail of laying type of metal strips reinforcement

5.2.3 Summary of construction features and materials

Table 11 Floor characteristics reinforced with steel plates

Beam		Simple boards	
n.	11	n.	80
Material	GL24c	Material	C22
E	11,6 GPa	E	10 GPa
Section	18x18 cm ²	Section	20x3 cm ²
Span	50 cm	Length	60-160 cm
Floor dim.	5,2x4,2 m ²	Total area	5,2x4,2 m ²
Boards connections		4 nails ø2,8x80 mm / beam	
Floor reinforcement - steel plates			
n.	16		
Material	Fe360		
E	210 GPa		
Section	80x2 mm ²		
Length	1,55-5,66 m		
Laying	45°		
Total area	5,2x4,2 m ²		
Connections	50 screws ø5x25 mm / plate		
Tie-beam reinforcement			
Parallel to load	Element dim.	80x5x3860 mm	
	Material	Fe430	
	E	210 GPa	
	Position	external beam	
	Connections	screws ø10x160 / 30 cm	
	Test	monotonic and cyclic test	
Orthogonal to load	Element dim.	75x5x5200 mm	
	Material	Fe430	
	E	210 GPa	
	Position	end of floor	
	Connections	screws ø10x160 / beam	
	Test	cyclic test	

5.3 Floor stiffness

The following figures represent the load-displacement curves coming out of experimental tests. Cases of floors with dimensions of 2x1 m and 5x4 m are especially represented. The latter with and without perimeter tie-beam.

Curves have been obtained from the experiments and from them the envelopes and then experimental stiffness. Stiffness determined from the load-displacement curves has also been documented in Table 12 for completing the picture obtained from numerical analysis.

The stiffness has been determined using procedure described in the EN12512:2006 with reference to load and displacement values relative to 10% and 40% of the maximum force registered. In the following figures the featured points used for determining such stiffness are highlighted.

Table 12 Floor stiffness reinforced with steel plates

Floor type	0,1 F_{max}	$d_{0,1F_{max}}$	0,4 F_{max}	$d_{0,4F_{max}}$	k
	[kN]	[mm]	[kN]	[mm]	[kN/mm]
Test 2x1m - no reinf.	6,51	1,22	26,06	5,81	4,26
Test 5x4m - reinf.	40,48	0,43	161,90	4,22	32,08
Model 2x1m - no reinf.	6,51	0,20	26,06	0,80	32,50
Model 5x4m - reinf.	40,48	0,57	161,90	4,69	29,47
Model 5x4m - no reinf.	40,48	0,92	161,90	8,89	15,24

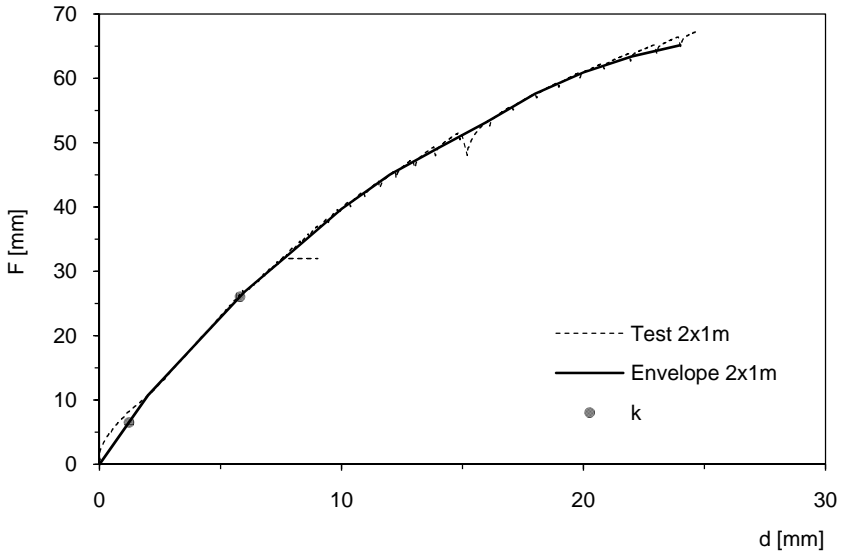


Fig. 60 Load-displacement curve of floor 2x1 m

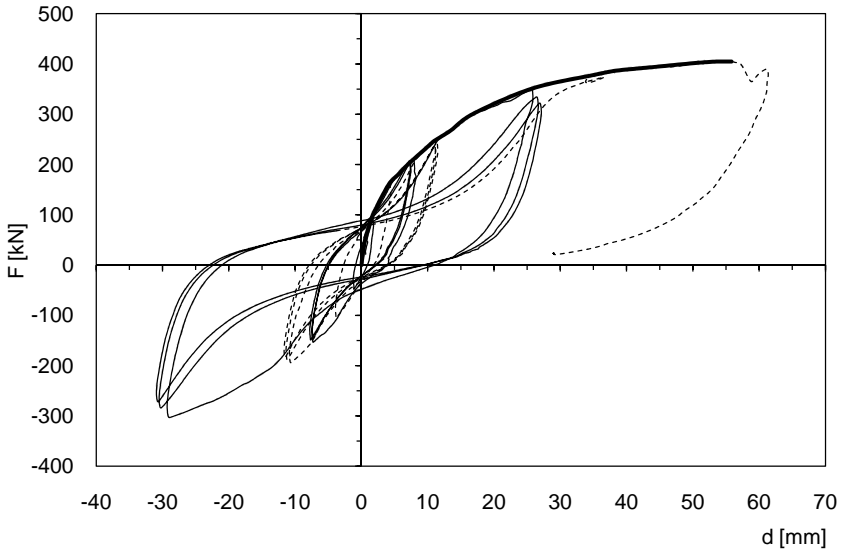


Fig. 61 Load-displacement curve of floor 5x4 m with tie-beam

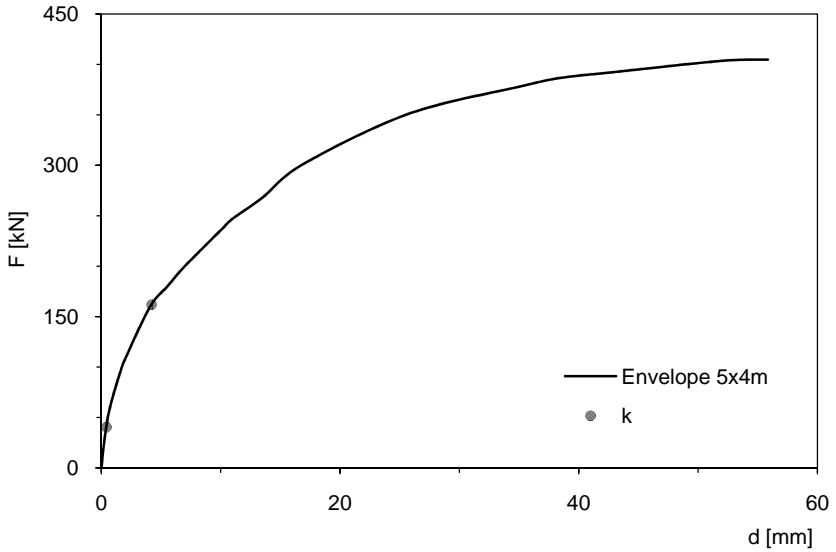


Fig. 62 Envelope load-displacement curve of floor 5x4 m with tie-beam

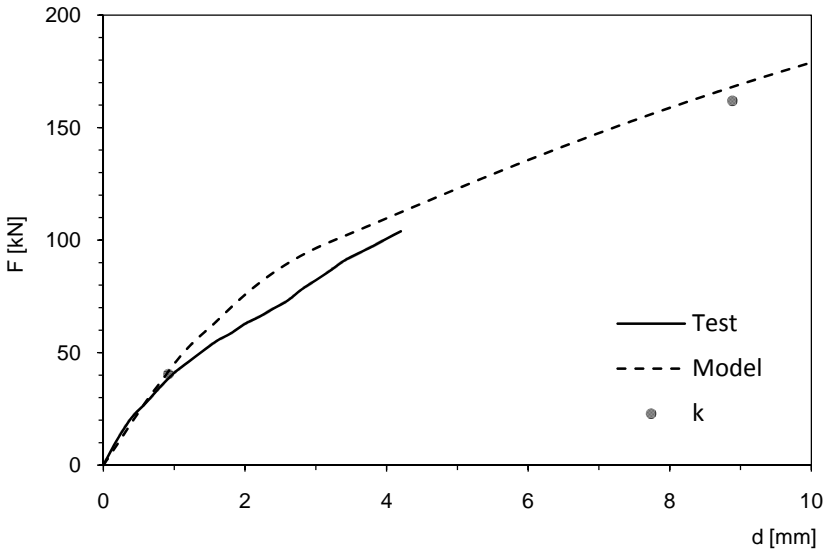


Fig. 63 Load-displacement curve of floor 5x4 m without tie-beam

5.4 Numerical model features

To define floor model it is necessary to determinate the force-displacement characteristic curve of link elements as described in paragraph 2.3.3.

In particular in Table 13 the load-displacement curves are documented related to experimental tests carried out on floors with dimensions of 5x4 m. In Fig. 64 is shown the assigned curve to link elements in the floor modelling case of 2x1 m; the model is the same of Fig. 30 and the characteristic parameters are $n_f=4$ e $n_d=2$.

Table 13 Load-displacement curve experimental test and link element

Test		Link	
d [mm]	F [kN]	d [mm]	F [kN]
-55,84	-404,76	-39,48	-71,55
-35,28	-378,64	-24,94	-66,93
-16,84	-300,60	-11,90	-53,14
-6,63	-195,32	-4,69	-34,53
-1,70	-99,16	-1,20	-17,53
-0,75	-61,00	-0,53	-10,78
-0,34	-34,64	-0,24	-6,12
0,00	0,00	0,00	0,00
0,34	34,64	0,24	6,12
0,75	61,00	0,53	10,78
1,70	99,16	1,20	17,53
6,63	195,32	4,69	34,53
16,84	300,60	11,90	53,14
35,28	378,64	24,94	66,93
55,84	404,76	39,48	71,55

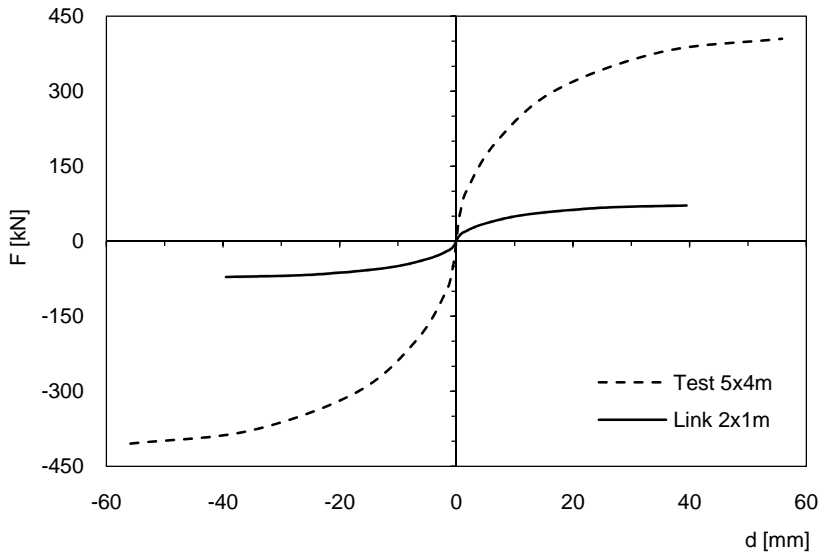


Fig. 64 Load-displacement curve of test and link element

5.5 Strength verification

This type of reinforcement as that with FRP strips includes an almost perfect connection between the timber boards and the diagonal reinforcement system. For this reason seismic action is absorbed, almost exclusively of tension and shear stresses by diagonal reinforcement elements while compression stress by timber boards with grain parallel to action. In the subsequent verifications, for simplicity and favouring safety, the diagonal reinforcement elements are presented schematically by the tension spring hinged at the ends.

5.5.1 Shear verification

For this check we refer to Fig. 65.

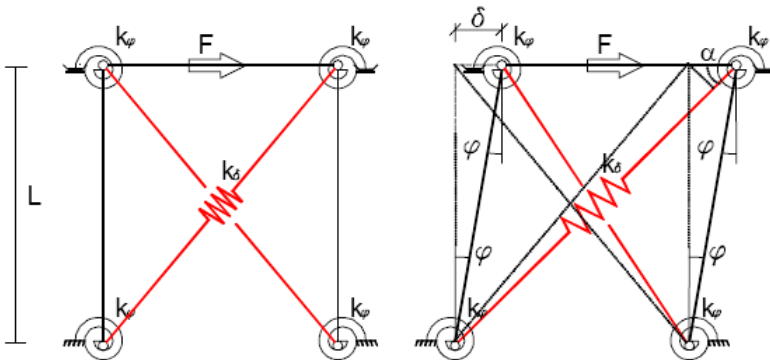


Fig. 65 Calculation model of floor reinforced with diagonal elements – shear

Applying a shear force F induces an action of tension in the diagonal spring.

$$N_{Sd} = F / \cos\alpha \quad (23)$$

The axial strength of diagonal elements can be obtained like this.

$$N_{Rd} = A \cdot f_{yd} \quad (24)$$

The verification is therefore achieved respecting the following equation.

$$N_{Sd} \leq N_{Rd} \quad (25)$$

For equilibrium the tension action of diagonal elements generates a deck compression which has to be absorbed by first timber layer parallel to action. In particular we hypothesise concentrating the compression on one plank. Noting area A_b of each plank the tension stress is the following.

$$\sigma_{c,0,d} = F \cdot \tan\alpha / A_b \quad (26)$$

The safety check is then carried out as indicated in Eurocode 5.

$$\sigma_{c,0,d} \leq f_{c,0,d} \quad (27)$$

5.5.2 Tension verification

Also for the tension check we only consider the strength of diagonal elements. The reference is to Fig. 66.

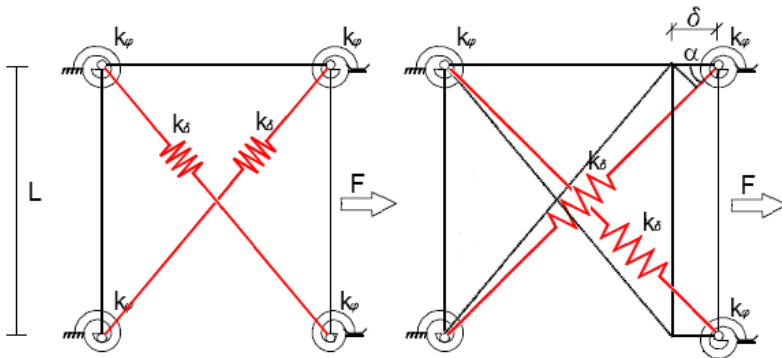


Fig. 66 Calculation model of floor reinforced with diagonal elements – tension

The tension force F induces a tension action in diagonal elements which can be calculated like this.

$$N_{sd} = F / (2 \cdot \cos \alpha) \quad (28)$$

The tension strength of each diagonal element is obtained with (24) while the safety check is completed using (25).

As for the shear verification, also in this case a compression on the deck is generated for equilibrium. Hypothesising, as before, concentrating compression on one plank. The action is calculated with (29) while for the check of strength we use (27).

$$\sigma_{c,0,d} = F \cdot \tan \alpha / (2 \cdot A_b) \quad (29)$$

The presence of tie-beam, needed for guaranteeing anchorage of masonry to floor, imposes a further check of same.

The tension check of element which constitutes the tie-beam is carried out using the Eurocode 3 formulation, with reference to Fig. 45.

$$N_{Sd} \leq N_{t,Rd} \quad (30)$$

In the end one needs to verify the connection of the curb with the main beams by means of (31). The action is obtained by analysis and by referring to Fig. 45.

$$F'_t = F_{V,Sd} \leq F_{V,Rd} \quad (31)$$

5.5.3 Compression verification

In compression diagonal elements are not considered so the check is the same to the one presented for floor with double layer.

The planks parallel to action and the tie-beam subject to compression must be checked with the following equations.

$$\sigma_{c,0,d} \leq f_{c,0,d} \quad (32)$$

$$N_{Sd} \leq N_{c,Rd} \quad (33)$$

5.5.4 Shear and tension verification of floor-wall connections

The load capacity of the floor-wall connections can be determined from experimental tests. Noting the strength, the safety verifications are the following.

$$N_{Sd} \leq N_{t,Rd} \quad (34)$$

$$F_{V,Sd} \leq F_{V,Rd} \quad (35)$$

6. FLOOR REINFORCED WITH FRP STRIPS

6.1 Introduction

The third reinforcement structure hypothesis was completed with laying CFRP strips placed at 45° above the existing timber boards. These strips are also supplied in rolls and can be cut to size. They are fixed with purpose made epoxy glue after the foundation has been prepared to render it flat enough.

Over this reinforcement a further layer can be put to obtain a coplanar surface for the subsequent finishing.



Fig. 67 Floor reinforced with FRP strips

6.2 Specimen construction features

6.2.1 Floor dimension 2x1 m

In this case a special type of reinforcement is foreseen made up of diagonal FRP strips. We are talking about the type of operation already schematically presented in the preceding chapter.

Also in this case the test specimen is obtained starting out from the deck made up of simple timber boards. The following figure documents a plan view of the laying scheme of diagonal reinforcement strips. As can be noted these are placed according to the angle of 45° compared to the horizontal and are glued to the layer under using epoxy glue.

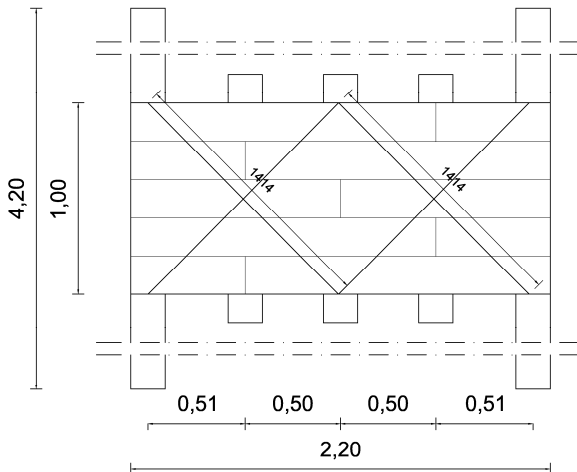


Fig. 68 Floor reinforced with FRP strips

In construction practice, as before illustrated in the course of the previous chapter, the reinforcement constituted by the fibre strips must be protected by laying of a second timber layer. This way of proceeding guarantees against wear of polymeric material during the phases of site work.

Moreover, the second layer allows for further deck rigidity limiting instability of FRP plates even if less than those of strips in metal. In this case the FRP plates are anchored to the layer with epoxy glue, so when there is instability of the FRP strips the in-plan stiffness of floor decrease with or without further upper layers.



Fig. 69 Detail of connection FRP strips-simple layer

6.2.2 Floor dimension 5x4 m

Analogously to description of reinforcement with metal plates, laying of FRP strips is included with variable length, anchored to first timber boards with epoxy glue.

In particular, 4 strips of 1550 mm, 4 strips of 2950 mm, 4 strips of 4350 mm and 4 strips of 5550 mm were used Fig. 70 shows the placing of reinforcement.

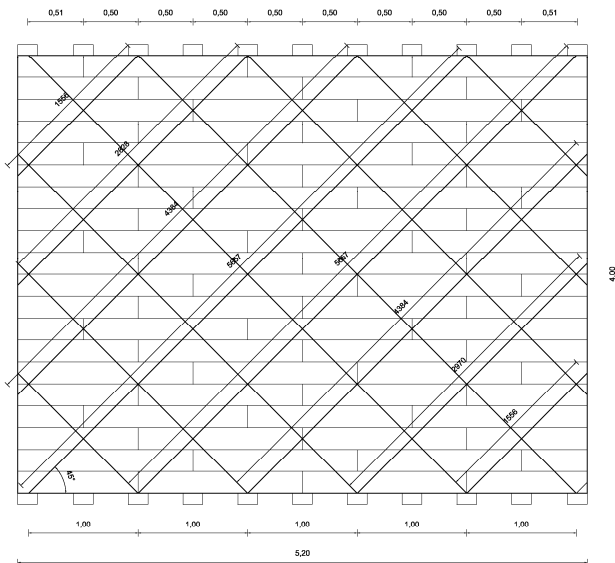


Fig. 70 Detail of laying method of FRP strips

6.2.3 Summary of construction features and materials

Table 14 Floor characteristics reinforced with FRP strips

Beam		Simple boards	
n.	11	n.	80
Material	GL24c	Material	C22
E	11,6 GPa	E	10 GPa
Section	18x18 cm ²	Section	20x3 cm ²
Span	50 cm	Length	60-160 cm
Floor dim.	5,2x4,2 m ²	Total area	5,2x4,2 m ²
Boards connections		4 nails ø2,8x80 mm / beam	
Floor reinforcement - FRP strips			
n.	16		
Material	Mapei Carboplate		
E	250 GPa		
Tension strength	2500 MPa		
Shear strength	79 MPa		
Section	50x1,4 mm ²		
Length	1,55-5,66 m		
Laying	45°		
Total area	5,2x4,2 m ²		
Connections	epoxy glue		
Tie-beam reinforcement			
Parallel to load	Element dim.	80x5x3860 mm	
	Material	Fe430	
	E	210 GPa	
	Position	external beam	
	Connections	screws ø10x160 / 30 cm	
	Test	monotonic and cyclic test	
Orthogonal to load	Element dim.	75x5x5200 mm	
	Material	Fe430	
	E	210 GPa	
	Position	end of floor	
	Connections	screws ø10x160 / beam	
	Test	cyclic test	

6.3 Floor stiffness

The following figures represent the load-displacement curves coming out of experimental tests. Cases of floors with dimensions of 2x1 m and 5x4 m are especially represented. The latter with and without perimeter tie-beam.

Curves have been obtained from the experiments and from them the envelopes and then experimental stiffness. Stiffness determined from the load-displacement curves has also been documented in Table 15 for completing the picture obtained from numerical analysis.

The stiffness has been determined using procedure described in the EN12512:2006 with reference to load and displacement values relative to 10% and 40% of the maximum force registered. In the following figures the featured points used for determining such stiffness are highlighted.

Table 15 Floor stiffness reinforced with FRP strips

Floor type	0,1 F_{max}	$d_{0,1F_{max}}$	0,4 F_{max}	$d_{0,4F_{max}}$	k
	[kN]	[mm]	[kN]	[mm]	[kN/mm]
Test 2x1m - no reinf.	3,32	0,09	13,30	0,52	23,18
Test 5x4m - reinf.	29,06	0,16	116,24	1,74	54,95
Model 2x1m - no reinf.	3,32	0,03	13,30	0,13	102,80
Model 5x4m - reinf.	29,06	0,20	116,24	1,87	52,29
Model 5x4m - no reinf.	29,06	0,32	116,24	3,33	28,98

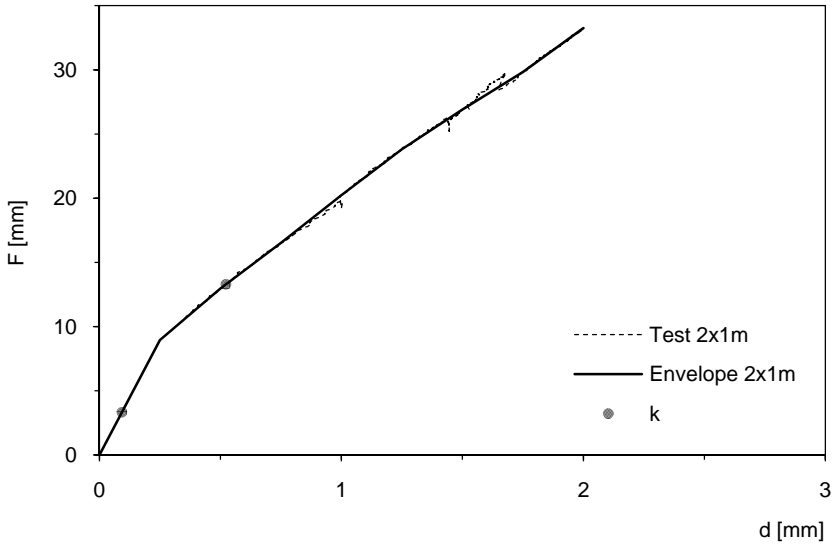


Fig. 71 Load-displacement curve of floor 2x1 m

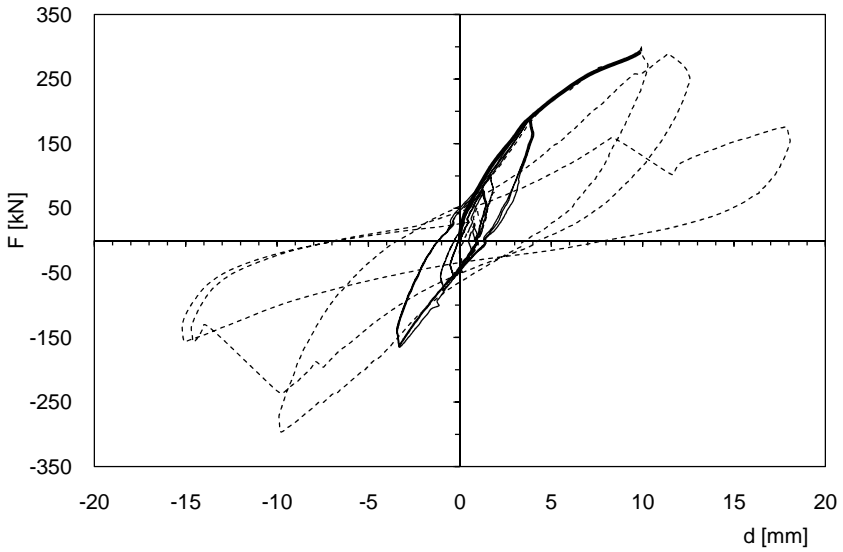


Fig. 72 Load-displacement curve of floor 5x4m with tie-beam

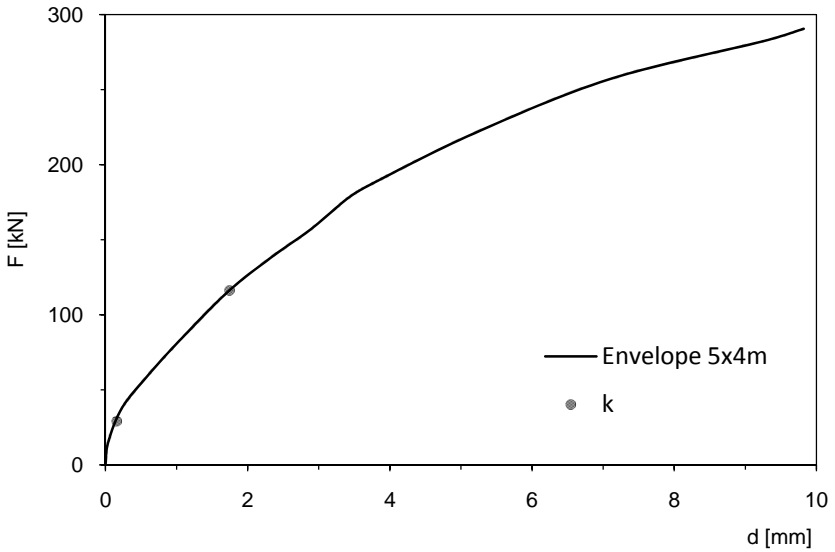


Fig. 73 Envelope load-displacement curve of floor 5x4m with tie-beam

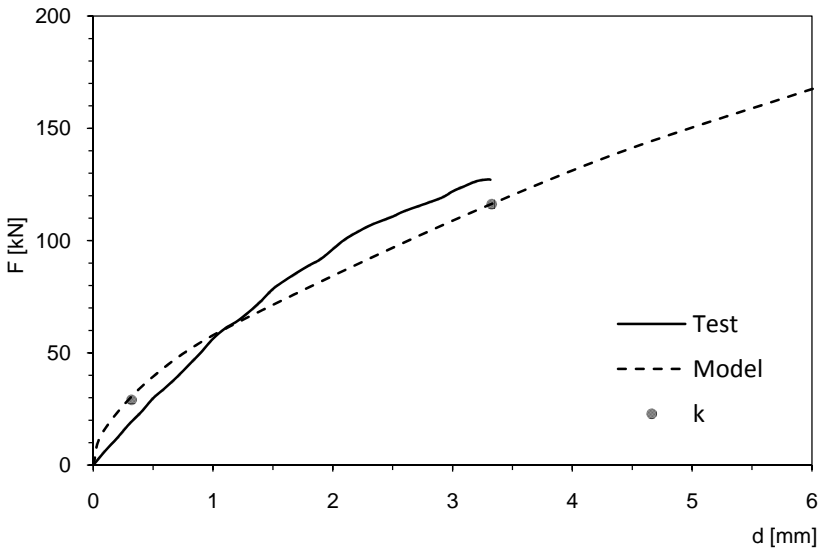


Fig. 74 Load-displacement curve of floor 5x4m without tie-beam

6.4 Numerical model features

To define floor model it is necessary to determinate the force-displacement characteristic curve of link elements as described in paragraph 2.3.3.

In particular in Table 16 the load-displacement curves are documented related to experimental tests carried out on floors with dimensions of 5x4 m. In Fig. 75 is shown the assigned curve to link elements in the floor modelling case of 2x1 m; the model is the same of Fig. 30 and the characteristic parameters are $n_f=4$ e $n_d=2$.

Table 16 Load-displacement curve experimental test and link element

Test		Link	
d [mm]	F [kN]	d [mm]	F [kN]
-9,82	-290,60	-6,94	-51,37
-5,19	-221,04	-3,67	-39,07
-2,88	-156,88	-2,04	-27,73
-1,72	-115,48	-1,22	-20,41
-0,62	-60,68	-0,44	-10,73
-0,24	-38,24	-0,17	-6,76
-0,04	-15,16	-0,03	-2,68
0,00	0,00	0,00	0,00
0,04	15,16	0,03	2,68
0,24	38,24	0,17	6,76
0,62	60,68	0,44	10,73
1,72	115,48	1,22	20,41
2,88	156,88	2,04	27,73
5,19	221,04	3,67	39,07
9,82	290,60	6,94	51,37

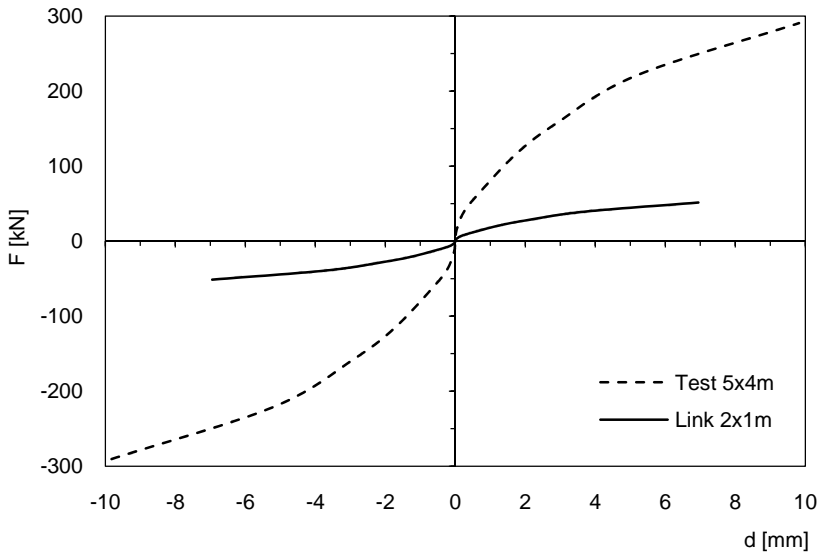


Fig. 75 Load-displacement curve of test and link element

6.5 Strength verification

The strength tests for this layer are the same presented in paragraph 5.5. This is related to the metal plate solution to which reference is advised.

7. FLOOR REINFORCED WITH PLYWOOD PANELS

7.1 Introduction

The fourth hypothesis for structural reinforcement includes laying three staggered plywood layers on the existing timber boards each having 21 mm of thickness.

This technique allows increase both in-plane stiffness and out of plane load-carrying capacity. The reduced size of plywood elements allow to use this technique for floors with different plan dimensions.

The plywood panels are glued to the first timber boards and also one to another with polyurethane glue and timber screws. Moreover, laying with threaded bars is foreseen injected with epoxy glue for completing the beam-deck connection.



Fig. 76 Floor reinforced with plywood panels

7.2 Specimen construction features

7.2.1 Floor dimension 2x1 m

As in the previously illustrated cases, the test specimen is obtained placing a package made up of three layers of plywood panels on to the first timber boards. Each panel is 220x110x2,1 cm. The following Fig. 77 documents a view in plan of floor at the final laying in plywood.

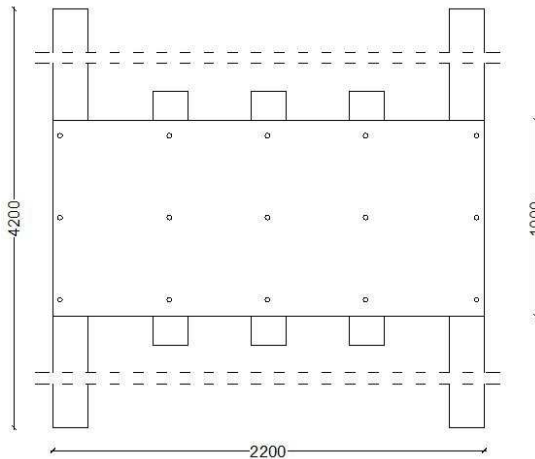


Fig. 77 View in plan of floor following laying of last plywood layer

All the plywood layers are glued to each other with polyurethane glue and are also glued to the first timber boards. The beam-deck connection are completed with threaded bars $\phi 10$ and length 150 mm, laid with span of 30 cm.

Fig. 78 represents the section of beam-deck connection.

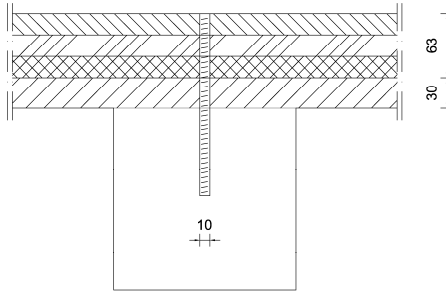


Fig. 78 Section view of connection between first timber boards and plywood panels

7.2.2 Floor dimension 5x4 m

For this type of specimen, as illustrated in the following Fig. 79, three layers of plywood of differing dimensions and 21 mm thickness have been used placed with staggered joints and glued one to another with polyurethane glue.

The beam-deck connectors were placed at span of 30 cm in correspondence to the beam ends while there was a span of 20 cm in the remaining part.

7.2.3 Summary of construction features and materials

Table 17 Floor characteristics reinforced with plywood panels

Beam		Simple boards	
n.	11	n.	80
Material	GL24c	Material	C22
E	11,6 GPa	E	10 GPa
Section	18x18 cm ²	Section	20x3 cm ²
Span	50 cm	Length	60-160 cm
Floor dim.	5,2x4,2 m ²	Total area	5,2x4,2 m ²
Boards connections		4 nails ø2,8x80 mm / beam	
Floor reinforcement - plywood panels			
n. layers		3	
Material		plywood (7 layers of spruce)	
Et,0		6,7 GPa	
Et,90		5,3 GPa	
Section		n. 3 x 21 mm	
Total area		5,2x4,2 m ²	
Connections		polyurethane glue	
		bars Fe360 ø10x150 mm / 20-30 cm	
Tie-beam reinforcement			
Parallel to load	Element dim.	80x5x3860 mm	
	Material	Fe430	
	E	210 GPa	
	Position	external beam	
	Connections	screws ø10x160 / 30 cm	
	Test	monotonic and cyclic test	
Orthogonal to load	Element dim.	75x5x5200 mm	
	Material	Fe430	
	E	210 GPa	
	Position	end of floor	
	Connections	screws ø10x160 / beam	
	Test	cyclic test	

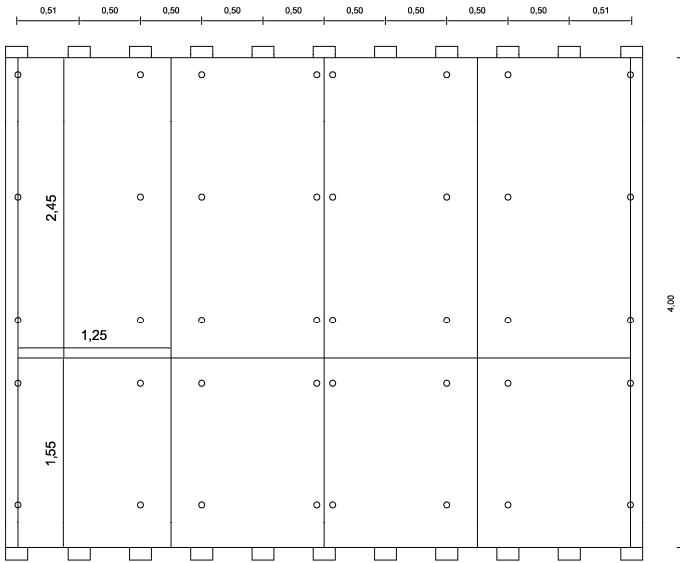


Fig. 79 In-plan view of last layer of plywood panel

7.3 Floor stiffness

The following figures represent the load-displacement curves coming out of experimental tests. Cases of floors with dimensions of 2x1 m and 5x4 m are especially represented. The latter with and without perimeter tie-beam.

Curves have been obtained from the experiments and from them the envelopes and then experimental stiffness. Stiffness determined from the load-displacement curves has also been documented in Table 18 for completing the picture obtained from numerical analysis.

The stiffness has been determined using procedure described in the EN12512:2006 with reference to load and displacement values relative to 10% and 40% of the maximum force registered. In the following figures the featured points used for determining such stiffness are highlighted.

Table 18 Floor stiffness reinforced with plywood panels

Floor type	0,1 F_{max}	$d_{0,1F_{max}}$	0,4 F_{max}	$d_{0,4F_{max}}$	k
	[kN]	[mm]	[kN]	[mm]	[kN/mm]
Test 2x1m - no reinf.	-	-	-	-	-
Test 5x4m - reinf.	30,48	0,11	121,92	0,74	144,01
Model 2x1m - no reinf.	11,13	0,13	44,51	0,55	79,21
Model 5x4m - reinf.	30,48	0,17	121,92	0,98	114,03
Model 5x4m - no reinf.	30,48	0,24	121,92	1,51	71,81

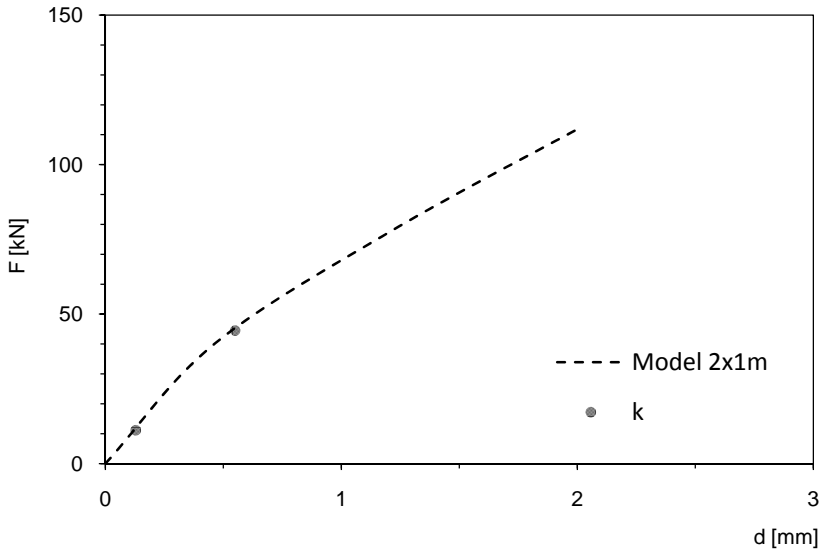


Fig. 80 Load-displacement curve of floor 2x1m

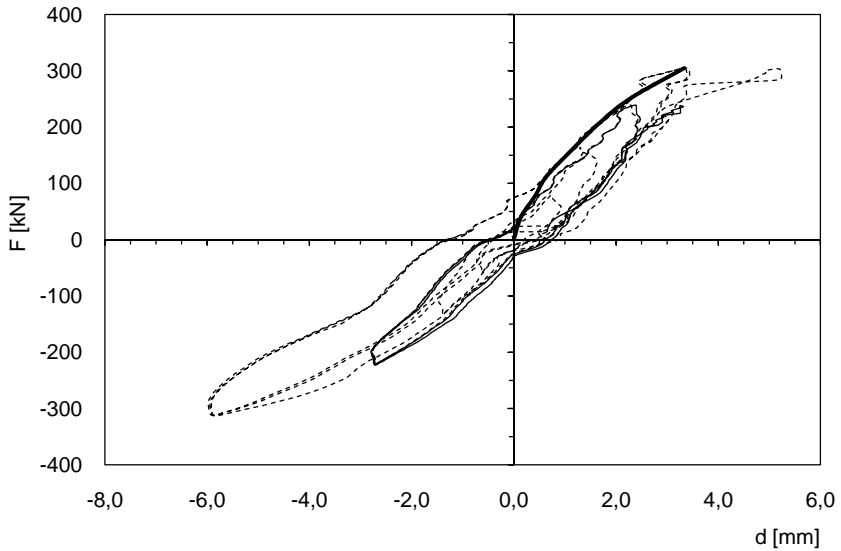


Fig. 81 Load-displacement curve of floor 5x4m with tie-beam

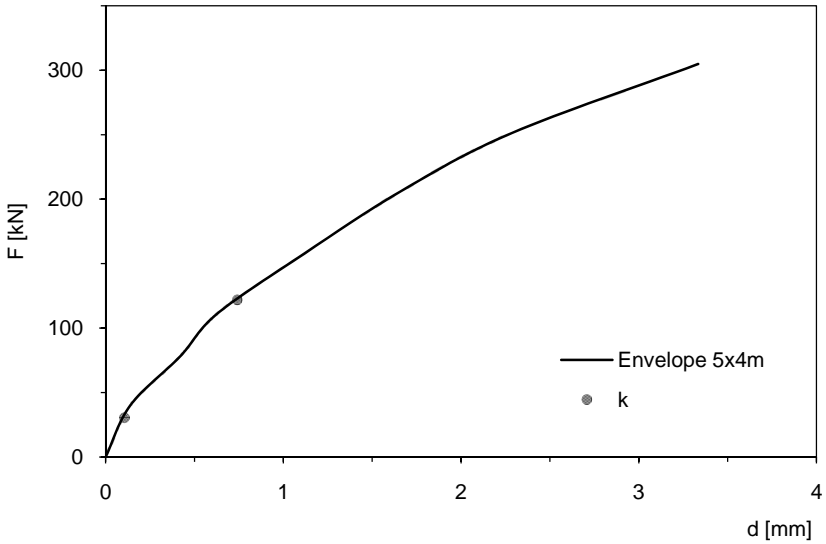


Fig. 82 Envelope load-displacement curve of floor 5x4m with tie-beam

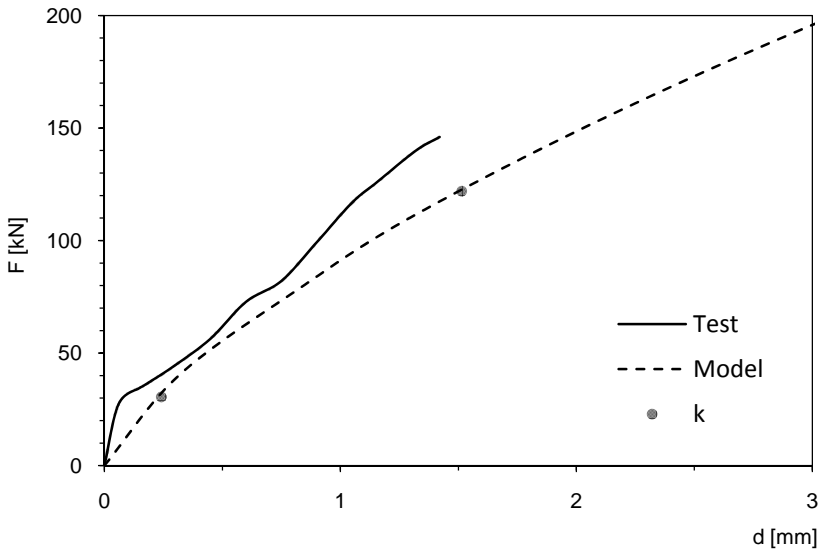


Fig. 83 Load-displacement curve of floor 5x4m without tie-beam

7.4 Numerical model features

To define floor model it is necessary to determinate the force-displacement characteristic curve of link elements as described in paragraph 2.3.3.

In particular in Table 19 the load-displacement curves are documented related to experimental tests carried out on floors with dimensions of 5x4 m. In Fig. 84 is shown the assigned curve to link elements in the floor modelling case of 2x1 m; the model is the same of Fig. 30 and the characteristic parameters are $n_f=4$ e $n_d=2$.

Table 19 Load-displacement curve experimental test and link element

Test		Link	
d [mm]	F [kN]	d [mm]	F [kN]
-3,33	-304,80	-2,36	-53,88
-2,29	-251,32	-1,62	-44,43
-1,66	-205,96	-1,17	-36,41
-1,12	-157,88	-0,79	-27,91
-0,63	-111,28	-0,44	-19,67
-0,42	-78,16	-0,30	-13,82
-0,14	-40,28	-0,10	-7,12
0,00	0,00	0,00	0,00
0,14	40,28	0,10	7,12
0,42	78,16	0,30	13,82
0,63	111,28	0,44	19,67
1,12	157,88	0,79	27,91
1,66	205,96	1,17	36,41
2,29	251,32	1,62	44,43
3,33	304,80	2,36	53,88

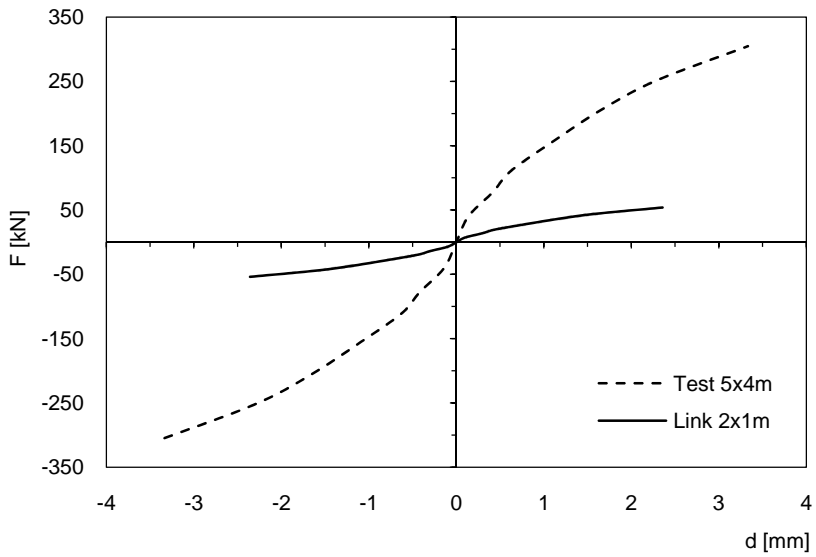


Fig. 84 Load-displacement curve of test and link element

7.5 Strength verification

Given the presence of three layers of plywood glued one to another, we hypothesise that seismic action is absorbed exclusively by the plywood, not considering the first timber layer.

7.5.1 Shear, tension and compression verification

Being the resisting element made of only plywood, noting the design strength we proceed to verify strength as indicated in Eurocode 5. The following equations will be checked.

$$\tau_d \leq f_{v,d} \quad (36)$$

$$\sigma_{t,0,d} \leq f_{t,0,d} \quad (37)$$

$$\sigma_{c,0,d} \leq f_{c,0,d} \quad (38)$$

The safety verifications in tension and compression of tie-beam are the following.

$$N_{Sd} \leq N_{t,Rd} \quad (39)$$

$$N_{Sd} \leq N_{c,Rd} \quad (40)$$

Moreover, it is necessary to verify connection of the tie-beam with the main beams.

$$F'_t = F_{V,Sd} \leq F_{V,Rd} \quad (41)$$

7.5.2 *Shear and tension verification of floor-wall connections*

The load capacity of the floor-wall connections can be determined from experimental tests. Noting the strength, the safety verifications are the following.

$$N_{Sd} \leq N_{t,Rd} \quad (42)$$

$$F_{V,Sd} \leq F_{V,Rd} \quad (43)$$

8. FLOOR REINFORCED WITH CONCRETE SLAB

8.1 Introduction

The fifth hypothesis of structural reinforcement is a concrete slab of 5 cm thickness built on the wood planks. The slab reinforcement is composed by welded steel mesh and perimeter bars that define tie-beam. The connections between the timber beam and the concrete slab is obtained by means of L shape connectors.



Fig. 85 Floor reinforced with concrete slab

8.2 Specimen construction features

8.2.1 Floor dimension 2x1 m

The last type of specimen is composed by concrete slab of 5 cm thickness connected to timber beam. These connections are obtained by means of L shape connector made up of reinforced bars $\phi = 14$ mm, $L = 200$ mm. Before concrete laying the connectors must be inserted inside holes done on the bearing beams and injected with epoxy glue. Connectors span is the same that previously illustrated in Paragraph 7.2.1.

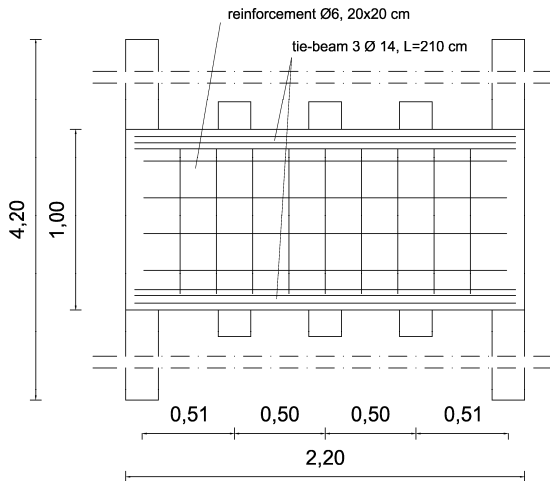


Fig. 86 Detail of reinforcement used in concrete slab

The test specimen is provided with a reinforcement made up of a welded steel mesh $\phi 6$ mesh 20x20 cm and 3 reinforced bars $\phi 14$ of 2 m length which constitute the tie-beam Fig. 86 documents the detail relative to the reinforcement used.

The following Fig. 87 shows the preparation of specimen before the concrete laying. You can see the connectors of the composed slab, the welded steel mesh and the tie-beam reinforced bars.



Fig. 87 Specimen view in the reinforced laying phase

8.2.2 Floor dimension 5x4 m

This specimen is wholly analogous to the one described in the previous Paragraph. For this type of floor purpose made hooks to be used the specimen movement in laboratory have been provided. To this end, 8 threaded bars M24 have been foreseen glued with epoxy resin to be inserted in the bearing beams. For the correct distribution of seismic action on the floor during moving operations of the specimen, the hooks were placed at a span reciprocal of 1 m. The following Fig. 88 documents the detail of the system of hooking described. We also note

the auxiliary hooks, laying in the slab, used in operations of dismantling of specimen at the end of the test.



Fig. 88 Detail of moving system of specimen

8.2.3 Summary of construction features and materials

Table 20 Floor characteristics reinforced with concrete slab.

Beam		Simple boards	
n.	11	n.	80
Material	GL24c	Material	C22
E	11,6 GPa	E	10 GPa
Section	18x18 cm ²	Section	20x3 cm ²
Span	50 cm	Length	60-160 cm
Floor dim.	5,2x4,2 m ²	Total area	5,2x4,2 m ²
Boards connections		4 nails \varnothing 2,8x80 mm / beam	
Floor reinforcement - concrete slab			
Layers		3	
Material		Rck 30	
E		30 GPa	
Thickness		5 cm	
Total area		5,2x4,2 m ²	
Connections		bars B450C \varnothing 14 / 20-30 cm	
Distribute reinforcement		B450C \varnothing 6, 20x20 cm	
Tie-beam reinforcement			
Parallel to load	Element dim.	3 \varnothing 14	
	Material	B450C	
	Position	external beam	
	Test	monotonic and cyclic test	
Orthogonal to load	Element dim.	3 \varnothing 14	
	Material	B450C	
	Position	end of floor	
	Test	monotonic and cyclic test	

8.3 Floor stiffness

The following figures represent the load-displacement curves coming out of experimental tests. Cases of floors with dimensions of 2x1 m and 5x4 m are especially represented. The latter with and without perimeter tie-beam.

Curves have been obtained from the experiments and from them the envelopes and then experimental stiffness. Stiffness determined from the load-displacement curves has also been documented in Table 21 for completing the picture obtained from numerical analysis.

The stiffness has been determined using procedure described in the EN12512:2006 with reference to load and displacement values relative to 10% and 40% of the maximum force registered. In the following figures the featured points used for determining such stiffness are highlighted.

Table 21 Floor stiffness reinforced with concrete slab

Floor type	0,1 F_{max}	$d_{0,1Fmax}$	0,4 F_{max}	$d_{0,4Fmax}$	k
	[kN]	[mm]	[kN]	[mm]	[kN/mm]
Test 2x1m - no reinf.	-	-	-	-	-
Test 5x4m - reinf.	37,85	0,24	151,39	1,80	72,69
Model 2x1m - no reinf.	8,90	0,11	35,60	0,63	51,81
Model 5x4m - reinf.	37,85	0,31	151,39	2,18	60,80
Model 5x4m - no reinf.	37,85	0,49	151,39	3,64	36,08

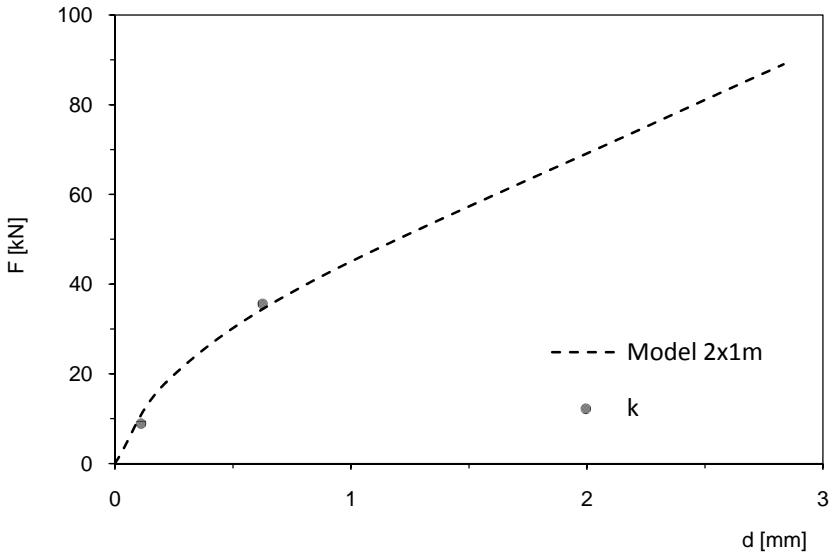


Fig. 89 Load-displacement curve of floor 2x1m

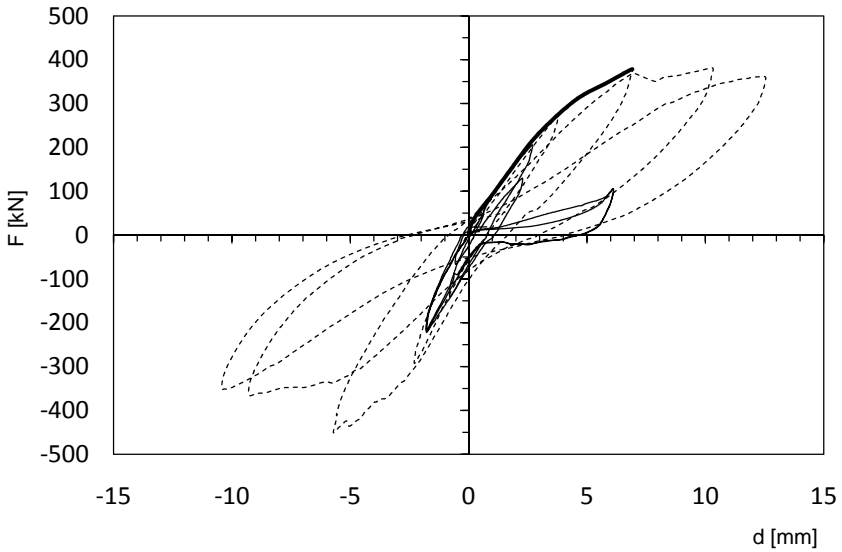


Fig. 90 Load-displacement curve of floor 5x4m with tie-beam

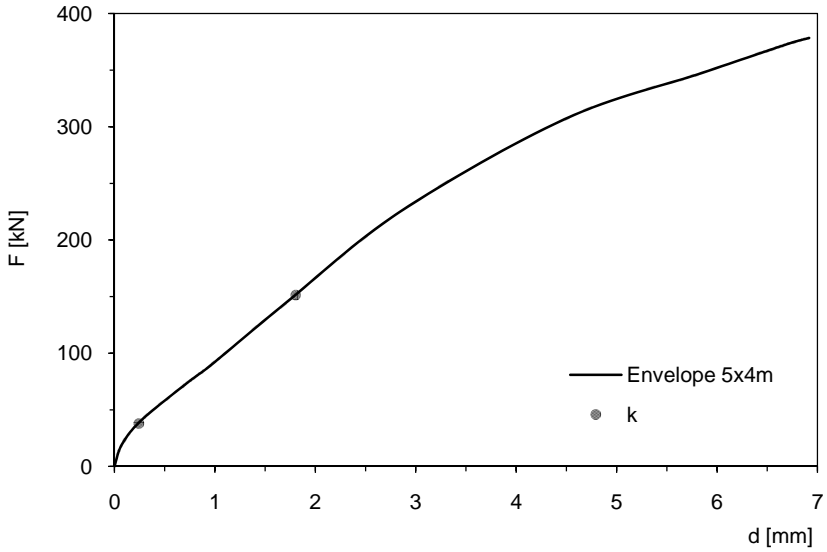


Fig. 91 Envelope load-displacement curve of floor 5x4m with tie-beam

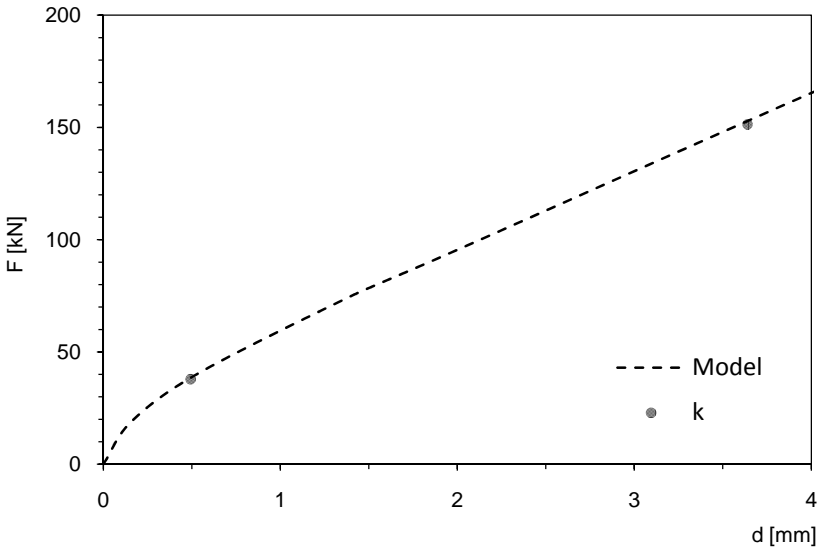


Fig. 92 Load-displacement curve of floor 5x4m without tie-beam

8.4 Numerical model features

To define floor model it is necessary to determinate the force-displacement characteristic curve of link elements as described in paragraph 2.3.3.

In particular in Table 22 the load-displacement curves are documented related to experimental tests carried out on floors with dimensions of 5x4 m. In Fig. 93 is shown the assigned curve to link elements in the floor modelling case of 2x1 m; the model is the same of Fig. 30 and the characteristic parameters are $n_f=4$ e $n_d=2$.

Table 22 Load-displacement curve experimental test and link element

Test		Link	
d [mm]	F [kN]	d [mm]	F [kN]
-6,92	-378,48	-4,89	-66,91
-4,48	-306,72	-3,17	-54,22
-2,85	-225,00	-2,01	-39,77
-0,96	-89,00	-0,68	-15,73
-0,75	-75,56	-0,53	-13,36
-0,27	-41,08	-0,19	-7,26
-0,07	-19,24	-0,05	-3,40
0,00	0,00	0,00	0,00
0,07	19,24	0,05	3,40
0,27	41,08	0,19	7,26
0,75	75,56	0,53	13,36
0,96	89,00	0,68	15,73
2,85	225,00	2,01	39,77
4,48	306,72	3,17	54,22
6,92	378,48	4,89	66,91

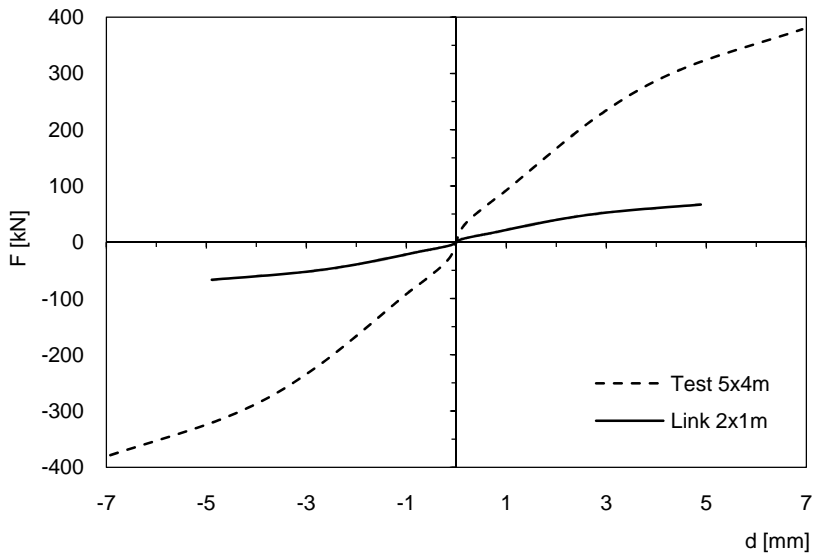


Fig. 93 Load-displacement curve of test and link element

8.5 Strength verification

Also in this case the verifications only refer to the concrete slab and to the connection of same with perimeter walls.

8.5.1 Shear verification

Taking the concrete slab as infinitely rigid, we consider the formation of a strength system made of compressed chords of concrete and tension curb of slab reinforcement.

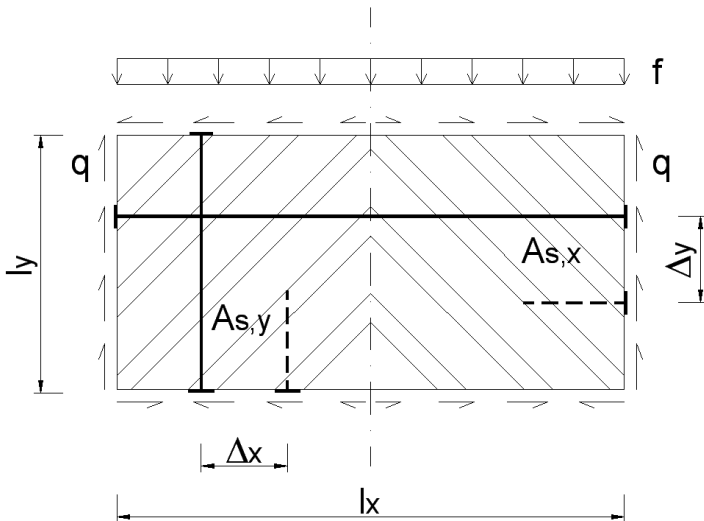


Fig. 94 Strength system to shear action

Fig. 94 shows the distribution of shear forces and the definition of strength system.

Equilibrium must be guaranteed at each node of this strength system. Fig. 95 illustrates the detail of node and the forces in play.

Noting the maximum shear force F_v it is necessary to check the chord of concrete in compression and the steel bar in tension. The inclination angle of the chord and its length depend on values of Δ_x and Δ_y that are the span between steel bars.

The resistant system just described must have efficient anchorage of the steel bar. In general, since the reinforcement is made of welded steel mesh, there are steel bar which connect the mesh to the curb or directly to the masonry.

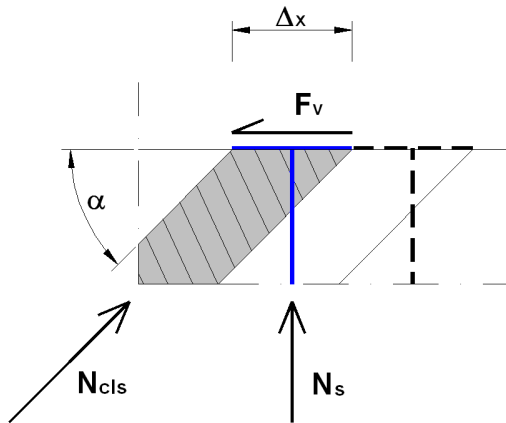


Fig. 95 Node of strength system to the shear action

The compression force of the chord is obtained with (44) while the safety check is (45).

$$N_{cls} = F_v / \cos \alpha \quad (44)$$

$$N_{cls} \leq f_{cd} \cdot \Delta_x \cdot \sin \alpha \cdot s \quad (45)$$

In (45), f_{cd} is the design compression strength of concrete while s is the thickness of slab.

Analogously the tension force of the steel bar and the relative safety check are carried out with (46) and (47).

$$N_s = F_Y \cdot \tan\alpha \quad (46)$$

$$N_s \leq f_{sd} \cdot A_{s,y} \quad (47)$$

As was done for the bars in vertical direction, if Δx differs from Δy , analogous verifications will have to be carried out for horizontal reinforced bars.

To guarantee a ductile behaviour it is necessary to ensure the yield of steel before concrete crush, and so it is necessary to verify the following equation.

$$\rho_{s,y} = A_{s,y}/\Delta_x s < f_{cd} \cdot \sin^2\alpha / f_{sd} \quad (48)$$

If Δx is different from Δy for the reinforcements in x direction there will have to be the following equation.

$$\rho_{s,x} = A_{s,x}/\Delta_x s < f_{cd} \cdot \sin^2\alpha / f_{sd} \quad (49)$$

In (48) and (49) $\rho_{s,y}$ and $\rho_{s,x}$ represent the shear relationships of reinforcement, respectively in y and x direction.

8.5.2 Tension verification

Subsequent to the seismic action we hypothesise that the concrete is cracked and so not able to develop any tension strength.

The tension at mid span to floor must be absorbed by purpose made reinforcements with ties near the edges and then by spreading reinforcement, added to that necessary to shear stresses.

Even though the curbs are inside the slab, they are separately modelled. In this way their tension verification is immediate as follows.

$$N_{t,Sd} \leq f_{sd} \cdot A_{s,c} \quad (50)$$

Noting span Δ_y of the added reinforcements and the tension in the slab $f_{t,Sd}$, the safety check is the following.

$$f_{t,Sd} \cdot \Delta_y \cdot s \leq f_{sd} \cdot A_{s,p} \quad (51)$$

8.5.3 Compression verification

The strengthening element in the compressed zone of floor is made up of concrete slab. The proposed check directly uses compression stress obtained from analysis with design compression strength of concrete.

$$\sigma_{c,Sd} \leq f_{cd} \quad (52)$$

The presence of tie-beam also in the compressed zone allows us to carry out its compression check. In reality this check is surely verified and only shows the compression in the bars that make up the tie.

$$N_{Sd} \leq N_{c,Rd} \quad (53)$$

8.5.4 Shear and tension verification of floor-wall connections

The difference compared to other types of floor refer to laying of these connections. In this case, in fact, the connection bars are inside of concrete slab for a length equal to the anchorage length.

The load capacity of the floor-wall connections can be determined from experimental tests. Noting the strength, the safety verifications are the following.

$$N_{Sd} \leq N_{t,Rd} \quad (54)$$

$$F_{V,Sd} \leq F_{V,Rd} \quad (55)$$

9. THE NUMERICAL EXAMPLE

9.1 Introduction

chapter the study of a numerical simulation is set out which was carried out on a building of three floors with plan dimensions of 14x8 m. The aim is to analyse behaviour of a whole building subject to seismic action, and investigate the influence on it of differing types of floor.

The entire building was modelled, including the masonry walls and timber floors with floor-wall connections, as previously described.

Analysis carried out included two for each type of floor. The first had tie-beam and the second was without.

The building was loaded applying design vertical loads and horizontal static forces equivalent to the seismic action. Such forces were applied at the level of each floor, uniformly distributed on the floor and perimeter wall. The distribution of the forces uses the equation (7.3.6) of D.M. 14/02/08 and subsequent modifications foreseen for a static linear analysis. This distribution is more onerous with regards to a proportional distribution to seismic masses.

Four different peak ground accelerations were considered and in detail they were 0,05g, 0,15g, 0,25g, 0,35g.

The building geometry is that studied by Gattesco (Gattesco et al., 2008) for a special type of reinforcement of timber floor therefore is possible to comparison of results obtained.

9.2 The geometry

The building modelled has plan dimensions of 14x8 m and is 8 m high. It develops on two levels, the first placed at 3 m height, the second at 6 m and the last completes the building roof at 8 m height.

The walls are not symmetric and have windows with different dimensions which are 150x225 cm, 100x175 cm, 100x125 cm and 100x75 cm.

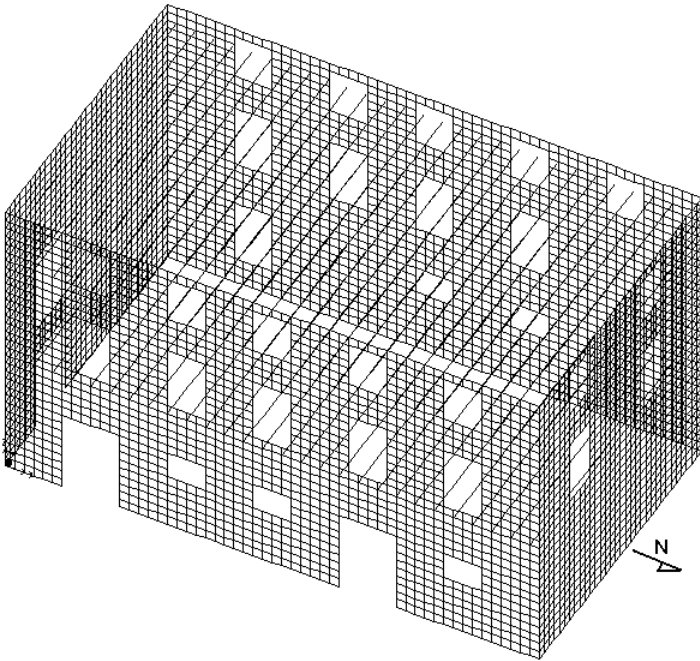


Fig. 96 Model of the entire building

9.3 The model

The masonry building walls were hypothesised with 40 cm thickness and modelled with bi-dimensional shell elements with four nodes. The mesh used has a characteristic dimensions in the two main directions of 25 cm. To model the masonry an orthotropic material was used with normal elastic module $E=1500$ MPa, shear module $G=600$ MPa and specific weight of 20 kN/m^3 .

The floors were modelled as described in Chapter 2, as with perimeter tie-beam.

As regards the floor-masonry connections, they were modelled on the basis of a shear and tension experimental test campaign (Giuriani, 2005). The compression behaviour of such connections was infinitely rigid hypothesised.

Table 23 Floor-masonry connections

Tension - Compression		Shear	
[mm]	[kN]	[mm]	[kN]
-3,00	-100,00	-10,00	-20,11
-0,10	-100,00	-1,29	-20,11
0,00	0,00	0,00	0,00
1,15	29,77	1,29	20,11
3,44	45,24	10,00	20,11

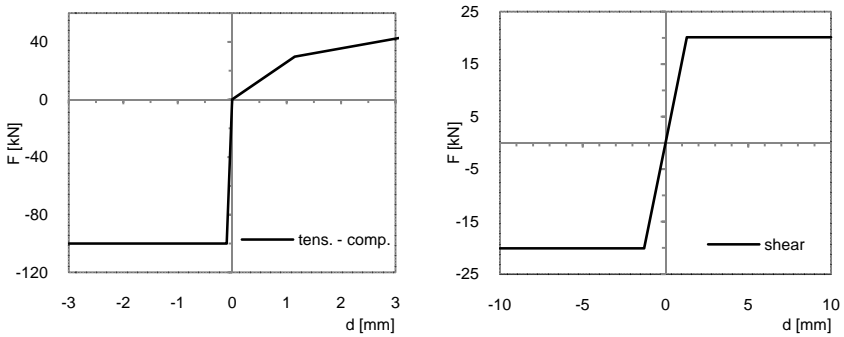


Fig. 97 Load-displacement diagram of floor-masonry connections

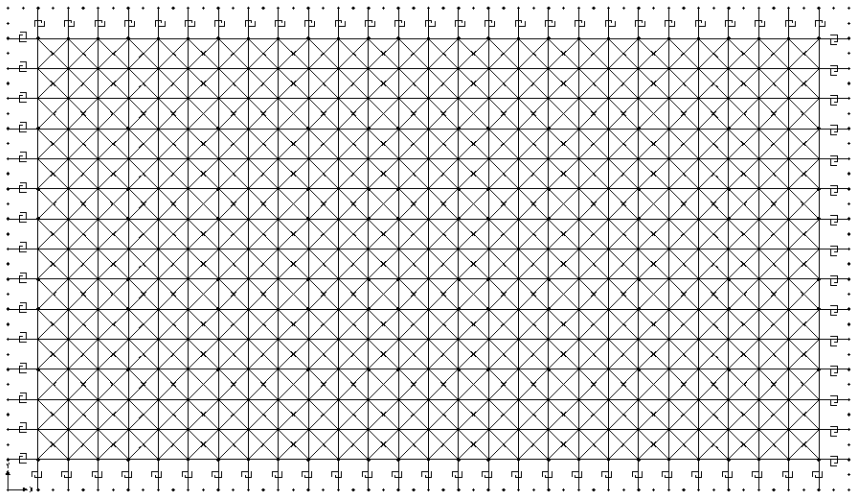


Fig. 98 Numerical floor model with floor-masonry connections

Analogously to the floor modelling, the floor-masonry connection was done using link elements of elastic-plastic behaviour of the “MultiLinear Plastic” kind.

To such elements the load-displacement curves were assigned represented in Fig. 97. Each of these elements is able to transfer tension, compression and shear forces.

In the numerical modelling there is a gap between floor and perimeter walls and they are connected by floor-masonry connection as shown in Fig. 98.

This modelling allows for entire representation of the building defining uniquely the load-displacement curves of floor and of floor-masonry connections to be assigned to respective link elements. The model can be loaded both with gravitational loads and seismic forces.

9.4 Analysis

The type of analysis applied is the lateral force method. It is function of the storey masses and their heights above the level of application of the seismic action. Noting the gravitational loads and self weights of each building elements the lateral forces are determined using the following equation.

$$F_i = F_h \cdot z_i \cdot W_i / \sum_j z_j W_j \quad (56)$$

In the preceding equation F_h represents the seismic base shear force, z_i the height of each storey and W_i the weight of each storey. The weights W_i include floor loads and weight of perimeter walls which act directly at level of storey under consideration.

Noting the force F_i to be applied to the height of each storey, these have been proportionally subdivided between floor and perimeter walls, so uniformly distributed on single floor and wall element.

This distribution of forces is more onerous with regard to proportional distribution to seismic weights. The forces were determined for peak ground accelerations equal to 0,05g, 0,15g, 0,25g, 0,35g and using a behaviour factor $q = 2,7$ considering the case of ordinary masonry structure of two or more storey, irregular in height.

Table 24 Load system of numerical model

LOAD							
First floor	[kN/m ²]	Second floor	[kN/m ²]	Third floor	[kN/m ²]	Walls	[kN/m ²]
Gk	3,4	Gk	3,4	Gk	1,9	Gk	8,0
Qk	2,0	Qk	2,0	Qk	2,0		
BUILDING PARAMETERS							
Floors	[m]	Height	[m]	Spectral parameters			
b	14,0	z1	3,0	Tb	0,2	S	1,3
h	8,0	z2	6,0	Tc	0,5	q	2,7
		z3	8,0	Td	2,0	ag	0,35g
WEIGHTS							
Floors	[kN]	Ortog. walls	[kN]	Paral. walls	[kN]	Total weight	[kN]
Ws1	434,6	P1	672,0	P1	384,0	W1	672,0
Ws2	434,6	P2	560,0	P2	320,0	W2	560,0
Ws3	266,6	P3	224,0	P3	128,0	W3	224,0
SEISMIC FORCES							
Floors	[kN]	Ortog. walls	[kN]	Paral. walls	[kN]	Total force	[kN]
Fs1	104,5	Fpo1	161,5	Fpp1	92,3	F1	358,3
Fs2	208,9	Fpo2	269,2	Fpp2	153,9	F2	632,0
Fs3	170,9	Fpo3	143,6	Fpp3	82,1	F3	396,5
						Fh	1386,9

La Fig. 99 documents, for floor with simple boards, the building weight and forces applied to model.

Non linear static analysis was carried out in displacement control. The control displacement was the centre of mass of the roof of the building. Final step of analysis was the state of incipient collapse through formation of overturn mechanism of walls or reaching maximum force applied to building.

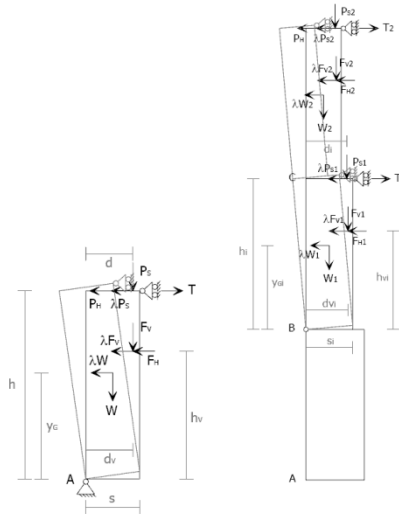


Fig. 99 Overturn kinematism

To determine the situation in which we would have formation of local collapse kinematism with out of plane overturn for perimeter walls, the point of control displacement of this limit state was previously determined.

Noting the geometry of the kinematics chain elements we proceeded to determine the maximum displacement of control point with non linear kinematics analysis.

In particular, the displacement which determines the collapse of the kinematics chain is determined putting to zero the collapse multiplier α in the following equation which refers to Fig. 99.

$$\alpha = (\sum_i W_i (s_i/2) + \sum_i P_{Si} d_i + \sum_i T_i h_i) / (\sum_i W_i y_{Gi} + \sum_i P_{Si} h_i) \quad (57)$$

The displacement of such control point for which we determine the condition of collapse of the kinematics chain is equal to $d_{k,0} = 28$ cm. The OPCM 3431 imposes displacement capacity for safety verifications equal to 40% of already determined displacement and so $d_u = 11$ cm. This value will be able to be compared with displacements obtained from building analysis.

9.5 Results

As mentioned in the preceding paragraphs, for each type of floor analysis has been done with and without perimeter tie-beam and increasing the forces until a value corresponding to $a_g = 0,35g$ or to the formation of a local kinematics collapse.

In the next paragraphs, the main results have documented in terms of displacements and stresses, coming out of numerical analysis. For each floor, as regards the F_r/W ratio, the profiles of deformation of the four perimeter walls are documented as well as the deformations of the three floors. The principal internal tension stresses of the perimeter walls are also documented. The comparisons between the different types of reinforcement as well as between solution with tie-beam and without it will be presented in detail in the next chapter.

9.5.1 Floor with simple timber boards

In Fig. 100 the building deformed configurations with and without perimeter tie-beam are compared in the conditions in which the horizontal seismic forces are equal to 40% of the weight of the whole building which corresponds to $a_g = 0,35g$.

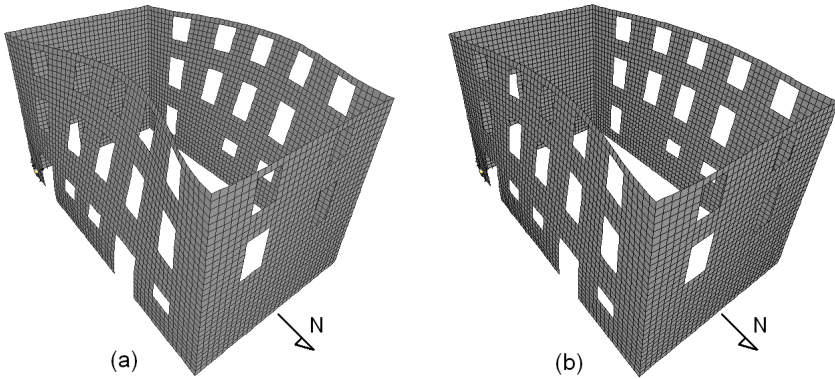


Fig. 100 Deformed configuration of structure for $Fh/W=0,40$ without tie-beam (a) and with tie-beam (b)

Fig. 101 and Fig. 102 shown the deformation profiles of the midpoint of each perimeter wall in function of adimensional height z/h_{tot} and the seismic base shear force. The situations in which the F_r/W ratio is at 8, 16, 28 and 40% respectively correspond to values of a_g equal to 0.05g, 0.15g, 0.25g, 0.35g. We can note as with the simple boards floors, without tie-beam, the midpoint displacements of walls orthogonal to seismic action are in the order of 10 cm such as to activate local collapse mechanisms for overturn outside the wall plane.

The entity of such displacements is in diagram form in Fig. 103 and Fig. 106 which document the deformation of each floor in function of adimensional length x/L of the wall orthogonal to the seismic action and of F_r/W ratio. Moreover, we note the beneficial effect offered by

perimeter tie-beam which determines on average reduction of midpoint displacements of 30%.

Fig. 104, Fig. 105, Fig. 107 and Fig. 108 show the principal tension forces of the perimeter walls. In white there are the compression stresses, in black the tension ones. Even though it is in examination a very flexible floor on its own plane we can note the contribution offered by tie-beam. In Fig. 104 the West wall present high tension forces along all of its length and in particular in correspondence of the corners, showing the formation of a mechanism of overturn outside of plane of wall. In Fig. 107 such stresses are reduced while tension forces increase in Fig. 108 in the South bracing wall determining a shear crack.

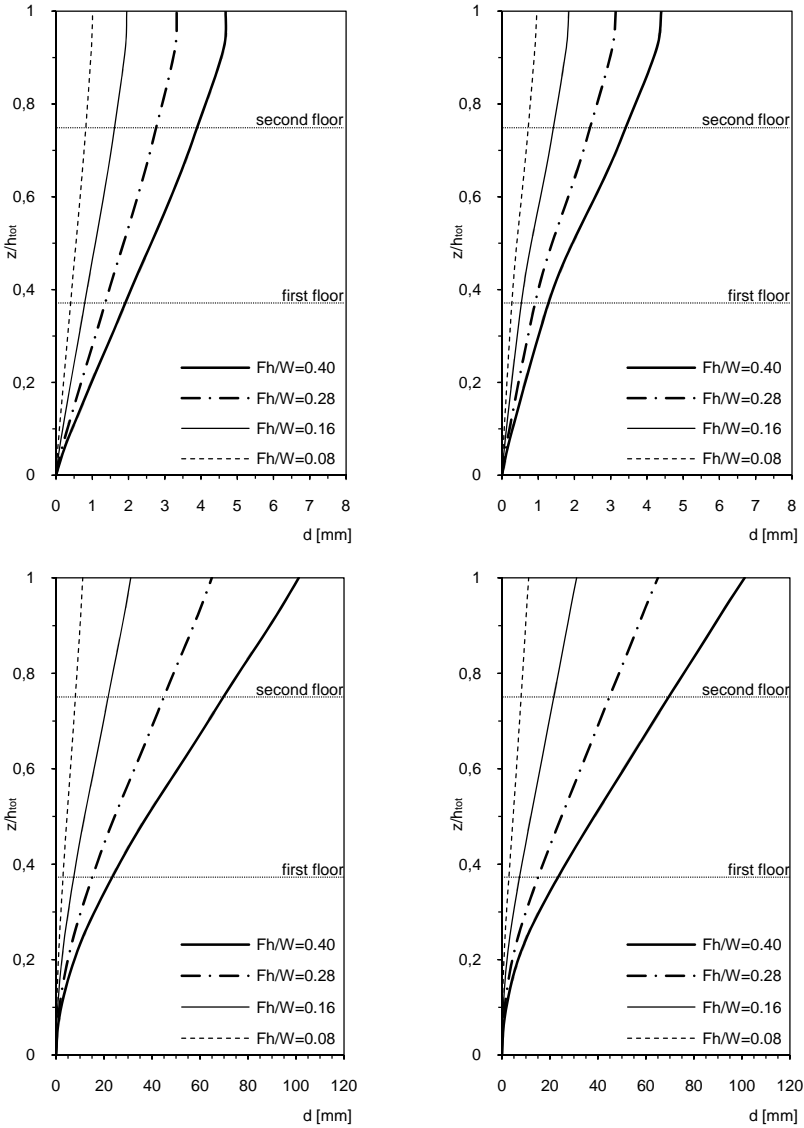


Fig. 101 | clock wise starting from above, horizontal midpoint displacements of South, North, East and West walls in function of building height, in the case of floor without perimeter tie-beam

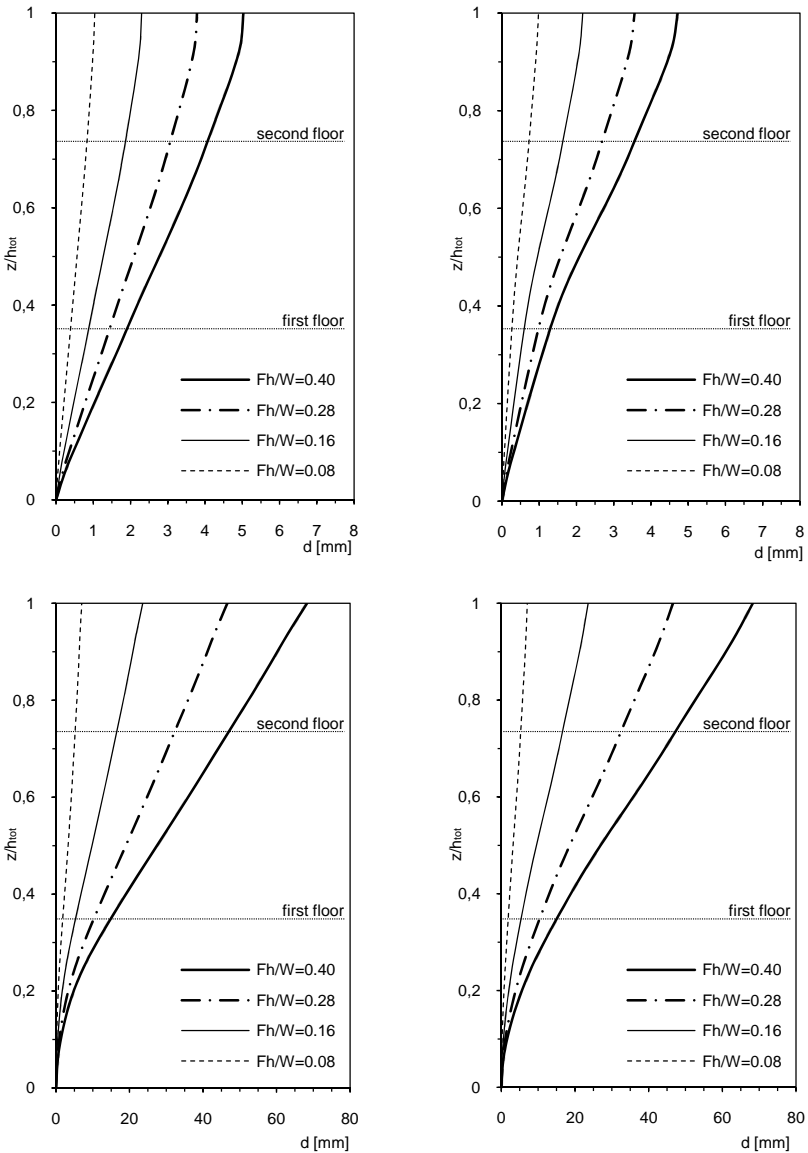


Fig. 102 Clock wise starting from above, horizontal midpoint displacements of South, North, East and West walls in function of building height, in the case of floor with perimeter tie-beam

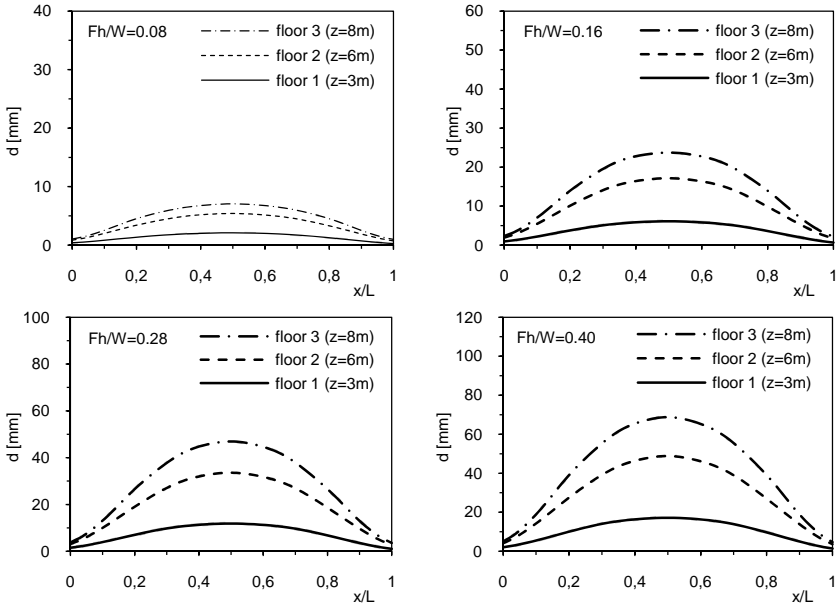


Fig. 103 Deformation of floor without tie-beam

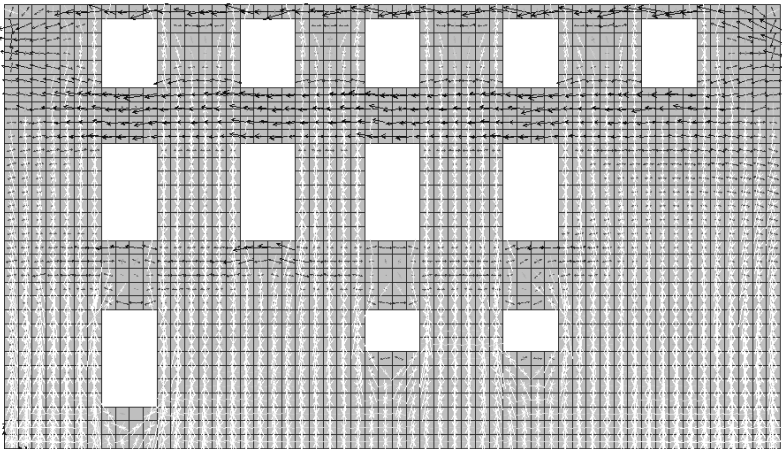


Fig. 104 Principal tension forces of West wall with floor without tie-beam

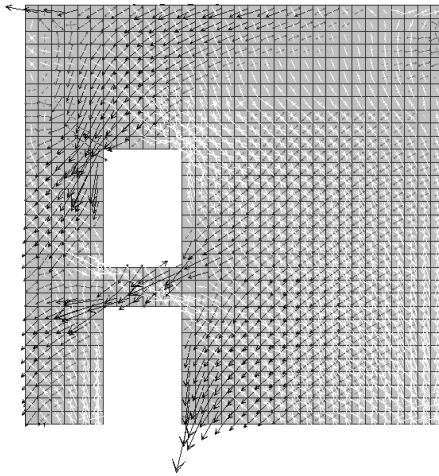


Fig. 105 Principal tension forces of South wall with floor without tie-beam

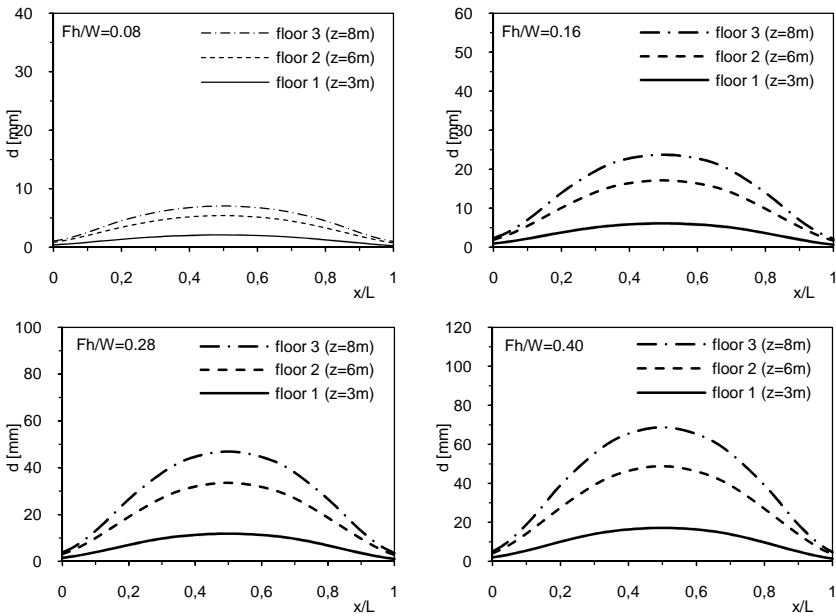


Fig. 106 Deformation of floor with tie-beam

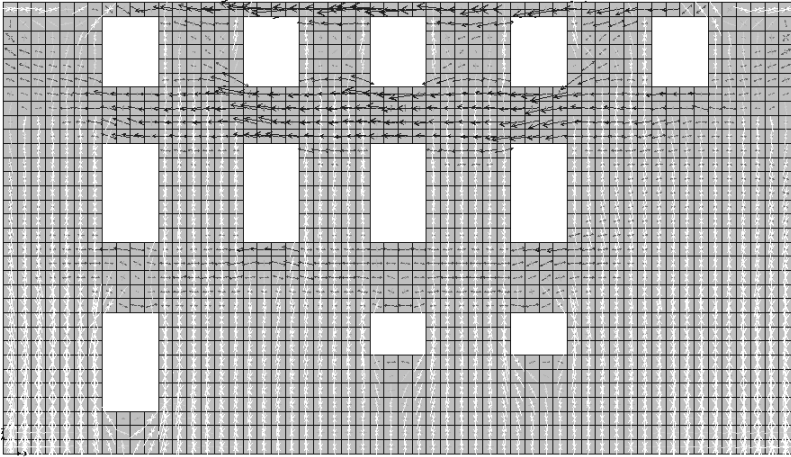


Fig. 107 Principal tension forces of West wall with floor with tie-beam

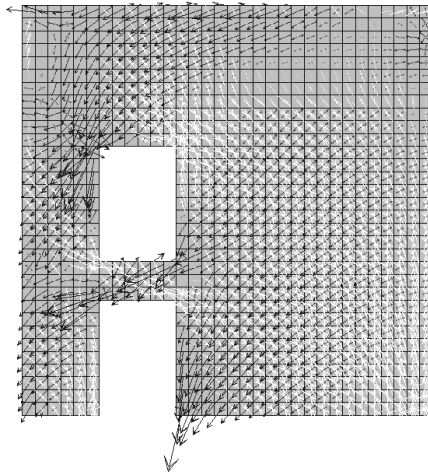


Fig. 108 Principal tension forces of South wall with floor with tie-beam

9.5.2 Floor reinforced with timber boards

In Fig. 109 the building deformed configurations with and without perimeter tie-beam are compared in the conditions in which the horizontal seismic forces are equal to 40% of the weight of the whole building which corresponds to $a_g = 0,35g$.

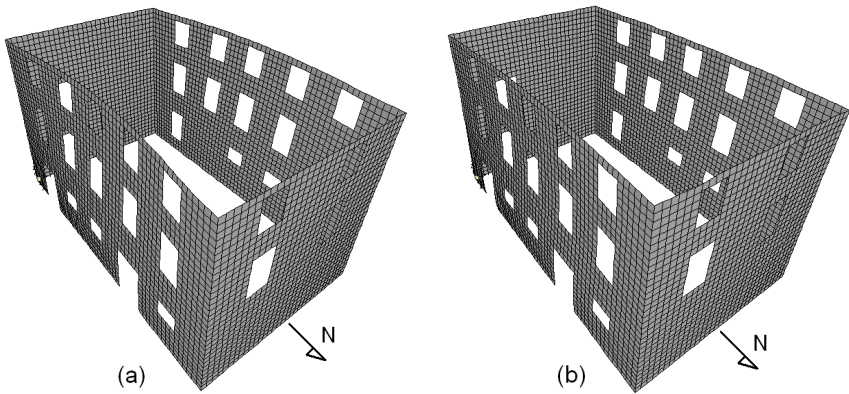


Fig. 109 Deformed configuration of structure for $F_r/W=0,40$ without tie-beam (a) and with tie-beam (b)

Fig. 110 and Fig. 111 shown the deformation profiles of the midpoint of each perimeter wall in function of adimensional height z/h_{tot} and the seismic base shear force. The situations in which the F_r/W ratio is at 8, 16, 28 and 40% respectively correspond to values of a_g equal to 0.05g, 0.15g, 0.25g, 0.35g.

The entity of such displacements is in diagram form in Fig. 112 and Fig. 115 which document the deformation of each floor in function of adimensional length x/L of the wall orthogonal to the seismic action and of F_r/W ratio. Moreover, we note the beneficial effect offered by perimeter tie-beam which determines on average reduction of midpoint displacements of 36%.

Fig. 113, Fig. 114, Fig. 116 and Fig. 117 show the principal tension forces of the perimeter walls. In white there are the compression stresses, in black the tension ones.

Passing from conditions without tie-beam to that in which such reinforcement element is present we note how tension stresses at the West wall midpoint decrease while shear stresses increase in the South and North walls due to greater floor stiffness effect.

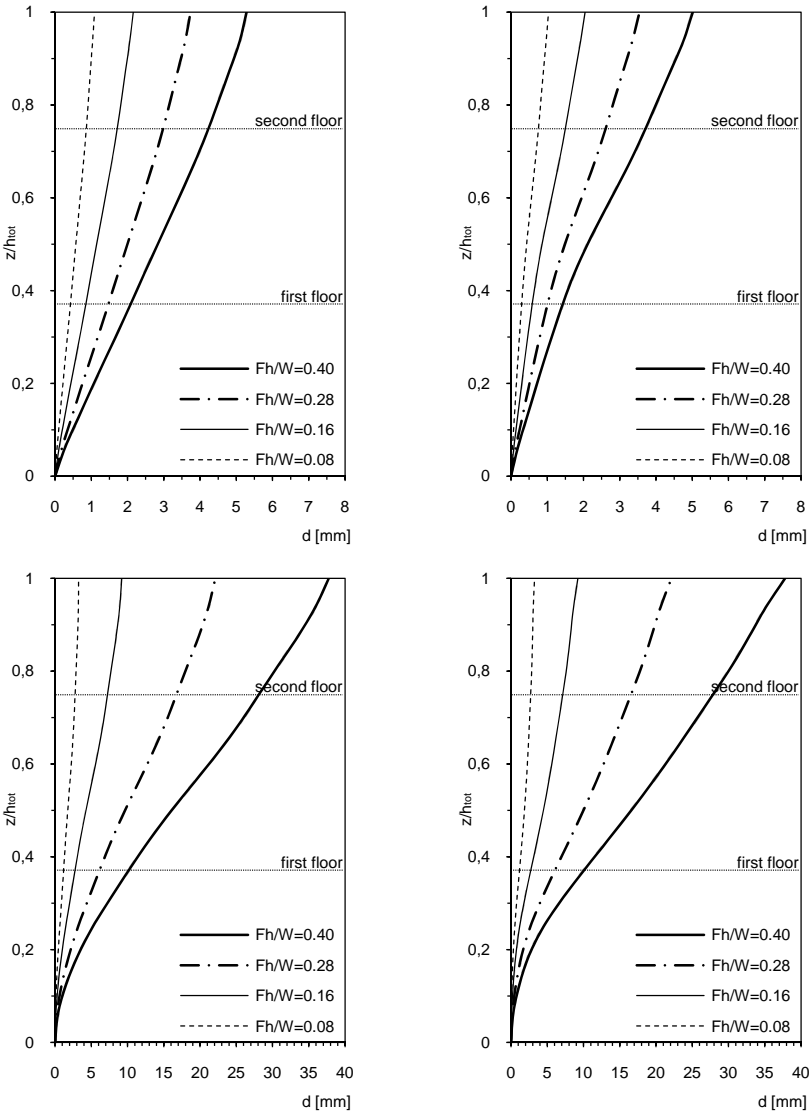


Fig. 110 Clock wise starting from above, horizontal midpoint displacements of South, North, East and West walls in function of building height, in the case of floor without perimeter tie-beam

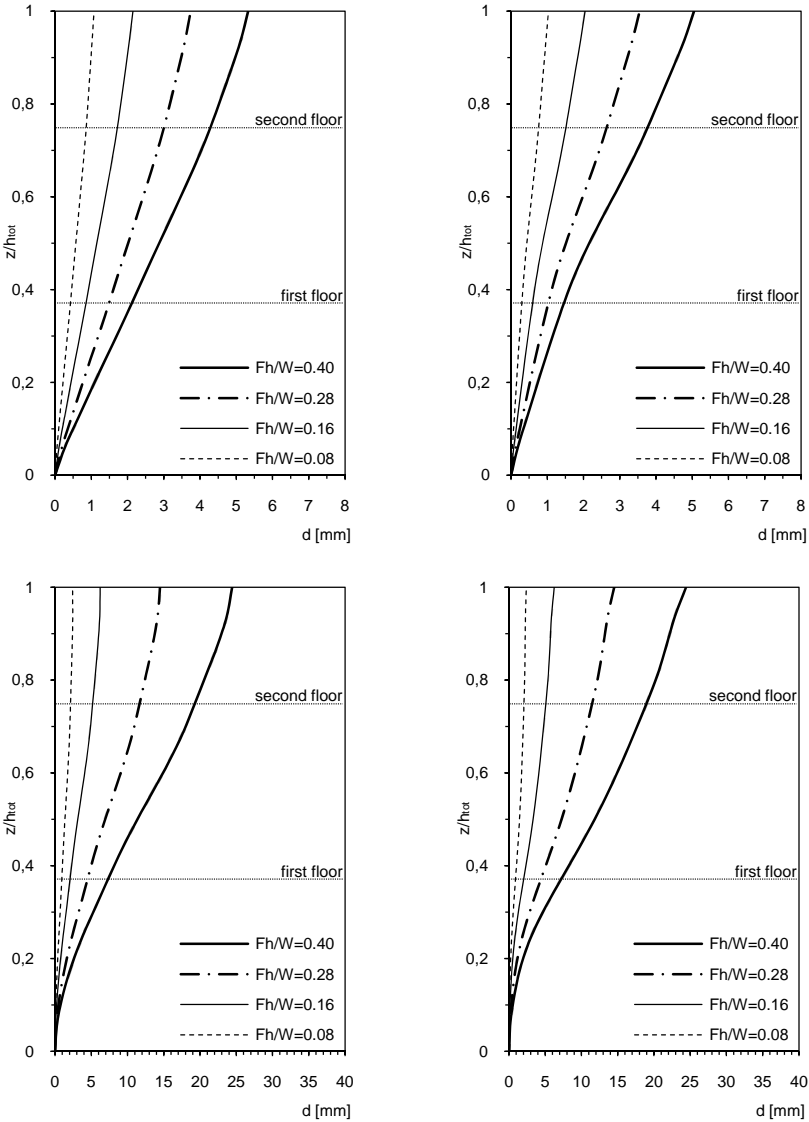


Fig. 111 Clock wise starting from above, horizontal midpoint displacements of South, North, East and West walls in function of building height, in the case of floor with perimeter tie-beam

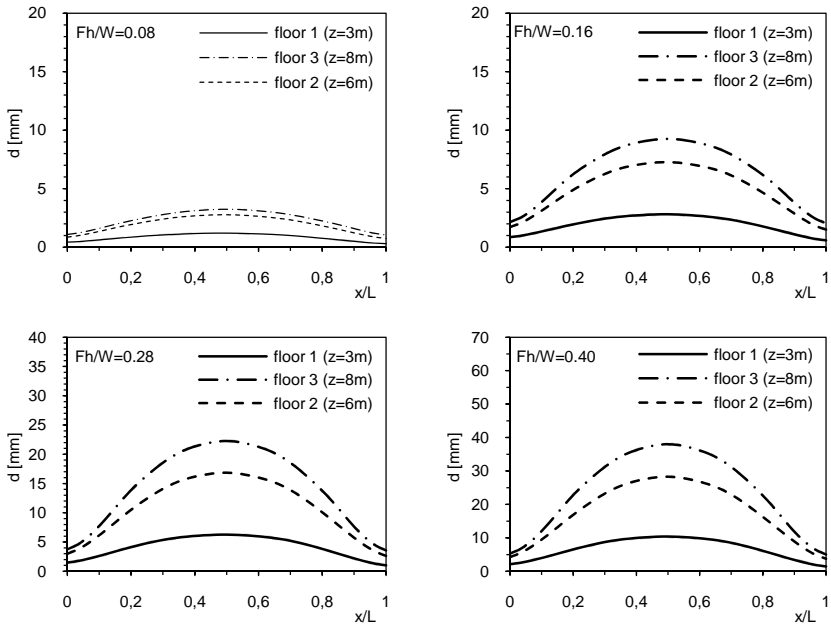


Fig. 112 Deformation of floor without tie-beam

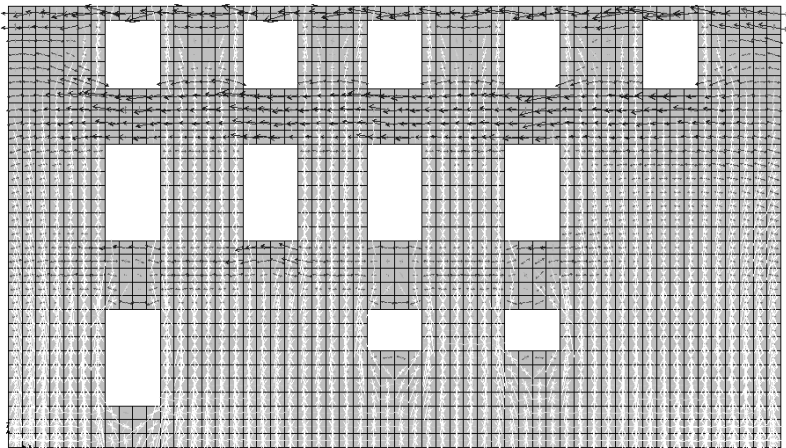


Fig. 113 Principal tension forces of West wall with floor without tie-beam

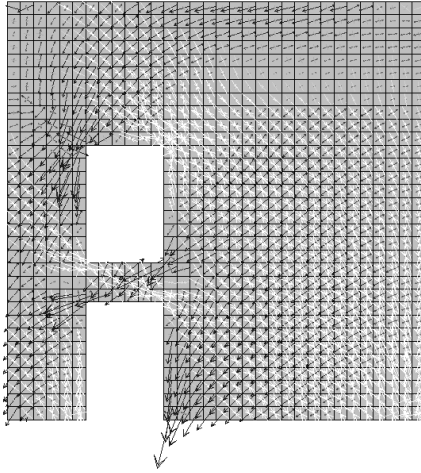


Fig. 114 Principal tension forces of South wall with floor without tie-beam

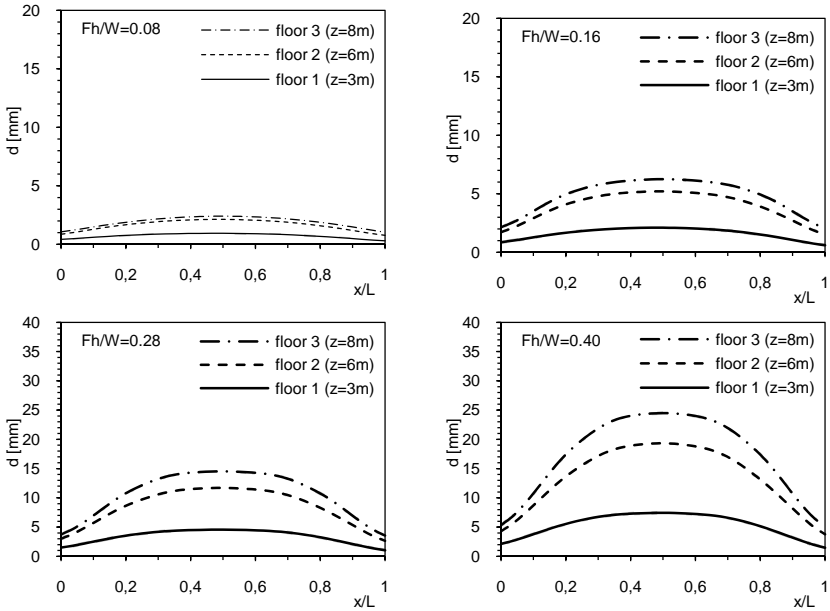


Fig. 115 Deformations of floor with tie-beam

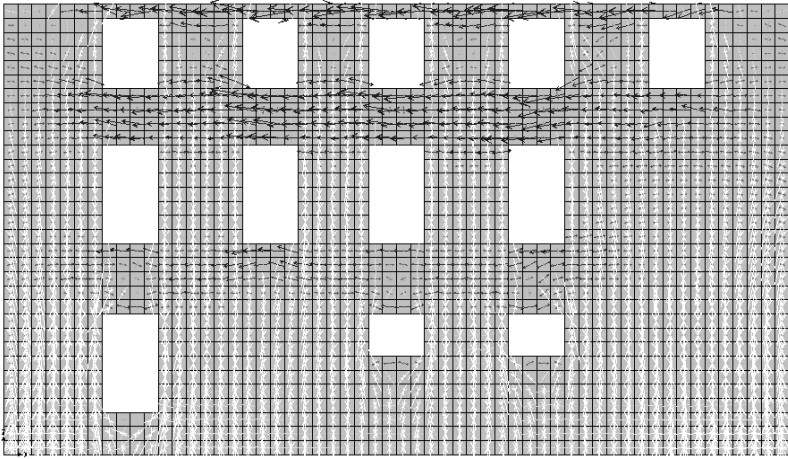


Fig. 116 Principal tension forces of West wall with floor with tie-beam

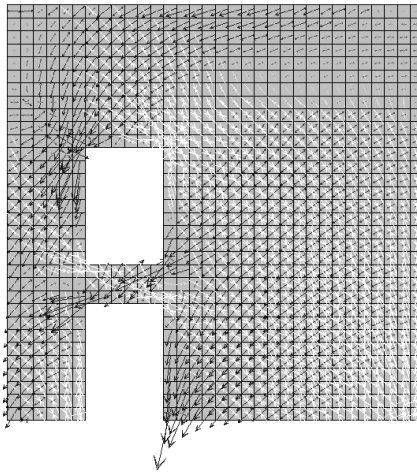


Fig. 117 Principal tension forces of South wall with floor with tie-beam

9.5.3 Floor reinforced with steel plates

In Fig. 118 the building deformed configurations with and without perimeter tie-beam are compared in the conditions in which the horizontal seismic forces are equal to 40% of the weight of the whole building which corresponds to $a_g = 0,35g$.

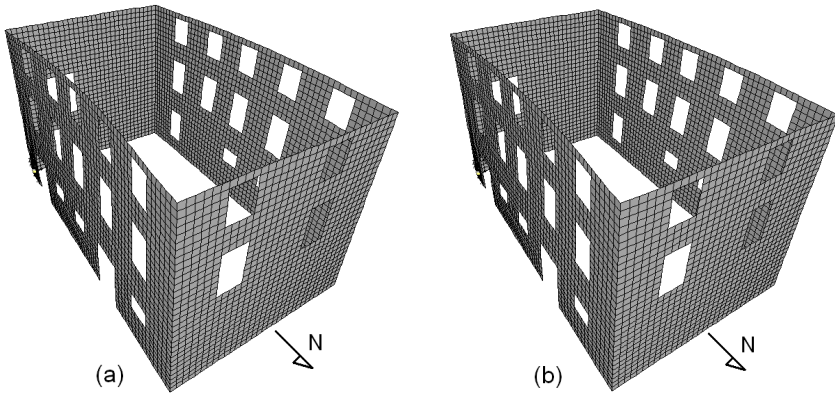


Fig. 118 Deformed configuration of structure for $F_h/W=0,40$ without tie-beam (a) and with tie-beam (b)

Fig. 119 and Fig. 120 shown the deformation profiles of the midpoint of each perimeter wall in function of adimensional height z/h_{tot} and the seismic base shear force. The situations in which the F_r/W ratio is at 8, 16, 28 and 40% respectively correspond to values of a_g equal to 0.05g, 0.15g, 0.25g, 0.35g.

The entity of such displacements is in diagram form in Fig. 121 and Fig. 124 which document the deformation of each floor in function of adimensional length x/L of the wall orthogonal to the seismic action and of F_r/W ratio. Moreover, we note the beneficial effect offered by perimeter tie-beam which determines on average reduction of midpoint displacements of 36%.

Fig. 122,

Fig. 123, Fig. 125 and Fig. 126 show the principal tension forces of the perimeter walls. In white there are the compression stresses, in black the tension ones.

Passing from conditions without tie-beam to that in which such reinforcement elements present we note how tension stresses at the West wall midpoint decrease while shear stresses increase in the South and North walls due to greater floor stiffness effect.

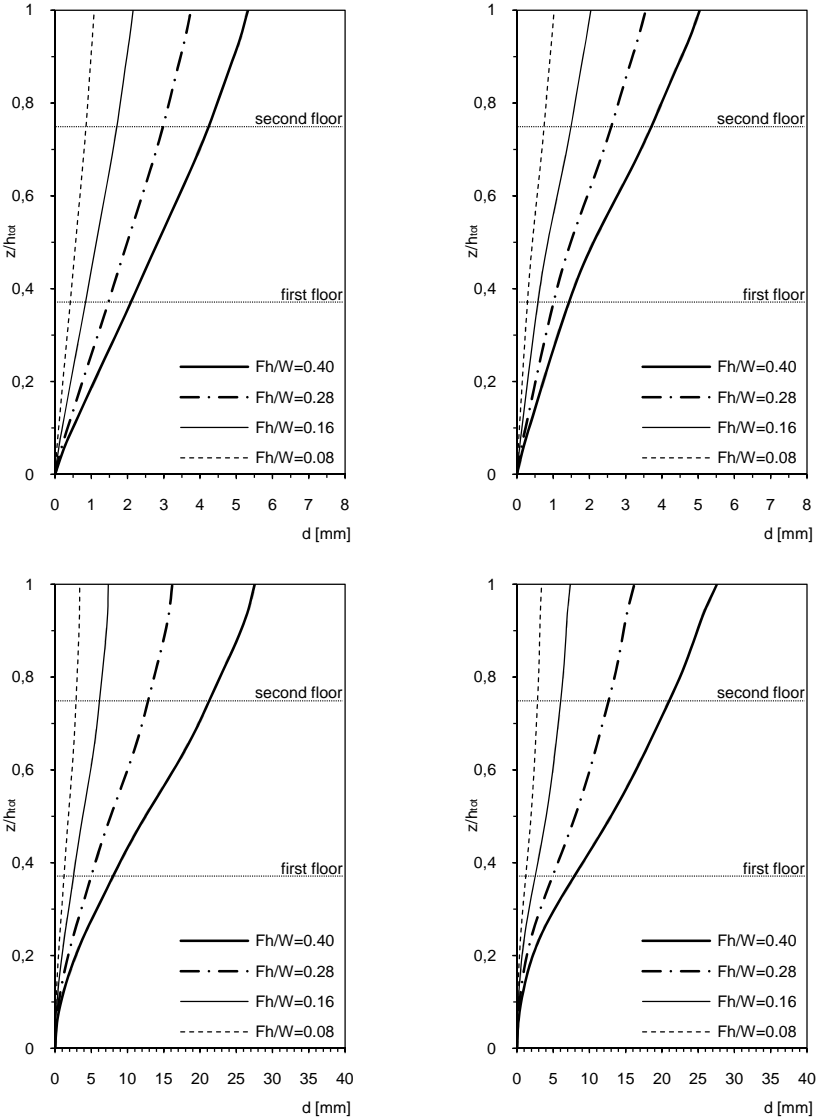


Fig. 119 Clock wise starting from above, horizontal midpoint displacements of South, North, East and West walls in function of building height, in the case of floor without perimeter tie-beam

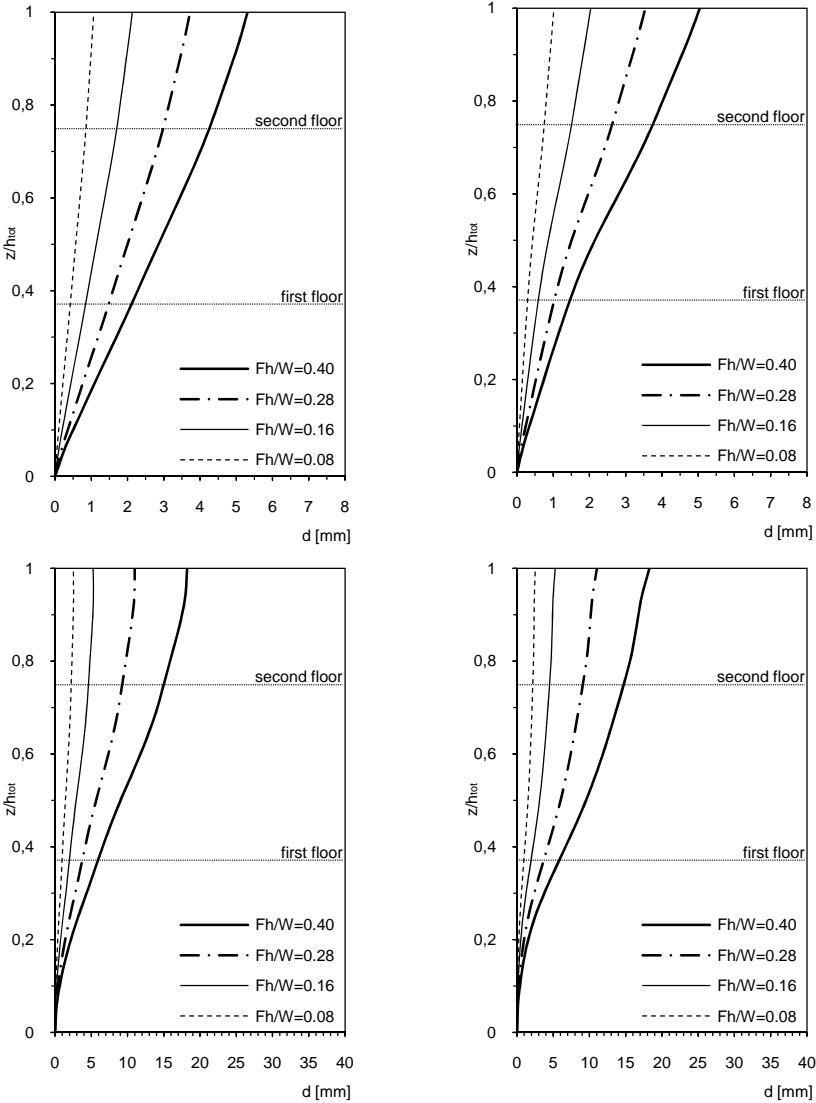


Fig. 120 Clock wise starting from above, horizontal midpoint displacements of South, North, East and West walls in function of building height, in the case of floor with perimeter tie-beam

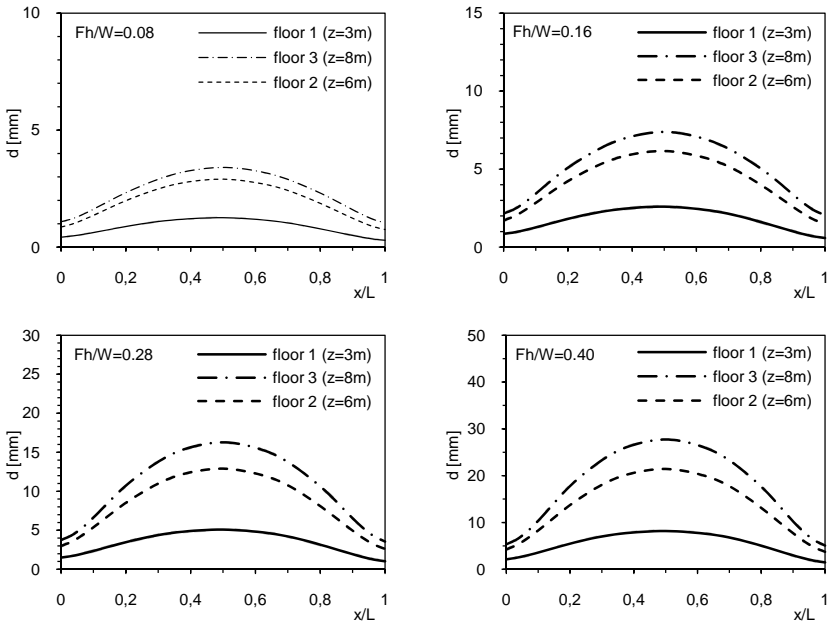


Fig. 121 Deformation of floor without tie-beam

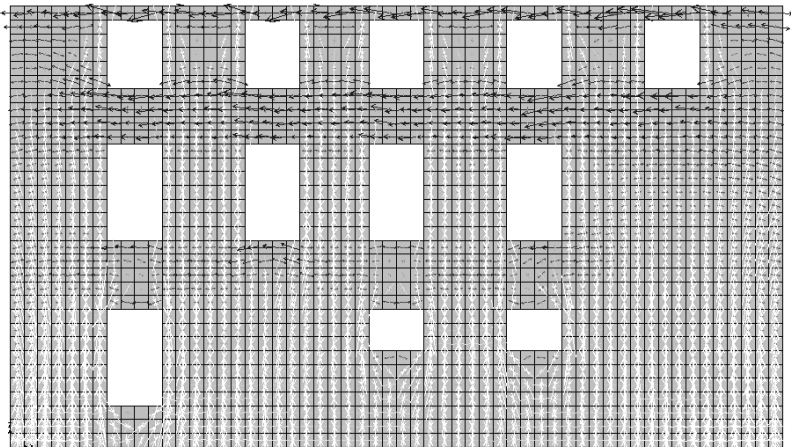


Fig. 122 Principal tension forces of West wall with floor without tie-beam

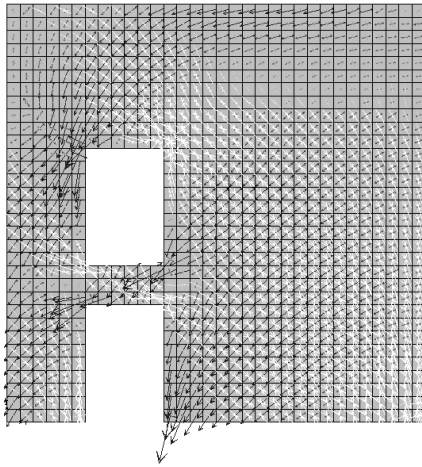


Fig. 123 Principal tension forces of South wall with floor without tie-beam

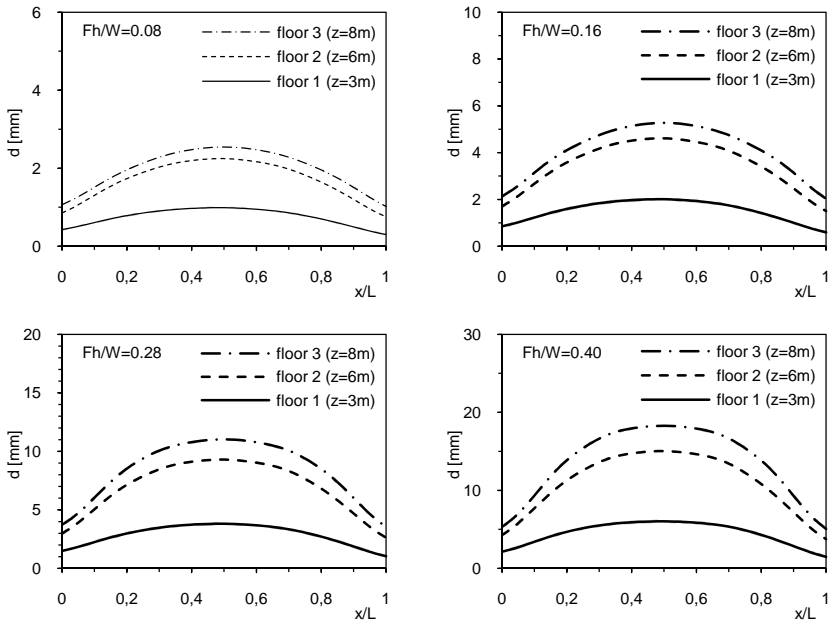


Fig. 124 Deformation of floor with tie-beam

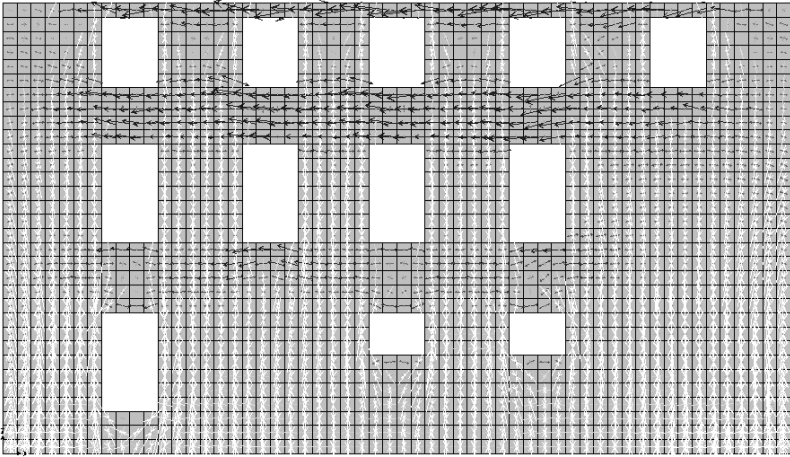


Fig. 125 Principal tension forces of West wall with floor with tie-beam

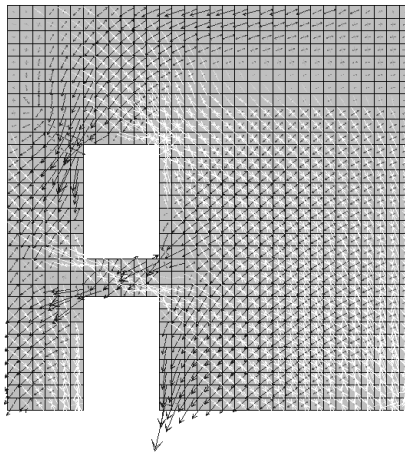


Fig. 126 Principal tension forces of South wall with floor with tie-beam

9.5.4 Floor reinforced with FRP strips

In Fig. 127 the building deformed configurations with and without perimeter tie-beam are compared in the conditions in which the horizontal seismic forces are equal to 40% of the weight of the whole building which corresponds to $a_g = 0,35g$.

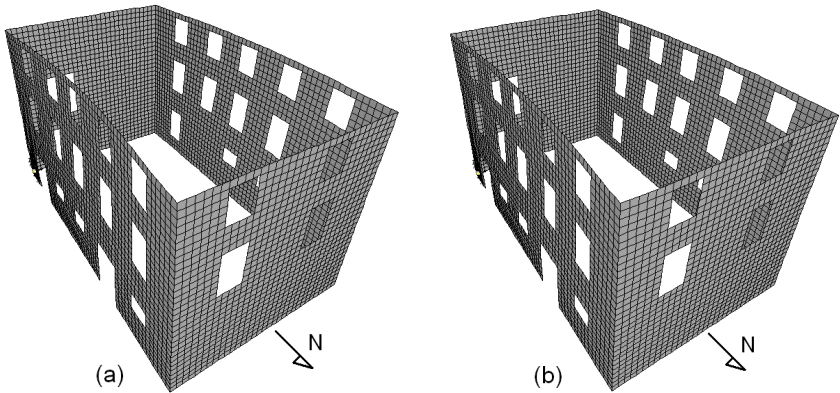


Fig. 127 Deformed configuration of structure for $Fh/W=0,40$ without tie-beam (a) and with tie-beam (b)

Fig. 128 and Fig. 129 shown the deformation profiles of the midpoint of each perimeter wall in function of adimensional height z/h_{tot} and the seismic base shear force. The situations in which the F_r/W ratio is at 8, 16, 28 and 40% respectively correspond to values of a_g equal to 0,05g, 0,15g, 0,25g, 0,35g.

The entity of such displacements is in diagram form in Fig. 130 and Fig. 133 which document the deformation of each floor in function of adimensional length x/L of the wall orthogonal to the seismic action and of F_r/W ratio. Moreover, we note the beneficial effect offered by perimeter tie-beam which determines on average reduction of midpoint displacements of 32%.

Fig. 131, Fig. 132, Fig. 134 and Fig. 135 show the principal tension forces of the perimeter walls. In white there are the compression stresses, in black the tension ones.

Passing from conditions without tie-beam to that in which such reinforcement element is present we note how tension stresses at the West wall midpoint decrease while shear stresses increase in the South and North walls due to greater floor stiffness effect.

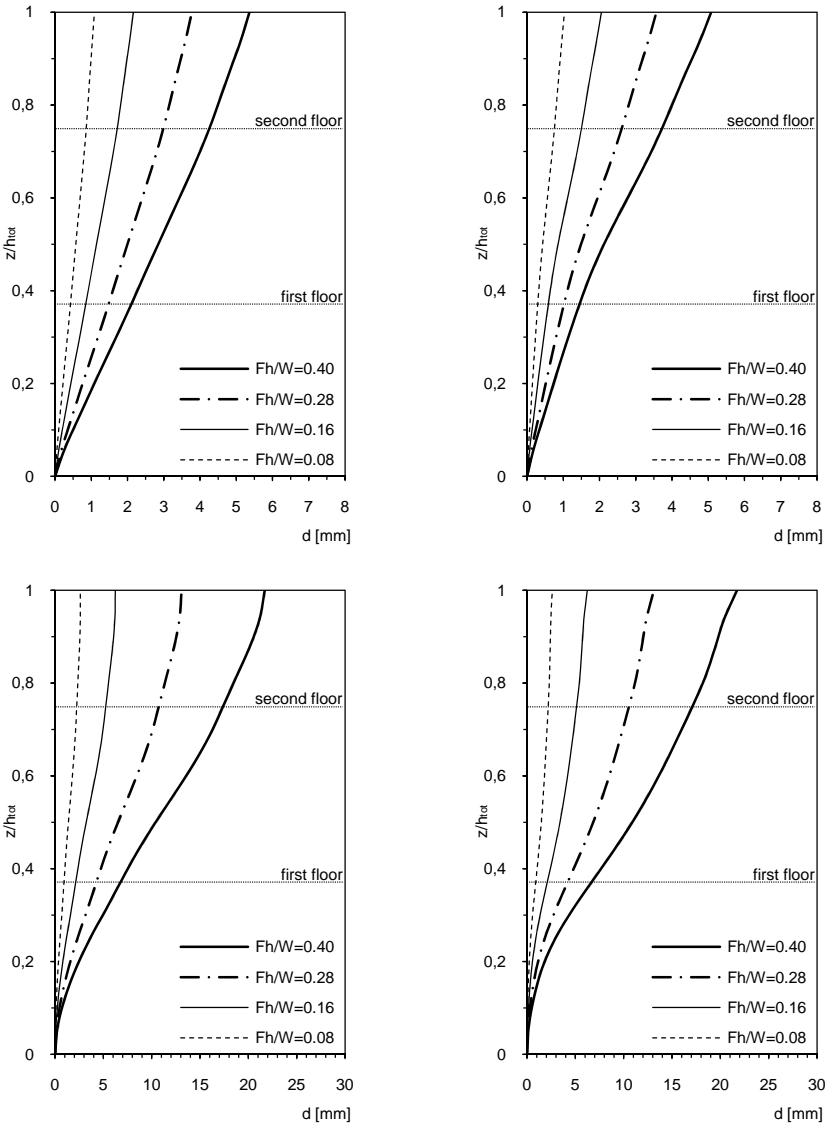


Fig. 128 Clock wise starting from above, horizontal midpoint displacements of South, North, East and West walls in function of building height, in the case of floor without perimeter tie-beam

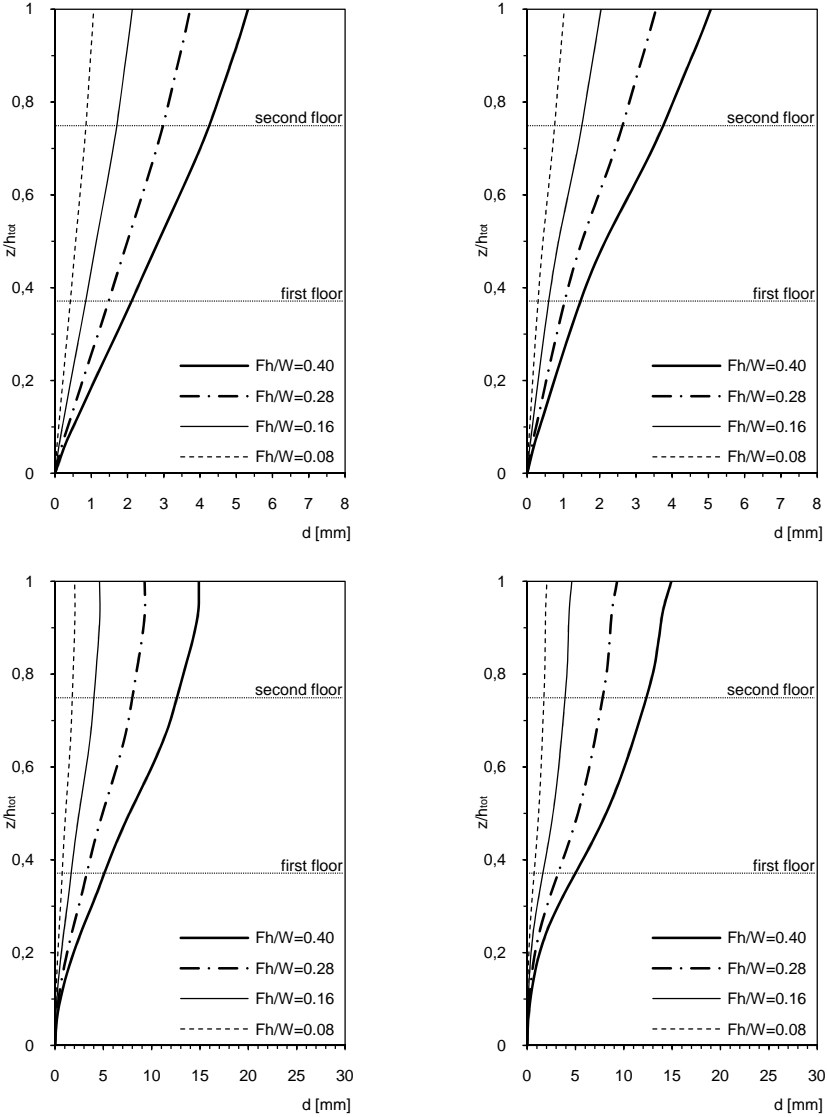


Fig. 129 Clock wise starting from above, horizontal midpoint displacements of South, North, East and West walls in function of building height, in the case of floor with perimeter tie-beam

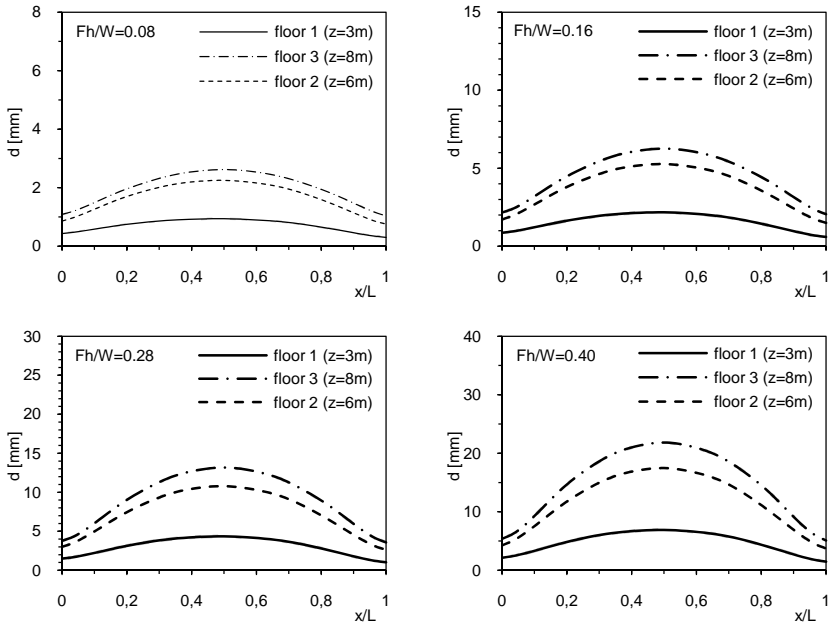


Fig. 130 Deformation of floor without tie-beam

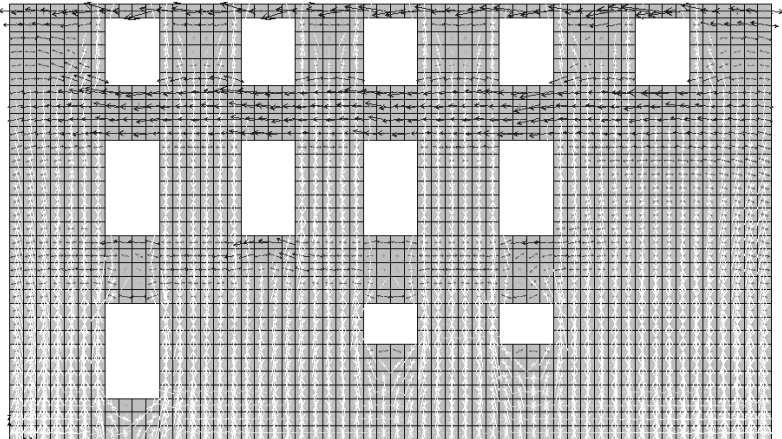


Fig. 131 Principal tension forces of West wall with floor without tie-beam

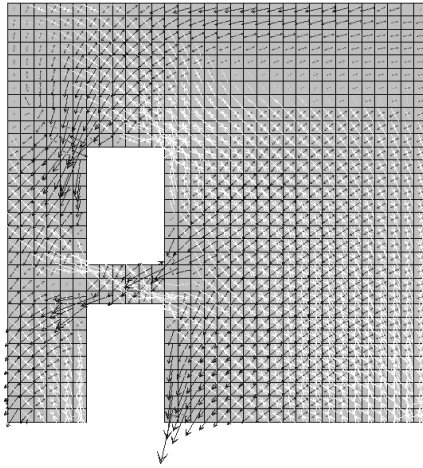


Fig. 132 Principal tension forces of South wall with floor without tie-beam

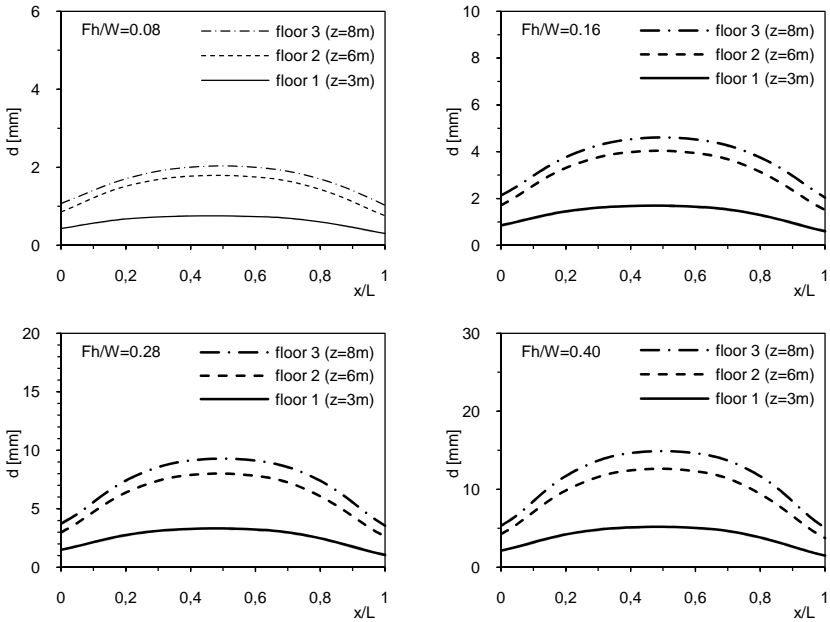


Fig. 133 Deformation of floor with tie-beam

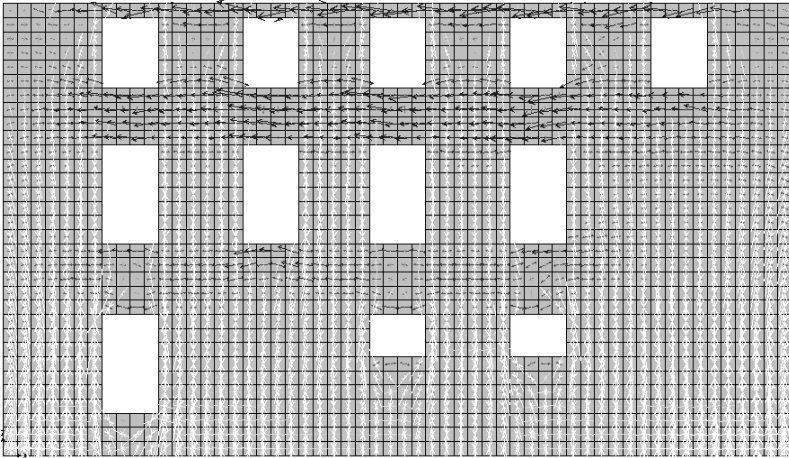


Fig. 134 Principal tension forces of West wall with floor with tie-beam

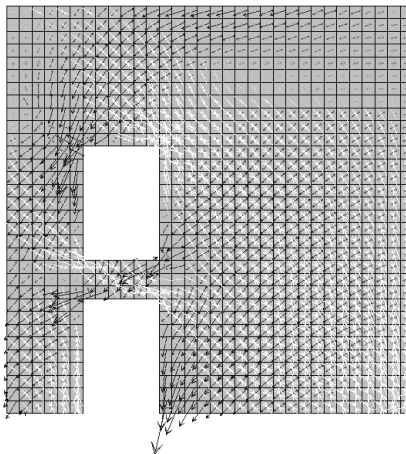


Fig. 135 Principal tension forces of South wall with floor with tie-beam

9.5.5 Floor reinforced with plywood panels

In Fig. 136 the building deformed configurations with and without perimeter tie-beam are compared in the conditions in which the horizontal seismic forces are equal to 40% of the weight of the whole building which corresponds to $a_g = 0,35g$.

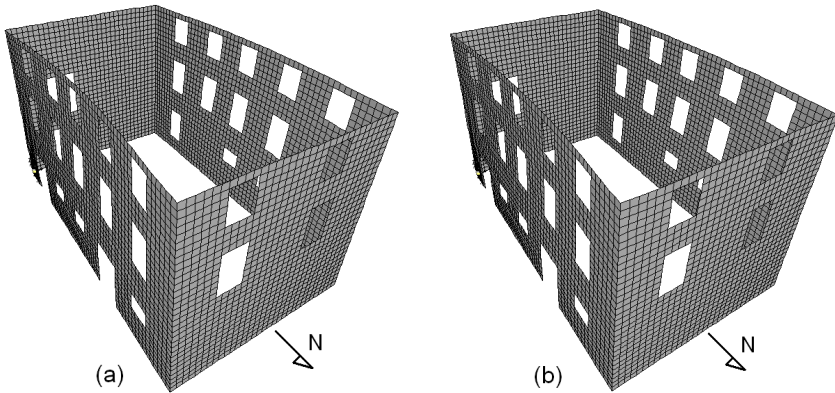


Fig. 136 Deformed configuration of structure for $Fh/W=0,40$ without tie-beam (a) and with tie-beam (b)

Fig. 137 and Fig. 138 shown the deformation profiles of the midpoint of each perimeter wall in function of adimensional height z/h_{tot} and the seismic base shear force. The situations in which the F_r/W ratio is at 8, 16, 28 and 40% respectively correspond to values of a_g equal to 0,05g, 0,15g, 0,25g, 0,35g.

The entity of such displacements is in diagram form in Fig. 139 and Fig. 142 which document the deformation of each floor in function of adimensional length x/L of the wall orthogonal to the seismic action and of F_r/W ratio. Moreover, we note the beneficial effect offered by perimeter tie-beam which determines on average reduction of midpoint displacements of 22%.

Fig. 140, Fig. 141, Fig. 143 and Fig. 144 show the principal tension forces of the perimeter walls. In white there are the compression stresses, in black the tension ones.

Passing from conditions without tie-beam to that in which such reinforcement element is present we note how tension stresses at the West wall midpoint decrease while shear stresses increase in the South and North walls due to greater floor stiffness effect.

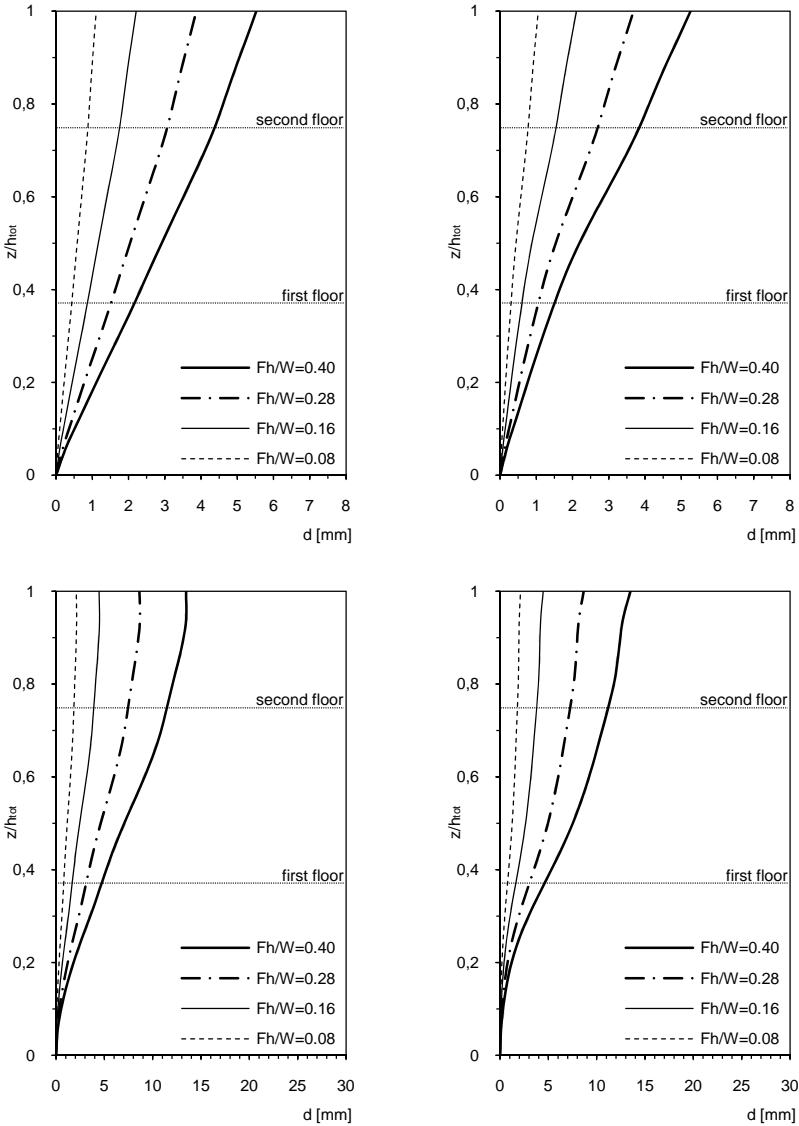


Fig. 137 Clock wise starting from above, horizontal midpoint displacements of South, North, East and West walls in function of building height, in the case of floor without perimeter tie-beam

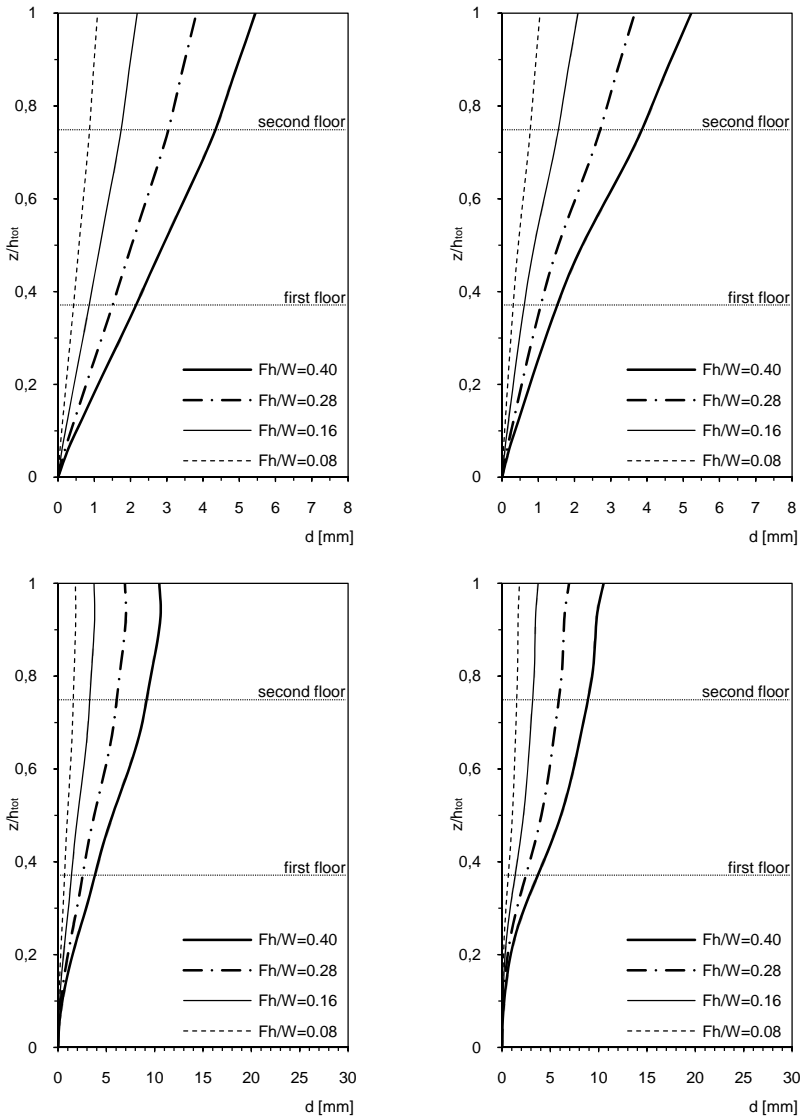


Fig. 138 Clock wise starting from above, horizontal midpoint displacements of South, North, East and West walls in function of building height, in the case of floor with perimeter tie-beam

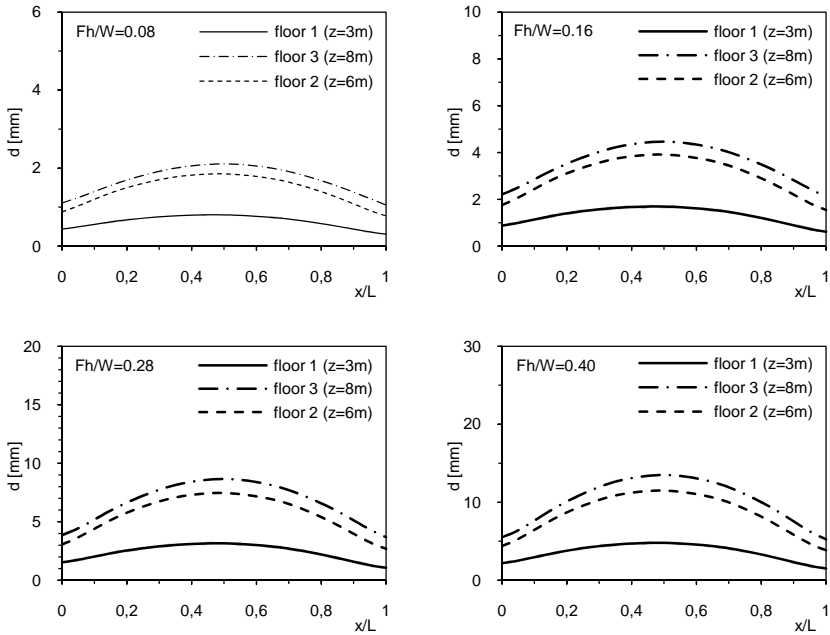


Fig. 139 Deformation of floor without tie-beam

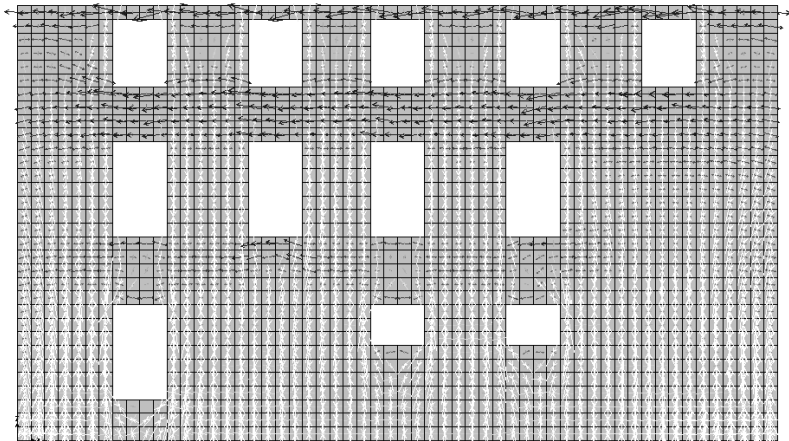


Fig. 140 Principal tension forces of West wall with floor without tie-beam

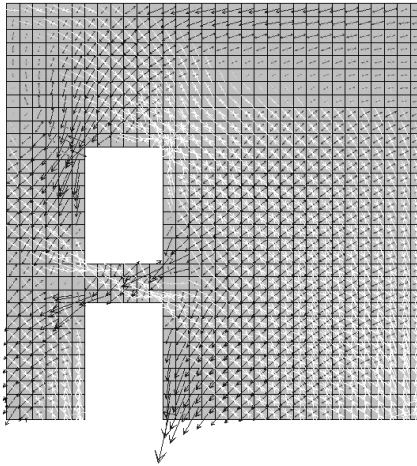


Fig. 141 Principal tension forces of South wall with floor without tie-beam

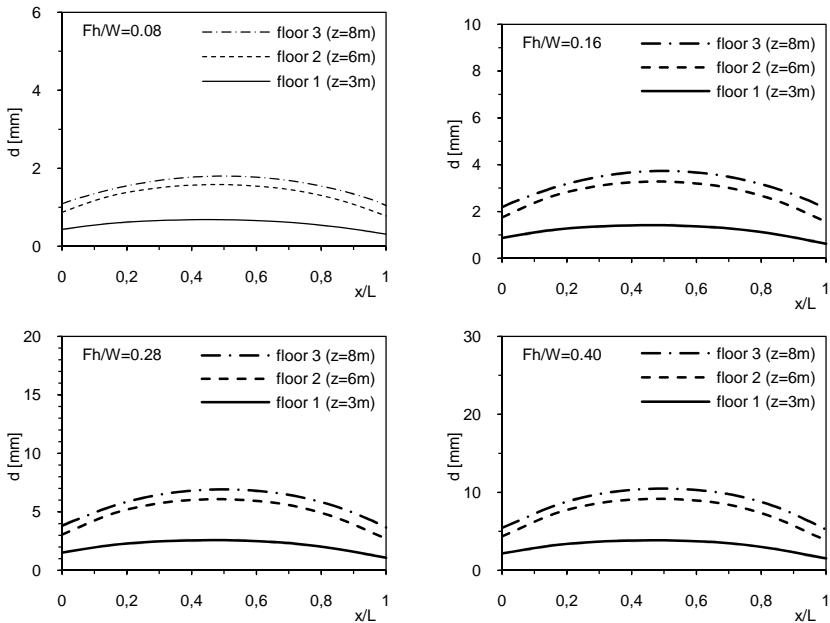


Fig. 142 Deformation of floor with tie-beam

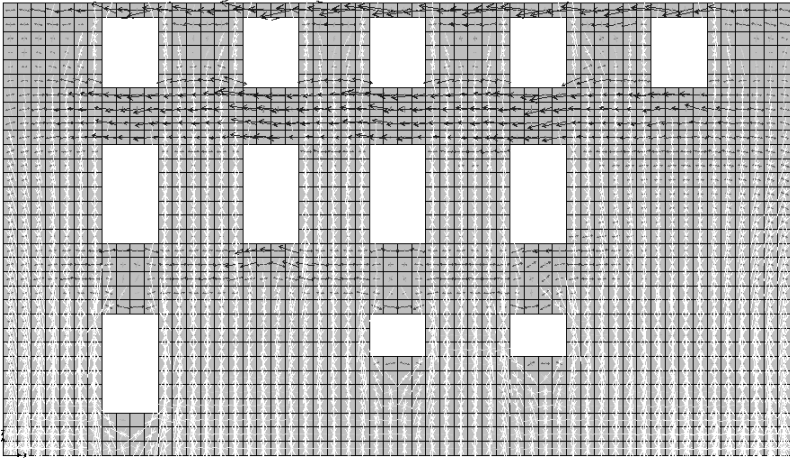


Fig. 143 Principal tension forces of West wall with floor with tie-beam

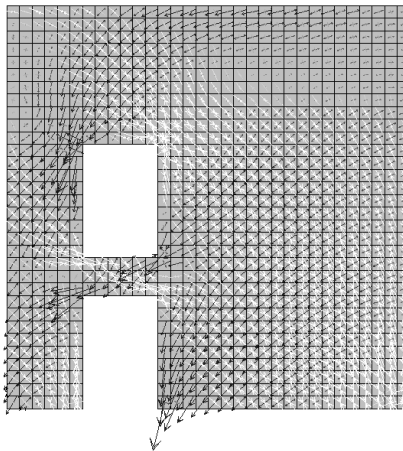


Fig. 144 Principal tension forces of South wall with floor with tie-beam

9.5.6 Floor reinforced with concrete slab

In Fig. 145 the building deformed configurations with and without perimeter tie-beam are compared in the conditions in which the horizontal seismic forces are equal to 40% of the weight of the whole building which corresponds to $a_g = 0,35g$.

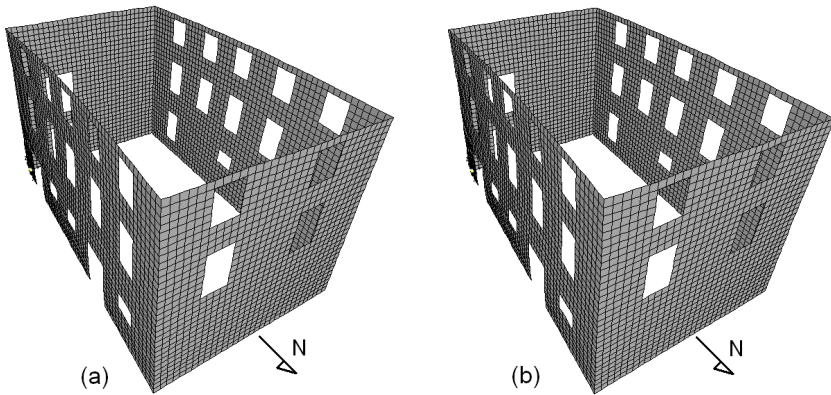


Fig. 145 Deformed configuration of structure for $Fh/W=0,40$ without tie-beam (a) and with tie-beam (b)

Fig. 146 e Fig. 147 shown the deformation profiles of the midpoint of each perimeter wall in function of adimensional height z/h_{tot} and the seismic base shear force. The situations in which the F_r/W ratio is at 8, 16, 28 and 40% respectively correspond to values of a_g equal to 0,05g, 0,15g, 0,25g, 0,35g.

The entity of such displacements is in diagram form in Fig. 148 and Fig. 151 which document the deformation of each floor in function of adimensional length x/L of the wall orthogonal to the seismic action and of F_r/W ratio. Moreover, we note the beneficial effect offered by perimeter tie-beam which determines on average reduction of midpoint displacements of 27%.

Fig. 149, Fig. 150, Fig. 152 and Fig. 153 show the principal tension forces of the perimeter walls. In white there are the compression stresses, in black the tension ones.

Passing from conditions without tie-beam to that in which such reinforcement element is present we note how tension stresses at the West wall midpoint decrease while shear stresses increase in the South and North walls due to greater floor stiffness effect.

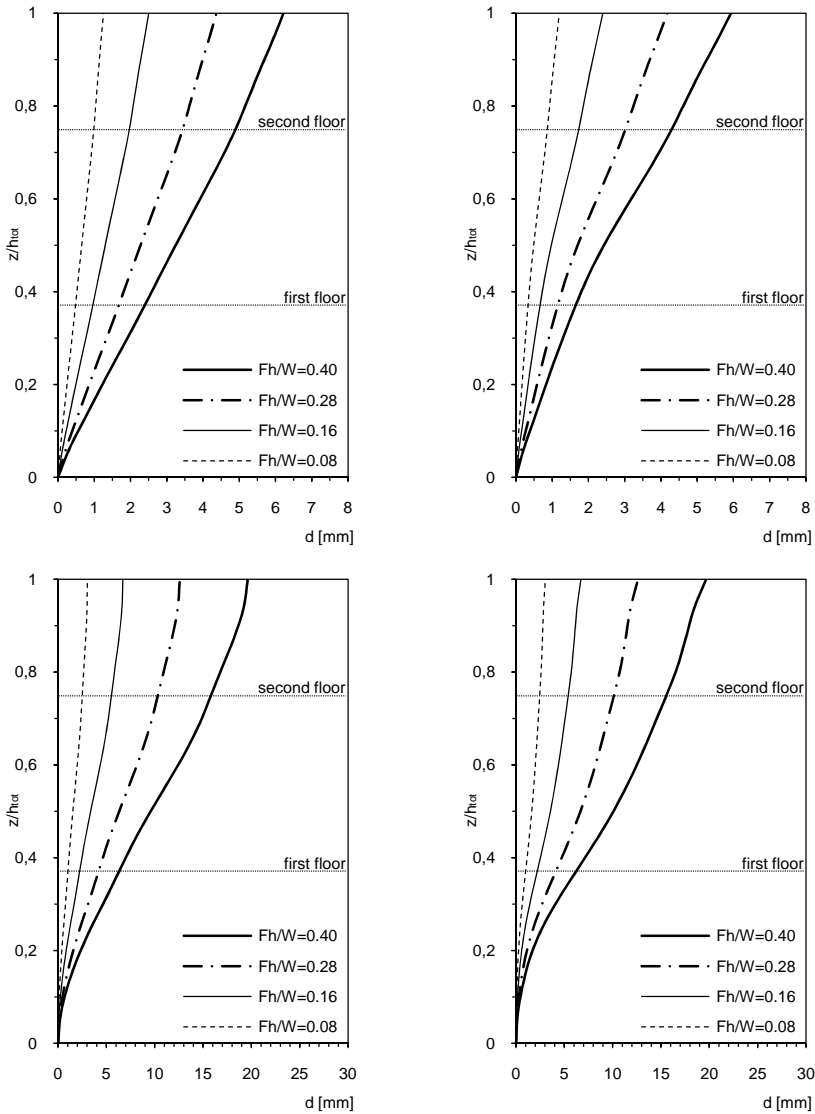


Fig. 146 Clock wise starting from above, horizontal midpoint displacements of South, North, East and West walls in function of building height, in the case of floor without perimeter tie-beam

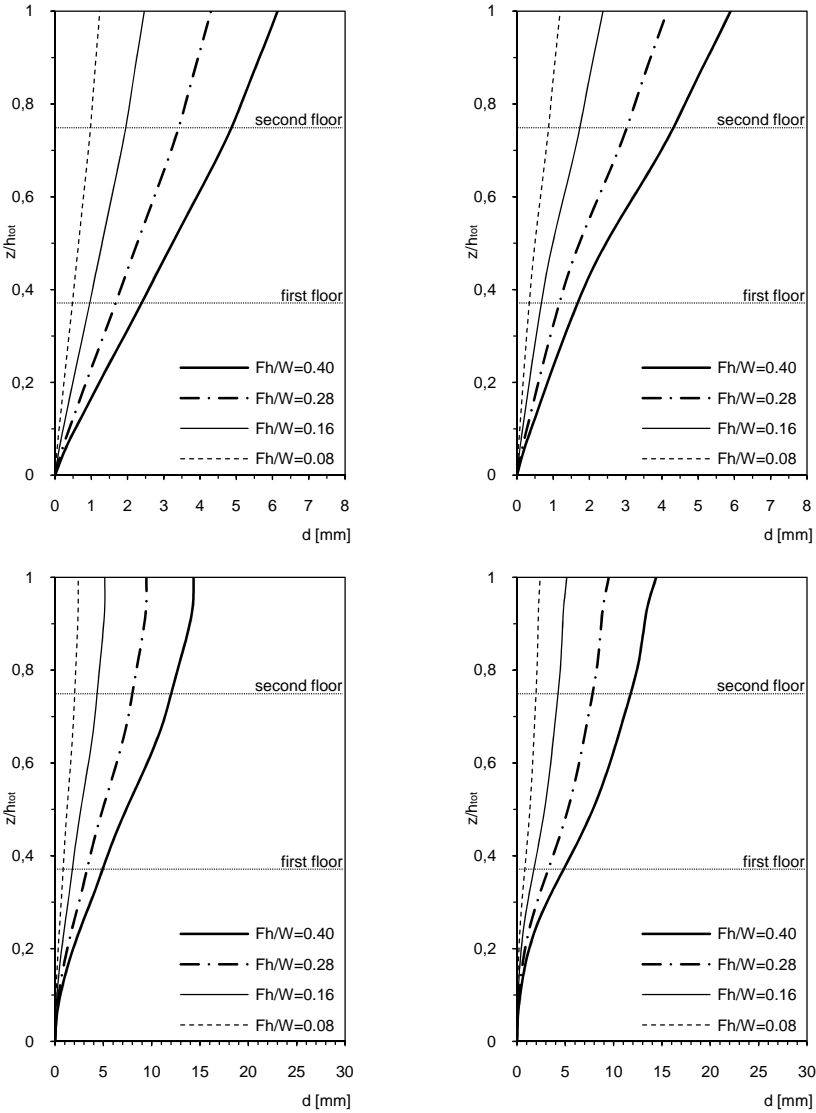


Fig. 147 Clock wise starting from above, horizontal midpoint displacements of South, North, East and West walls in function of building height, in the case of floor with perimeter tie-beam

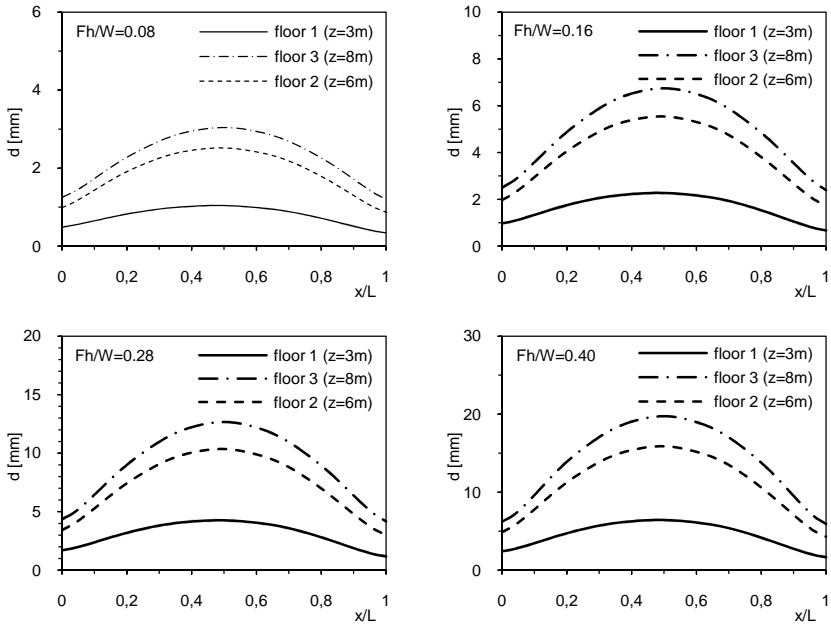


Fig. 148 Deformation of floor without tie-beam

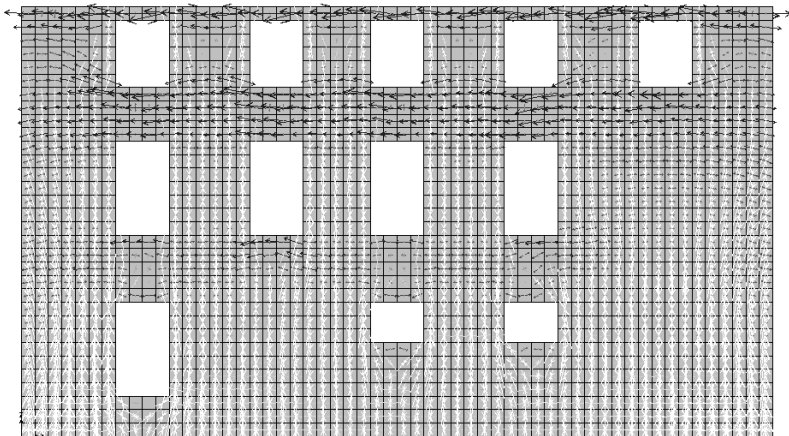


Fig. 149 Principal tension forces of West wall with floor without tie-beam

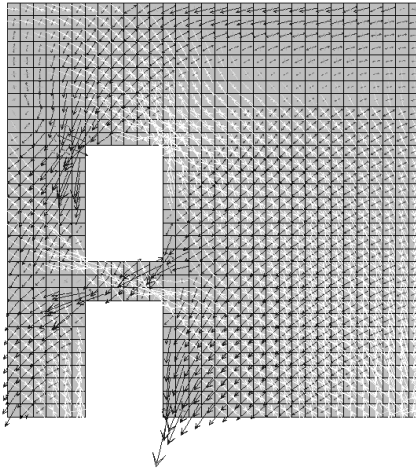


Fig. 150 Principal tension forces of South wall with floor without tie-beam

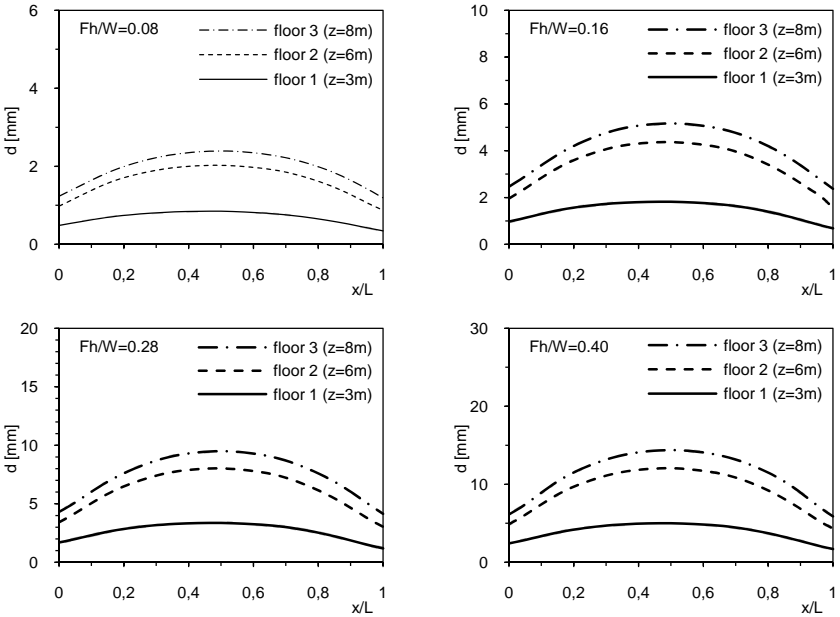


Fig. 151 Deformation of floor with tie-beam

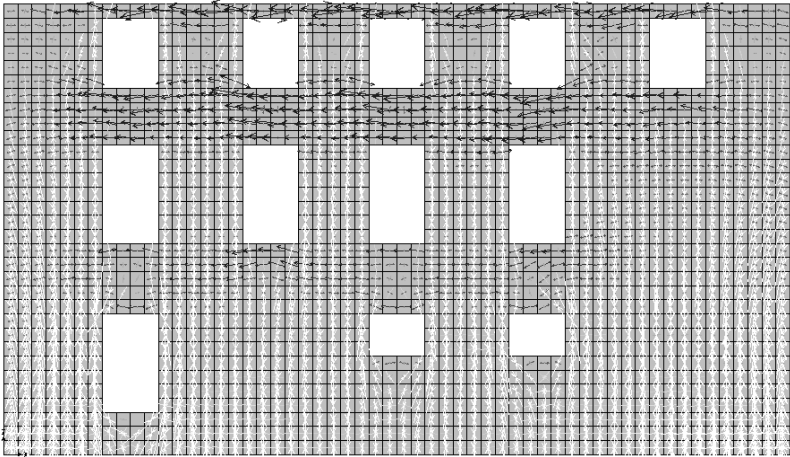


Fig. 152 Principal tension forces of West wall with floor with tie-beam

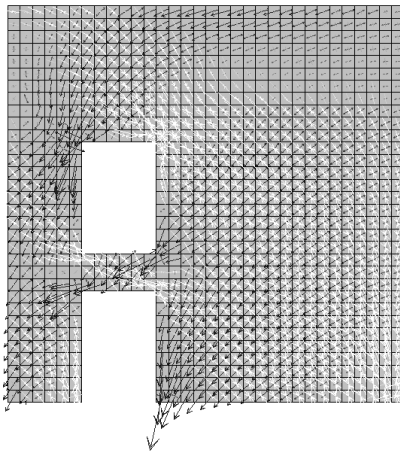


Fig. 153 Principal tension forces of South wall with floor with tie-beam

10. REINFORCEMENT COMPARISON

10.1 Introduction

This chapter summarises the results obtained from experimental tests and from numerical analysis in terms of load-displacement curves, floor stiffness and floor stresses.

What emerges from the experimental tests is compared with results obtained from numerical analyses both in the case of floors with dimensions of 2x1 m and those of 5x4 m. The contribution in terms of stiffness offered by perimeter tie-beam is highlighted.

10.2 Experimental tests and modelling

10.2.1 *The load-displacement curves*

Fig. 154 shows the comparison between the load-displacement curves obtained in the experimental tests. We can see the high in-plane deformation of floor with simple boards which requires a in-plane reinforcement to be able to efficiently transfer seismic actions to bracing walls avoiding overturn outside of wall plane.

Laying a second layer of wood planks at 45° compared to the first, in-plane stiffness increase in eight times greater than the solution with

simple boards. The other types of reinforcement further increase in-plane stiffness passing from the metal plates to the FRP strip to the reinforced concrete slab and finally to plywood panels. The last solution most increments such stiffness, in the order of seventy times that offered by simple boards.

Next figures document for each type of floor the comparison between load-displacement curves obtained by experimental tests with those produced from numerical analysis and then the comparison between load-displacement curves with tie-beams and those without perimeter tie-beams. We note the minimum deviation present between experimental results and the numerical analysis confirming the high quality of numerical modelling.

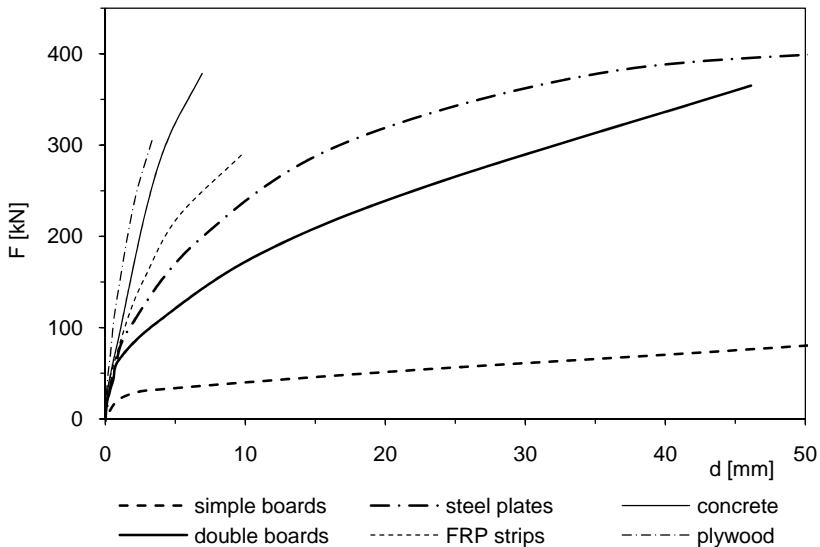


Fig. 154 Load-displacement experimental curves

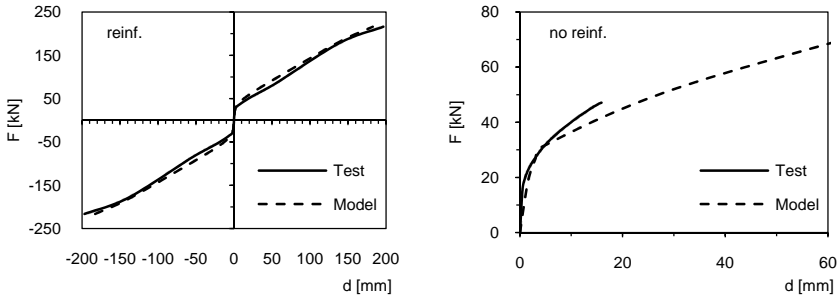


Fig. 155 Comparison load-displacement curves between experimental tests and numerical analysis of floors with dimensions 5x4 m – simple boards

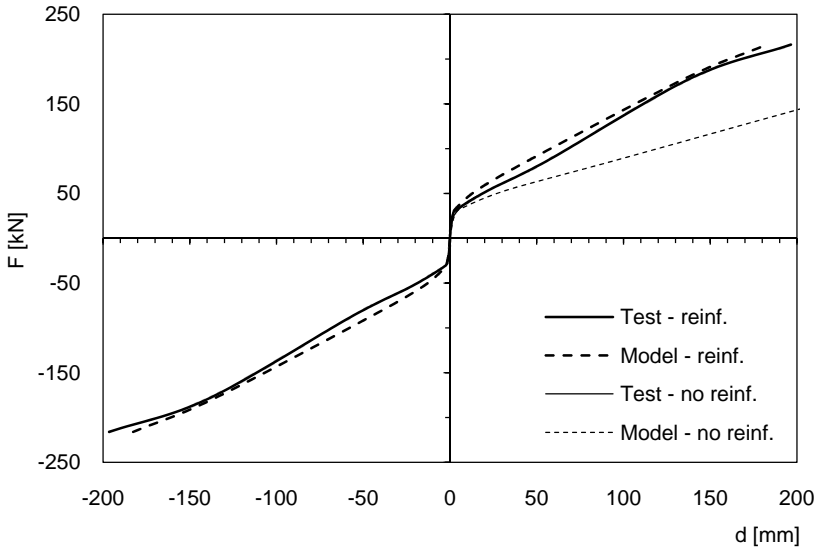


Fig. 156 Comparison load-displacement curves with and without perimeter tie-beam for floors with dimensions 5x4 m.– simple boards

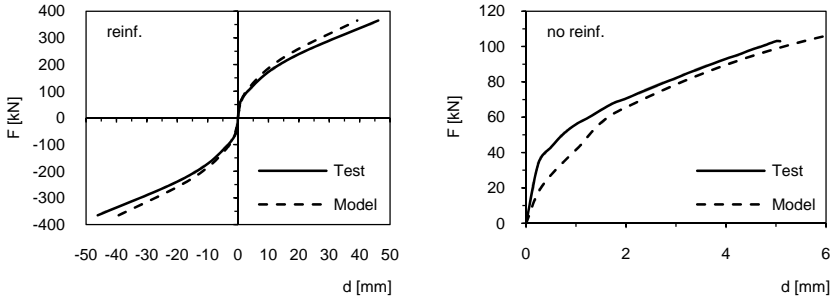


Fig. 157 Comparison load-displacement curves between experimental tests and numerical analysis of floors with dimensions 5x4 m – double boards

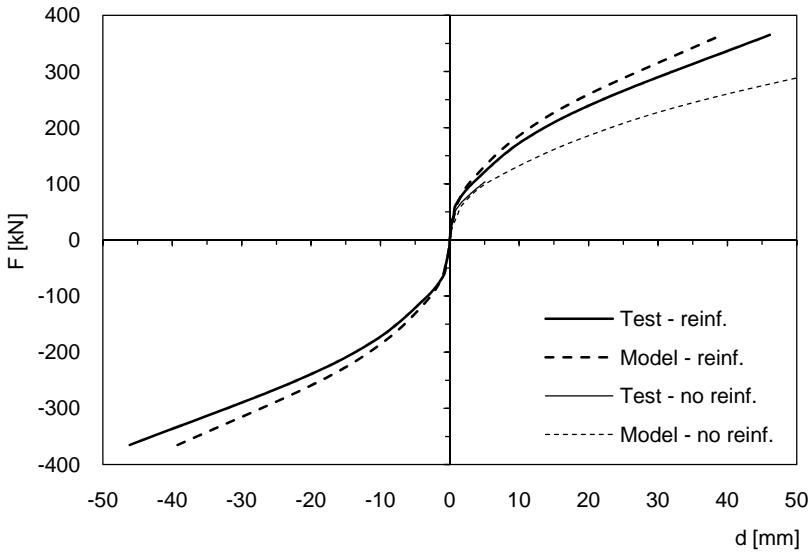


Fig. 158 Comparison load-displacement curves with and without perimeter tie-beam for floors with dimensions 5x4 m – double boards

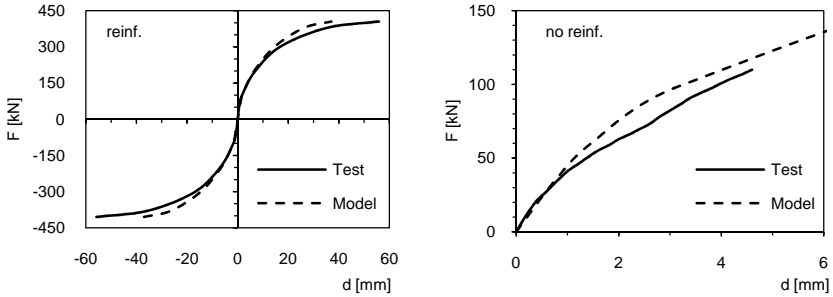


Fig. 159 Comparison load-displacement curves between experimental tests and numerical analysis of floors with dimensions 5x m – metal plates

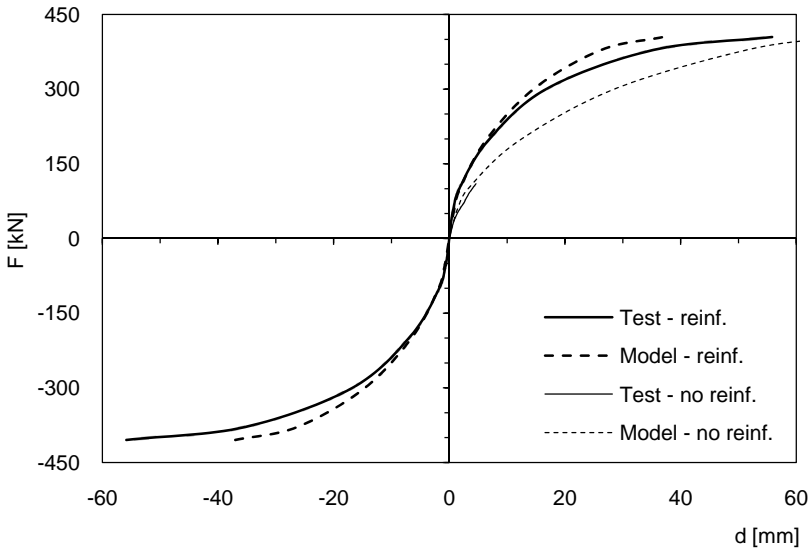


Fig. 160 Comparison load-displacement curves with and without perimeter tie-beam for floors with dimensions 5x4 m – metal plates

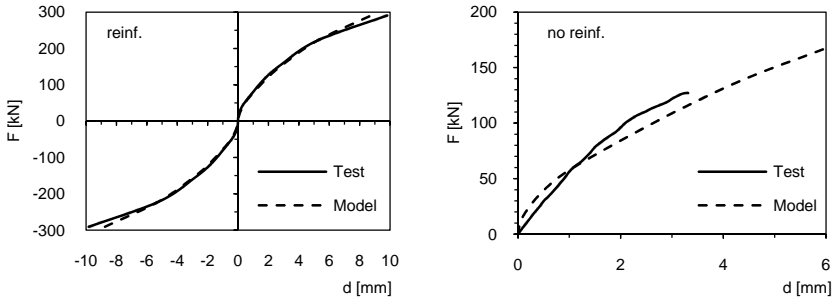


Fig. 161 Comparison load-displacement curves between experimental tests and numerical analysis of floors with dimensions 5x4 m – FRP strips

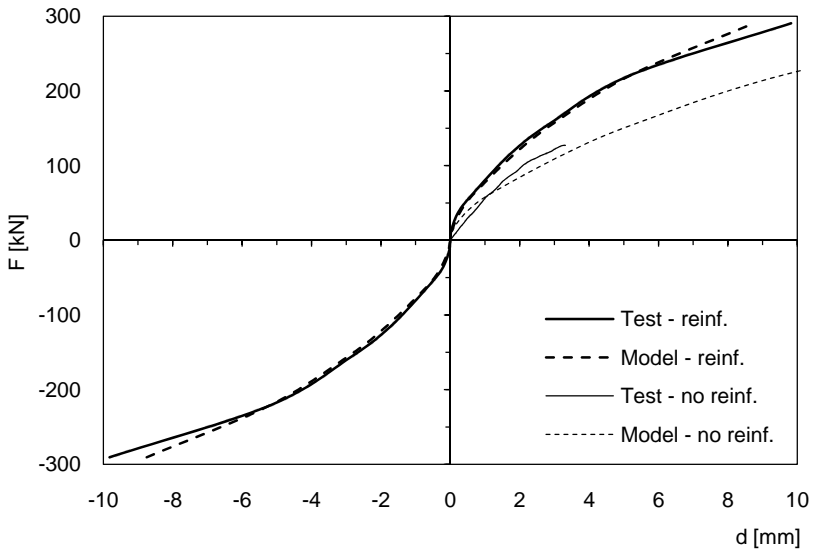


Fig. 162 Comparison load-displacement curves with and without perimeter tie-beam for floors with dimensions 5x4 m – FRP strips

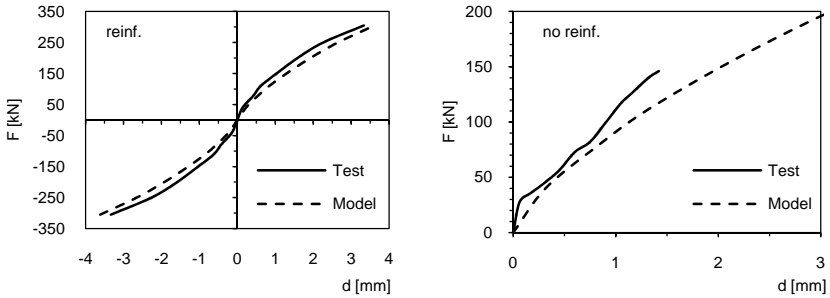


Fig. 163 Comparison load-displacement curves between experimental tests and numerical analysis of floors with dimensions 5x4 m – plywood panels

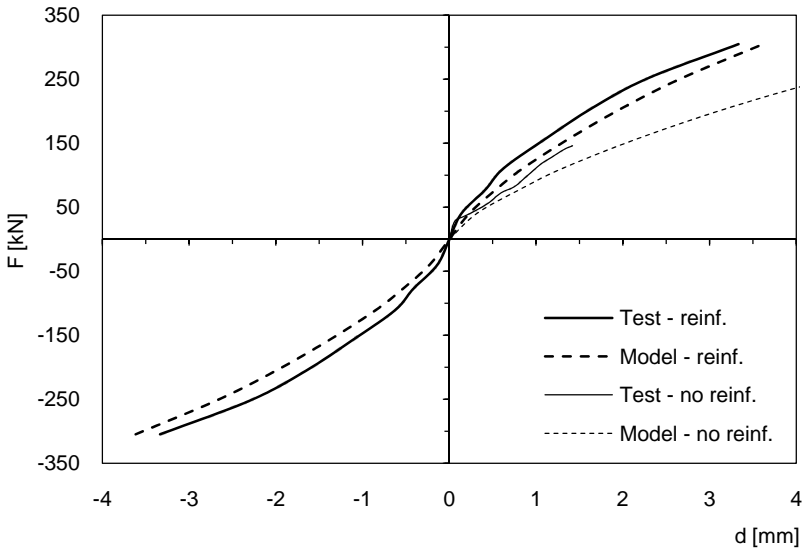


Fig. 164 Comparison load-displacement curves with and without perimeter tie-beam for floors with dimensions 5x4 m – plywood panels

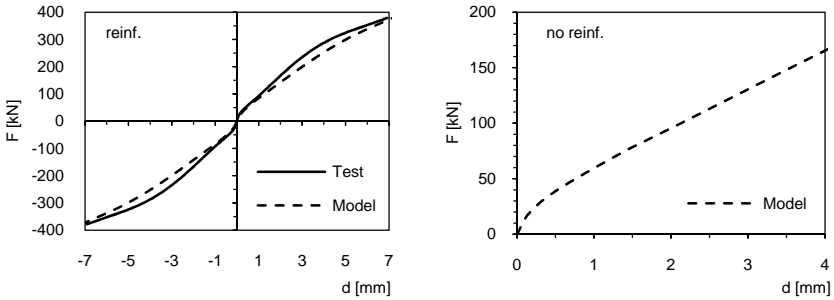


Fig. 165 Comparison load-displacement curves between experimental tests and numerical analysis of floors with dimensions 5x4 m – concrete slab

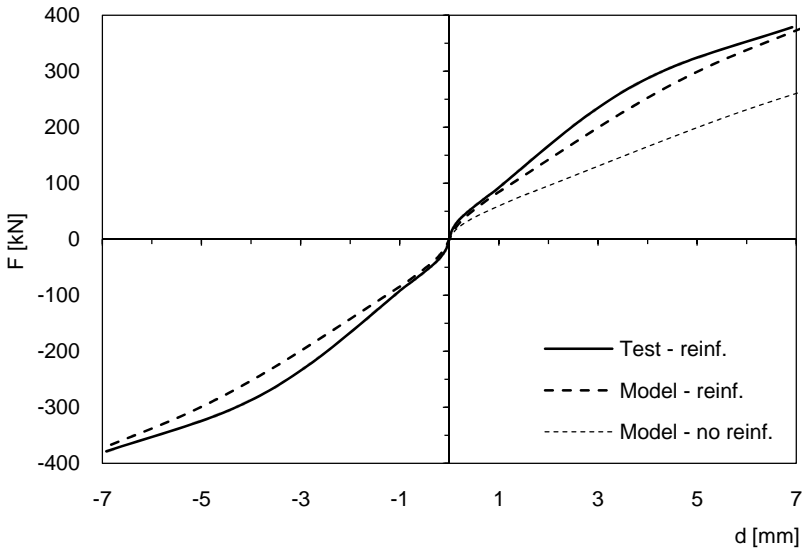


Fig. 166 Comparison load-displacement curves with and without perimeter tie-beam for floors with dimensions 5x4 m – concrete slab

10.2.2 *Stiffness*

In this paragraph there are comparisons between the stiffness of the different types of floor.

The results obtained from experimental tests in the case of floors of 2x1 m dimensions are compared with those of 5x4 m, with and without perimeter tie-beam.

Finally the comparison is between the stiffness obtained by experimental tests with those calculated in numerical analysis. From this latter comparison we see the quality of the numerical model in the case of floors of 5x4 m dimensions but a deviation with regards to that obtained by the experimental tests in the case of floors of dimensions of 2x1 m.

Such difference is strongly due to the low reliability of experimental tests in the case of floors of small dimensions being comparable to the dimensions of the elements that make up the sample. The load-displacement curve obtained by these tests was not characteristic to real behaviour of specimen and in some situations, as with the floors reinforced with plywood panels and concrete slab, it was not even possible to determine it being moved the specimen like rigid motion.

In the end it is important to underline the comparison in terms of stiffness between the floors with tie-beam and those without such element of reinforcement. The increase in stiffness offered by perimeter tie-beam is on average equal to 100%, redoubling the initial floor stiffness.

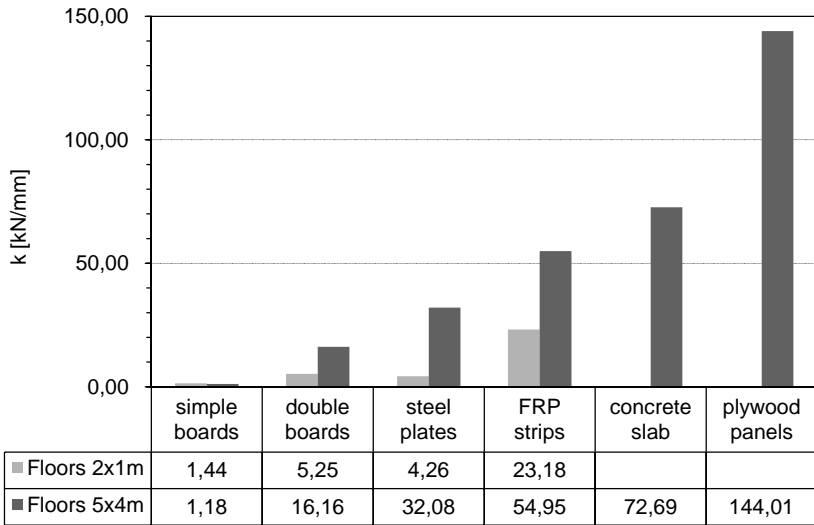


Fig. 167 Comparison experimental stiffness of floors of 2x1m and 5x4m

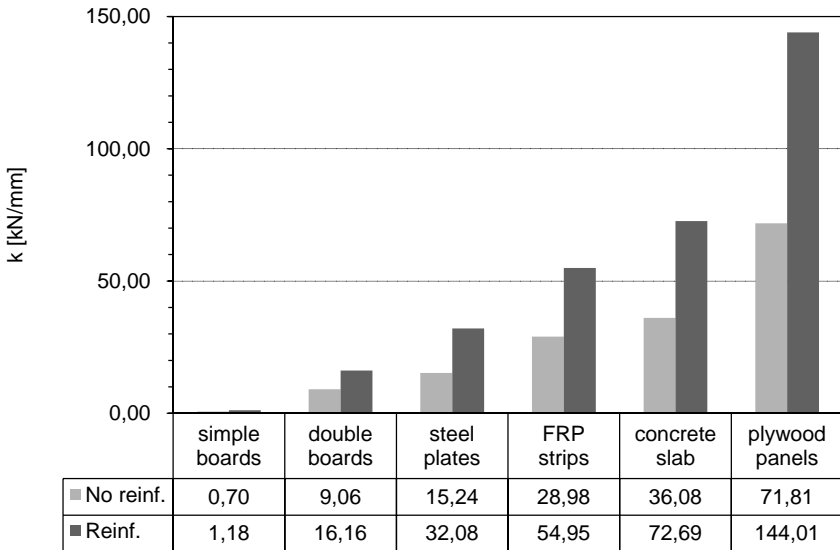


Fig. 168 Comparison experimental stiffness of floors of 5x4 m with and without tie-beam

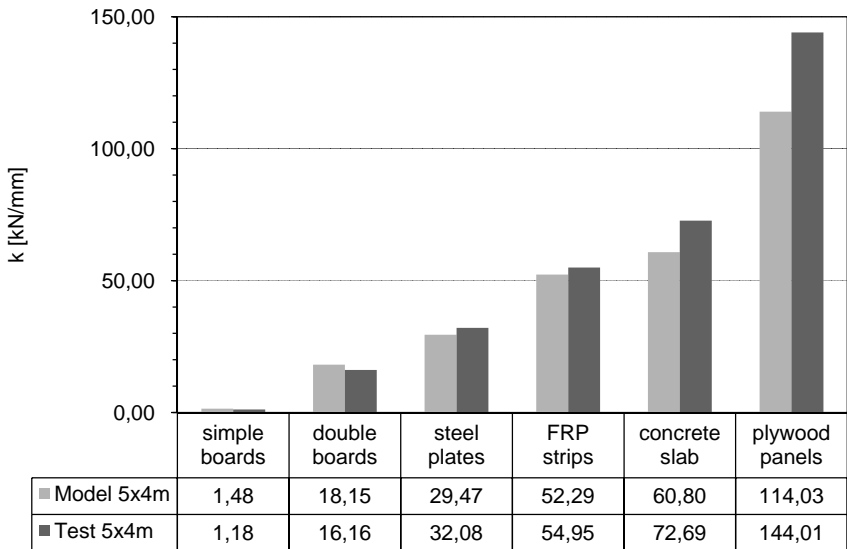


Fig. 169 Comparison experimental stiffness with numerical analysis of floors of 5x4m

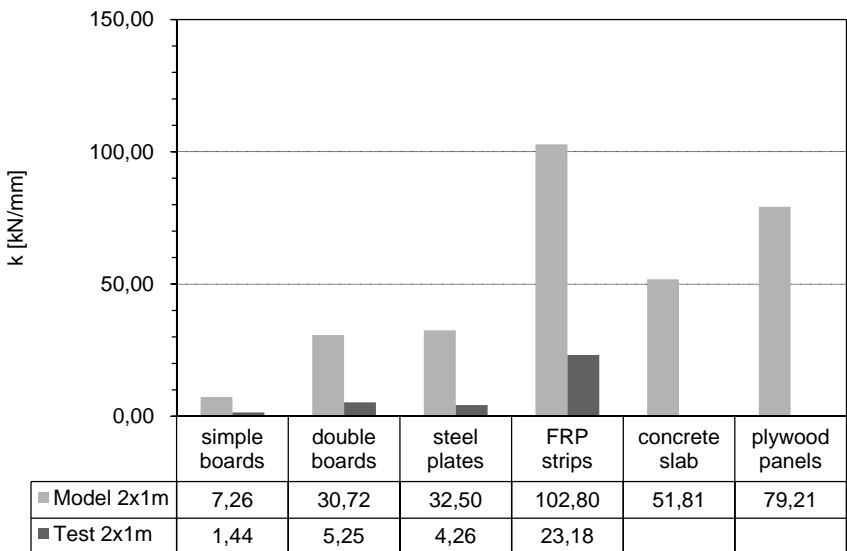


Fig. 170 Comparison experimental stiffness with numerical analysis of floors of 2x1m

10.2.3 Stresses

In this paragraph are compared the stresses recorded by wood and steel strain gauges placed at the midpoint of floor with those obtained by numerical analyses.

We can immediately note how the numerical stresses is not close to experimental ones. In particular the model underestimates the stresses on the timber boards and overestimates the stresses on perimeter tie-beam. These difference are due in part to the difficulty of laying the strain gauges on test specimens, in fact, in some cases it was not possible to obtain the measures for the drift of the strain gauges, but, in particular for the type of chosen modelling.

The model was chosen with the aim of simulating most faithfully the global in-plane behaviour of the floor. The model, in fact, not being continuous but made up of a series of elements between each other linked at the ends, limited the possibility to estimate the local stresses privileging simplicity of modelling and its easy implementation in study of floors have different shape and dimension.

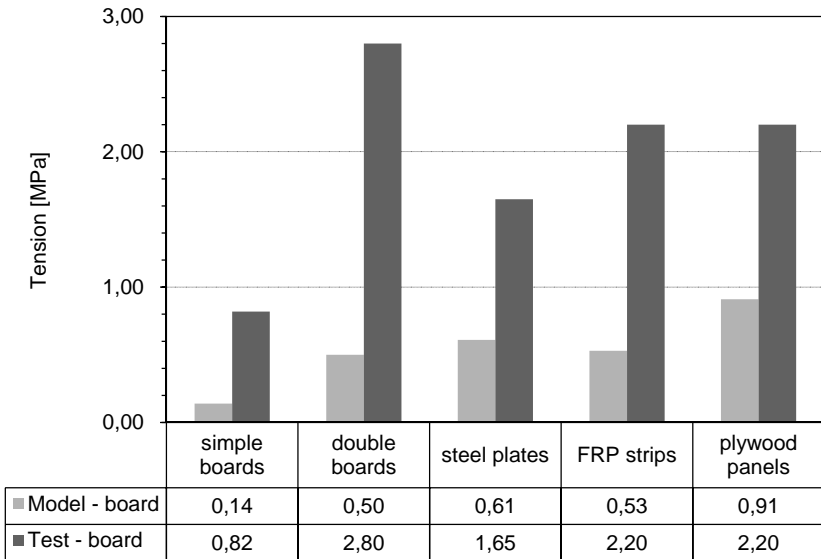


Fig. 171 Comparison experimental stresses with model – wood planks

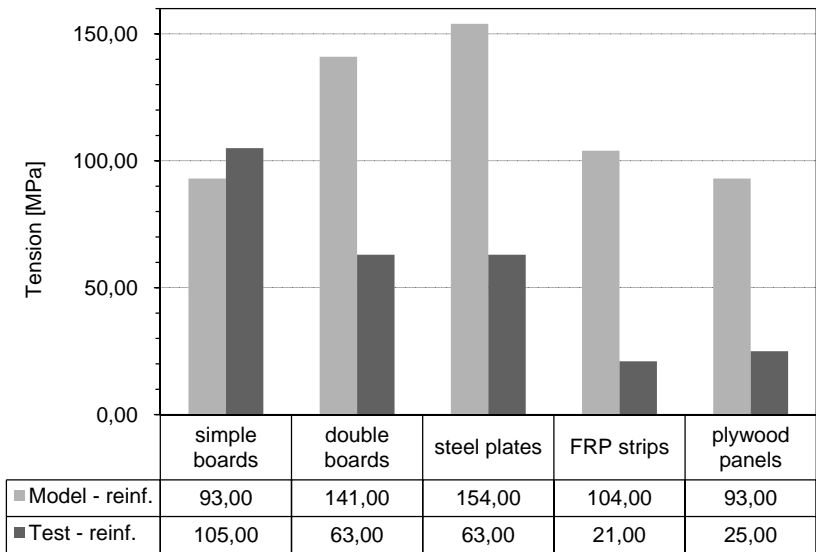


Fig. 172 Comparison experimental stresses with model - tie-beam

10.3 Numerical example

In this paragraph are presented numerical analysis comparisons between different types of reinforcement in terms of perimeter walls deformations and in-plane bending of floor, both with and without perimeter tie-beam.

10.3.1 *Tie-beam contribution*

Figures from

Fig. 173 to Fig. 178 represent for each type of reinforcement the contribution offered by tie-beam. In particular the midpoint deformation of West and South walls and midpoint displacements of second and third floor.

We can note how the presence of tie-beams has little influence on the bracing South and North walls in fact they are stressed with the same seismic action while it determines an important decrement of East and West walls deformations being they orthogonally to seismic action.

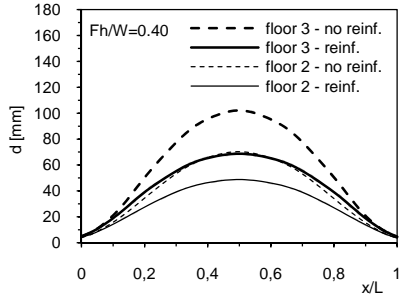
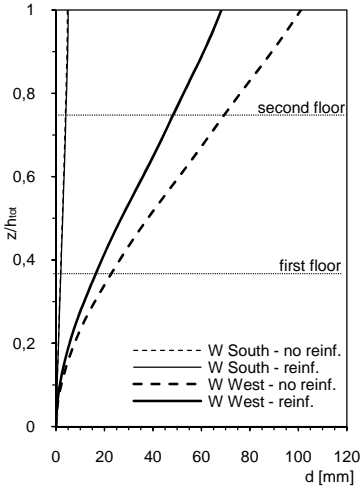


Fig. 173 Contribution of tie-beam in the case of floors with simple boards

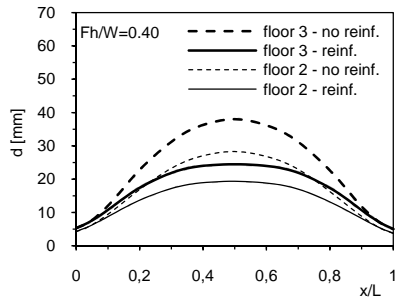
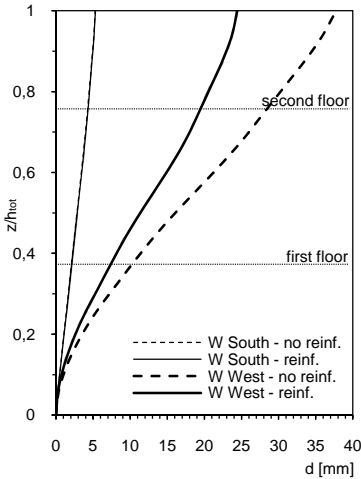


Fig. 174 Contribution of tie-beam in the case of floors with double boards

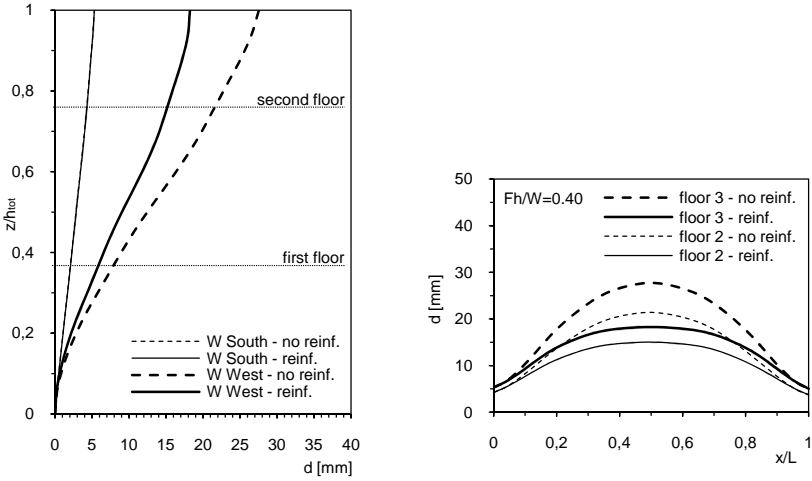


Fig. 175 Contribution of tie-beam in the case of floor reinforced with metal plates

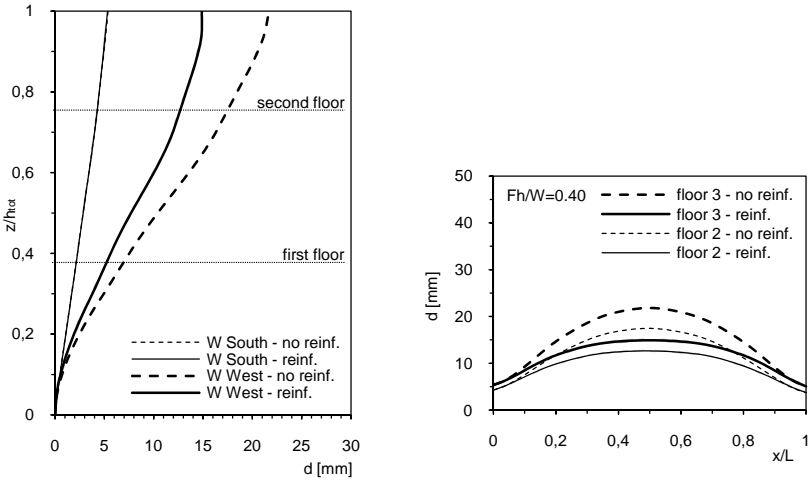


Fig. 176 Contribution of tie-beam in the case of floors reinforced with FRP strips

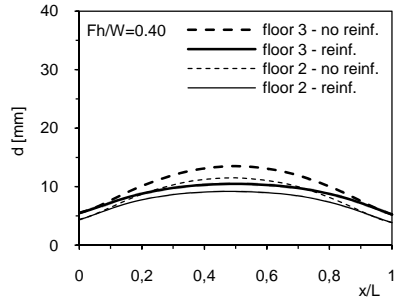
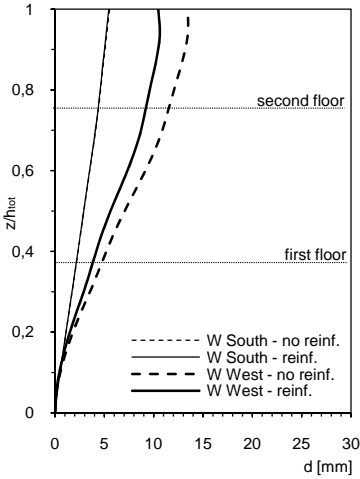


Fig. 177 Contribution of tie-beam in the case of floors reinforced with plywood panels

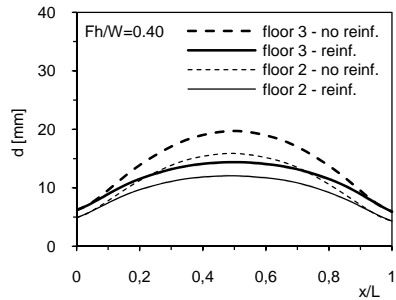
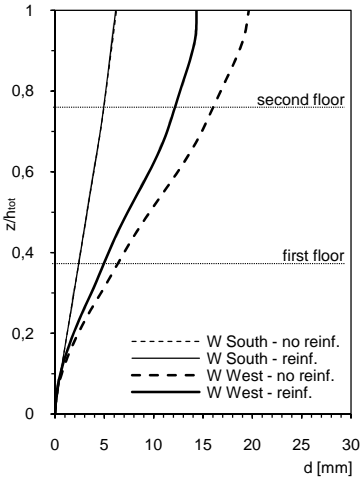


Fig. 178 Contribution of tie-beam in the case of floors reinforced with concrete slab

10.3.2 *Comparison between different reinforcement – walls*

Figures from Fig. 179 to Fig. 182 represent deformation profiles of South and West walls with and without tie-beam.

We can note how the displacements in the midpoint of South wall do not change much varying the floor type, in fact it is stressed by the same seismic action. We note an increase in deformation only in the case of floor reinforced with concrete slab which increments the seismic weights and then also the equivalent seismic forces on the bracing walls.

Regarding the West wall, orthogonal to seismic action, we note a difference between the solution with simple boards and all the other solutions which foresee stiffening of floor on its own plane.

We pass, in fact, from a maximum displacement to the building of around 102 mm in the case of simple board to displacements in the order of 38 mm for the double board until lessening to 10 mm corresponding to the reinforcement with plywood panels. A further reduction is obtained with the application of perimeter tie-beam.

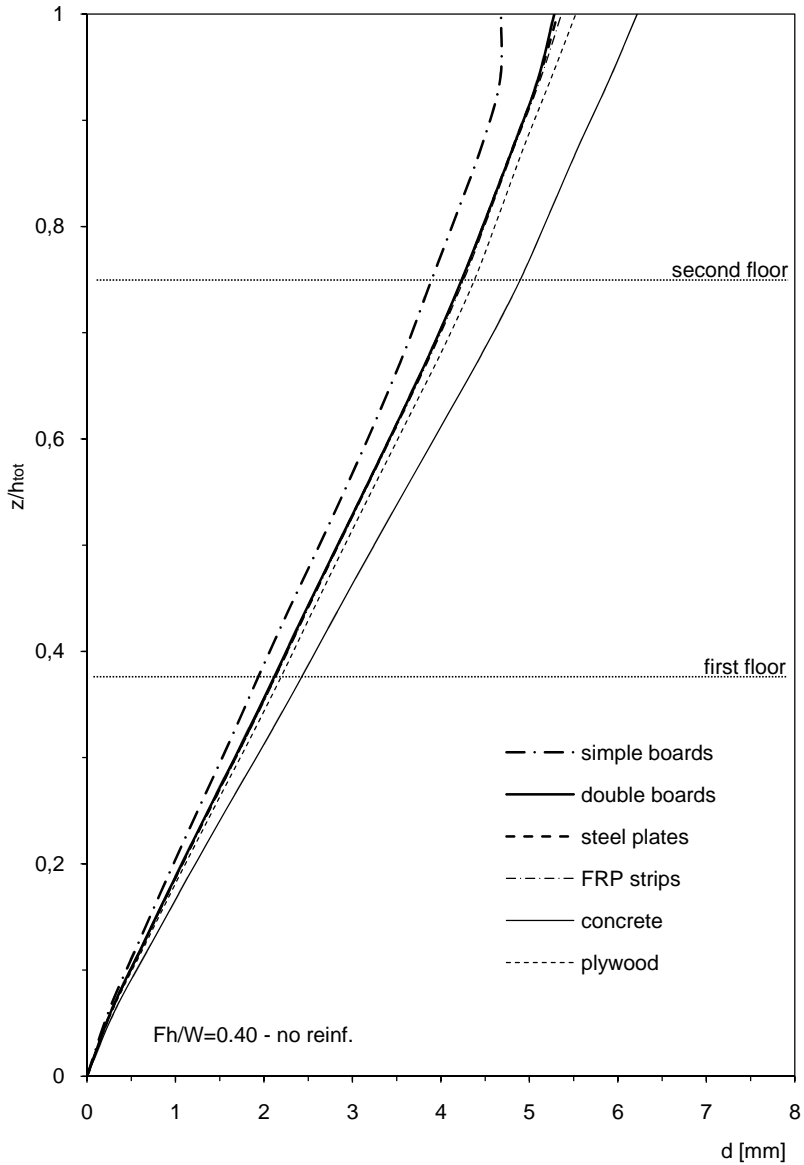


Fig. 179 Comparison deformed configuration of South wall without tie-beam

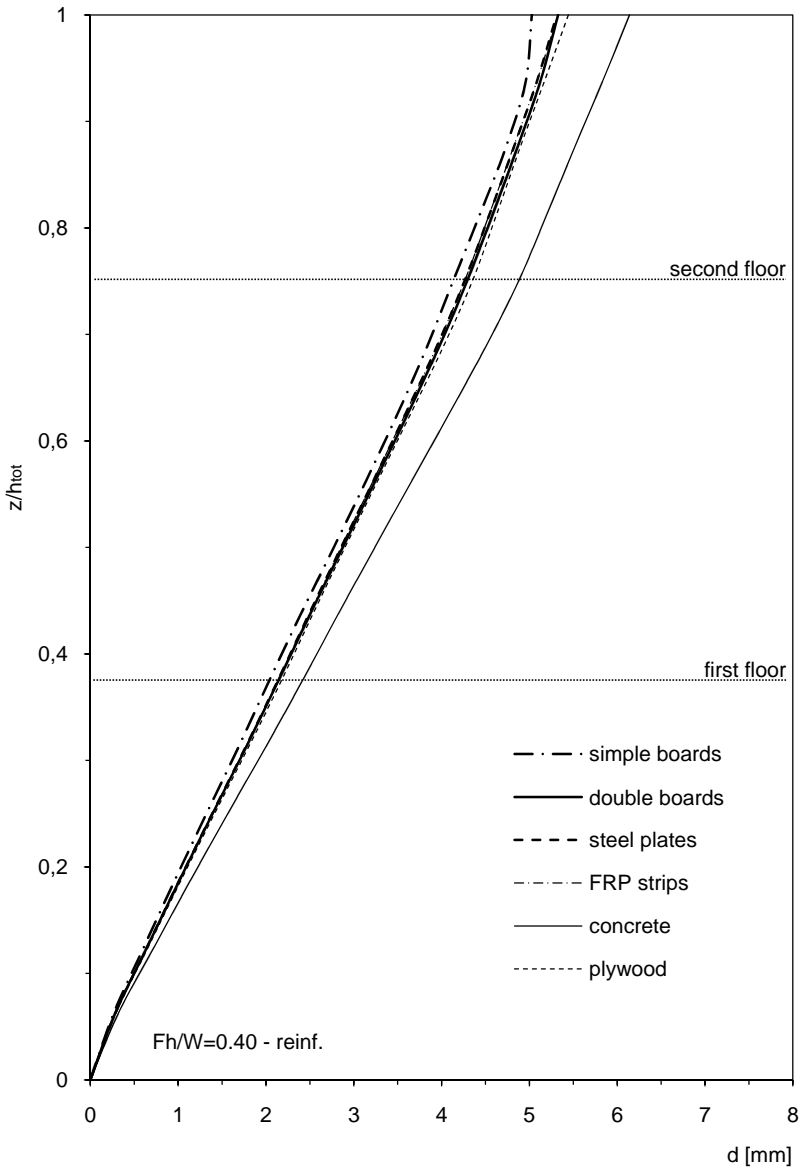


Fig. 180 Comparison deformed configuration of South wall with tie-beam

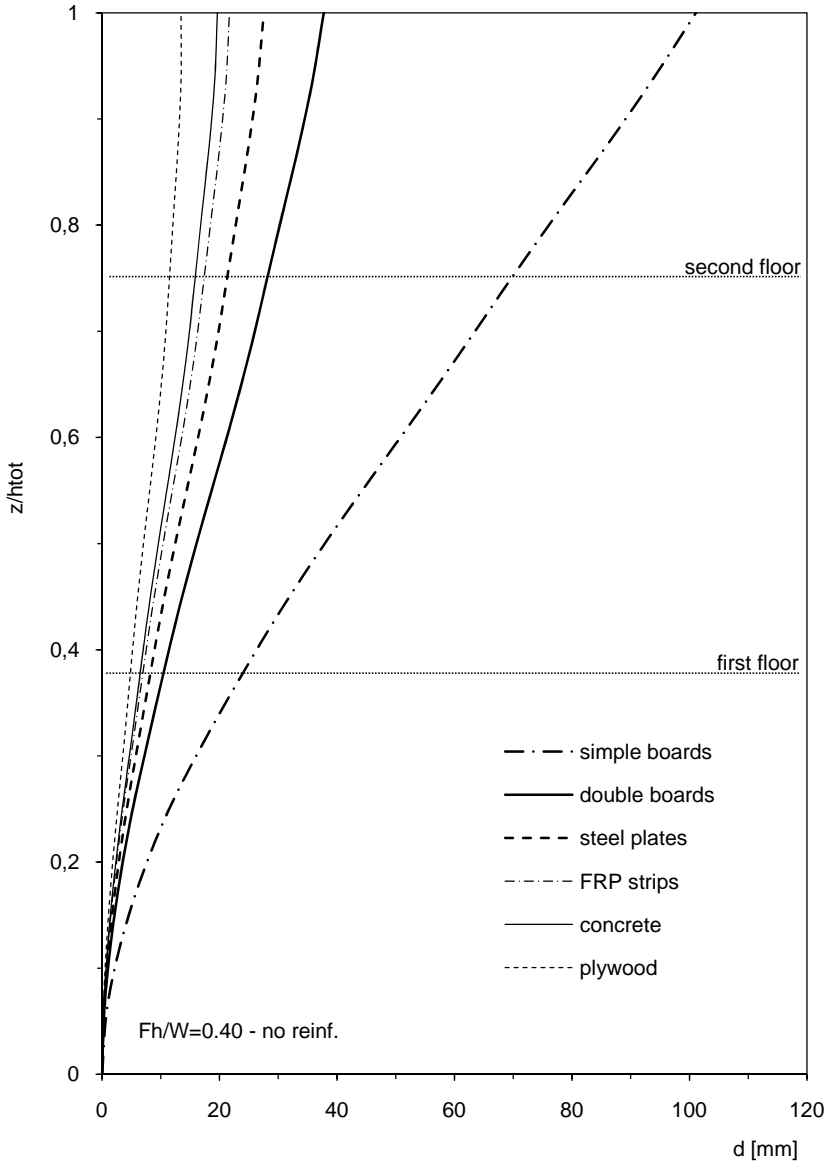


Fig. 181 Comparison configuration deformed of West wall without tie-beam

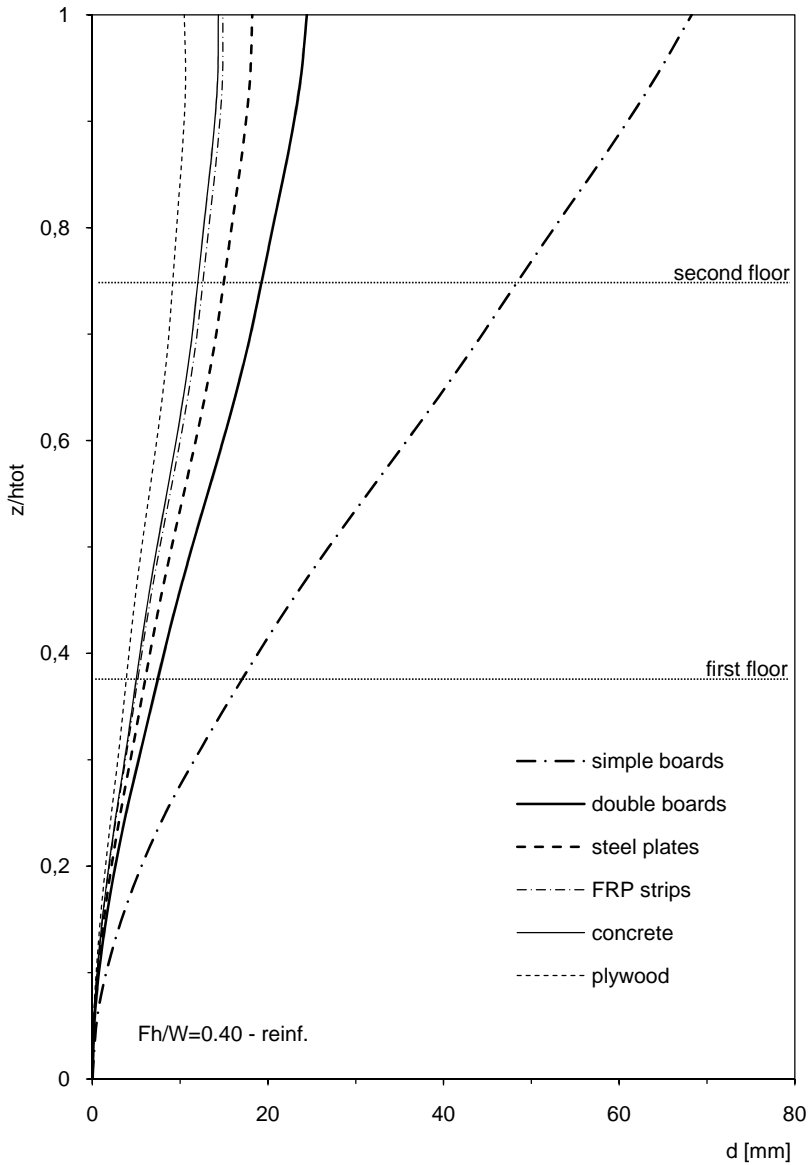


Fig. 182 Comparison deformed configuration of West wall with tie-beam

10.3.3 *Comparison between different reinforcement – floors*

The figures from Fig. 183 to Fig. 186 represent the in-plane displacements of second and third floor with and without perimeter tie-beam.

The same valid considerations are described in the preceding paragraph and in particular we note the difference between solution with simple boards and all the other solutions which foresee the stiffness of own in-plane floor.

We pass, in fact, from a maximum top building displacement of around 102 mm in the case of simple boards to a displacement in the order of 38 mm for the double boards until decreasing to 10 mm corresponding to reinforcement with plywood panels. The application of perimeter tie-beam determines a further reduction of in-plane deformations redoubling on average the in-plane stiffness of each floor.

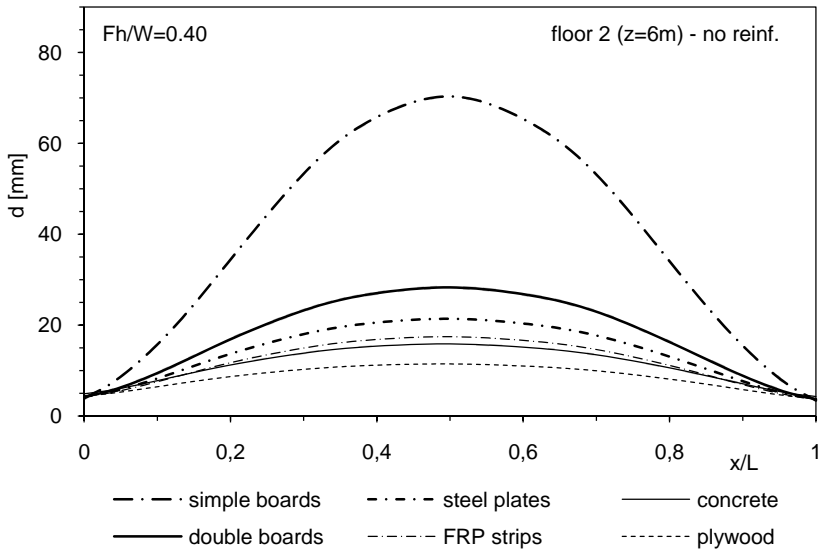


Fig. 183 Comparison displacements of second floor without tie-beam

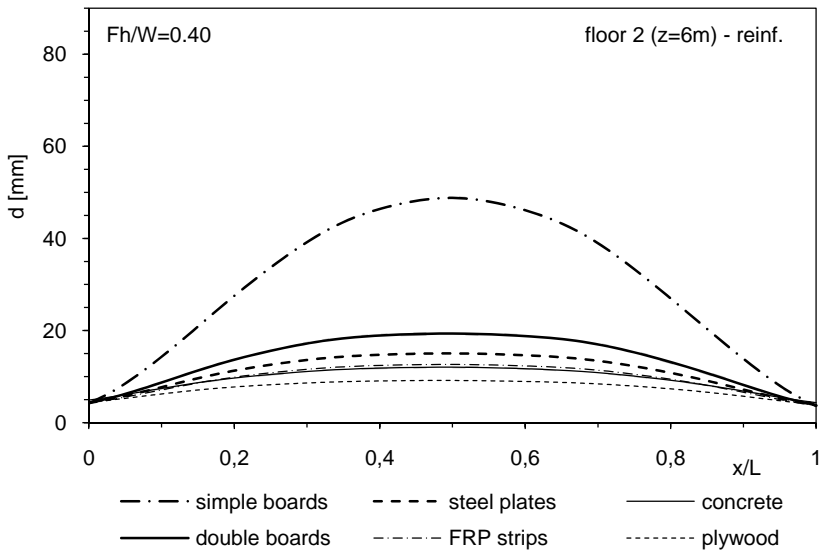


Fig. 184 Comparison displacements of second floor with tie-beam

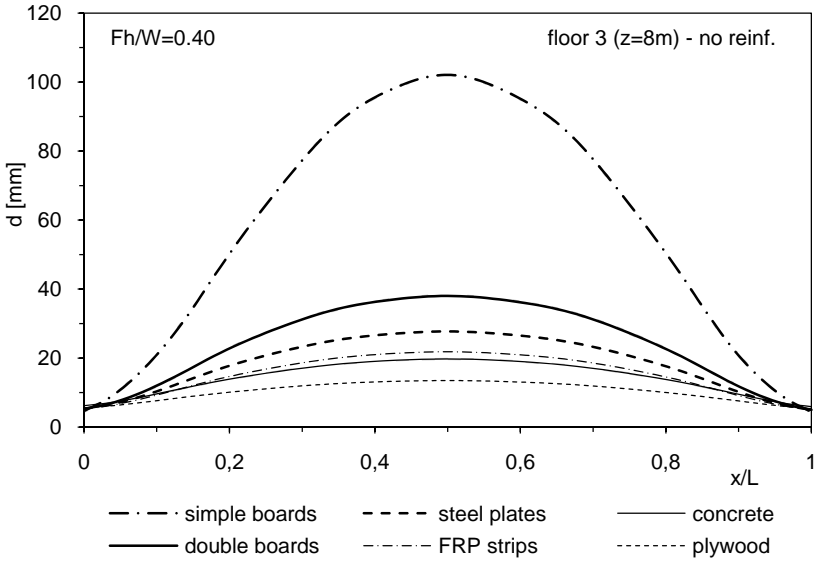


Fig. 185 Comparison displacements of third floor without tie-beam

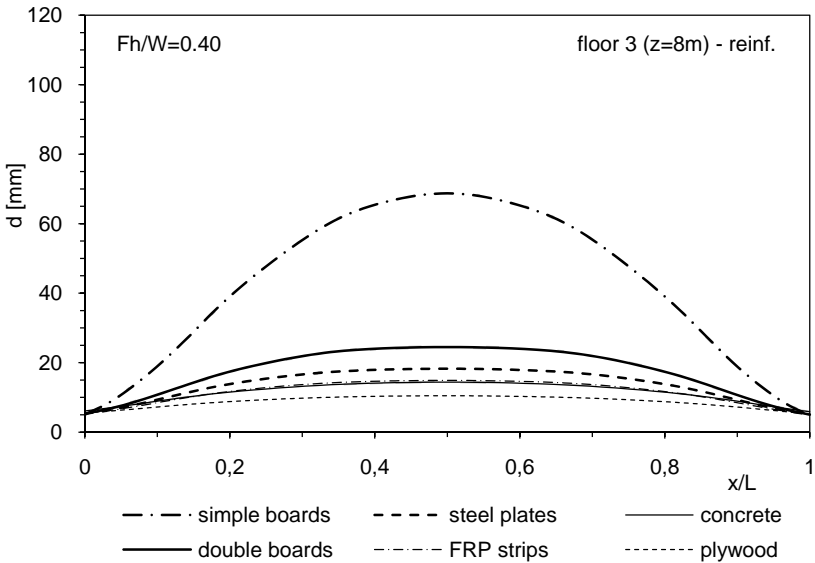


Fig. 186 Comparison displacements of third floor with tie-beam

11. CONCLUSIONS AND FUTURE DEVELOPMENTS

11.1 Conclusions

This work has analysed the in-plane behaviour of six kinds of timber floor with different in-plane stiffness. The starting solution is the one mostly used in historic buildings and it is floor with simple boards. How has been amply shown in the preceding chapters its limited in-plane stiffness is inadequate to resisting to horizontal loads of seismic action.

Excessive deformations, in fact, determine the impossibility of the floor to efficiently counteract the overturn outside plane of walls orthogonal to seismic action.

Application of perimeter tie-beam, even if indispensable for transferring seismic forces to bracing walls and doubling in-plane stiffness of floor, for this solution it is not enough to avoid local collapse mechanisms due to overturn of perimeter walls.

The remaining five types of floor analysed foresee a system of reinforcement with different operation techniques.

The numerical example presented in this work is not meant to be exhaustive but surely can be representative of main operation techniques adopted for in-plane reinforcing timber floors.

The first in-plane technique analysed was the diagonal laying of a second layer of wood planks on top of the existing one; increase in terms of stiffness is notable, passing from 1 kN/mm to 16 kN/mm. Doing this is a relatively simple job. It does not require specialised labour, it is adaptable also to confined situations laying given the reduced dimensions of necessary elements and foresees the connections of the second layer to the first with screws of $\varnothing 6 \times 90$ mm.

As well as being among the reinforcement techniques which slightly increments the in-plane stiffness, it is also among the most valid, together with plywood, as regards strength to cyclic load path and also able to dissipate more energy. Such properties are due essentially to numerous connections which link the two timber boards which are able to dissipate energy while not damaging excessively. At the end of the experimental test, in fact, most of the connecting screws between the two layers did not show evident signs of damage.

The second kind of reinforcement includes diagonal laying of metal drilled plates above the existing layer, anchored to it with $\varnothing 5 \times 25$ mm screws. In this case the role of the perimeter tie-beam is very important, in fact define with steel plates a closed strength system, that notable increases the in-plan stiffness which passes from 4 kN/mm to 32 kN/mm. Also this solution is easy to achieve and together with the preceding one it is able to dissipate greater energy given the presence of a great quantity of metal components and of connections with the existing layer. The main weak point of this technique is instability of steel plates when subject to compression stresses. Such instability, which have origin in the over positioning points of the metal plates, is what determines their detachment from support when stressed by cyclic action determining loss of efficiency of reinforcement. The phenomenon may be limited by laying further layers of boards above the steel plates with the function of confinement in particular in correspondence with over positioning points.

The third reinforcement solution foresees laying FRP strips placed diagonally above the existing layer. This technique further increments stiffness which passes to 55 kN/mm but it throws up some problems.

Its use includes, in fact, availability of specialised labour for the careful preparation of support and for the laying of reinforcement carried out with epoxy glue. As with the metal plates there is also the phenomenon of instability of plates starting out from over positioning points. However, in this case laying of a second upper layer does not allow the efficient confinement FRP plates being notable the differences of outside of plane

stiffness between this second layer and the glued connection. In the end, even guaranteeing an elevated stiffness in its own plane, it offers a limited dissipation of energy being strongly affected by compression instability of FRP plates, which determines support detachment.

The fourth reinforcement system is made up of three layers of plywood, each with 21 mm thickness, laid with staggered joints above the existing layer. The connection between panels and with timber boards is achieved with polyurethane glue. Moreover, connections with threaded bars $\varnothing 10 \times 150$ mm are also foreseen injected with epoxy resin, so as to achieve a composite system able to increase floor bearing capacity. This solution turns out to be the stiffest offering an in-plane stiffness equal to 144 kN/mm. It also lends itself to use in cramped situations, given the limited dimensions of plywood panels and the ease of cutting. The inconvenience is the difficulty of removal and so the limited reversibility.

The last intervention technique foresees the concrete slab of 5 cm thickness above the existing layer anchored to the bearing beams with bars of reinforcement B450C $\varnothing 14$, bent at L, so as to complete a composite wood-concrete system. The final system gives us an in-plane stiffness of 73 kN/mm. The lesser stiffness with regards to the plywood panel solution is the consequence of formation of local cracks nearest of the bracing walls, due to mainly the limited thickness of slab if related to the connector diameter. Among the proposed solutions it is the only one which increases permanent floor dead load so increasing also seismic actions on bracing walls. As with the plywood panel solution, the technique is also hardly reversible and it is the only wet solution.

As far as the experimental tests it is important to underline the dimension specimen choices. The tests on specimens of 2x1 m dimensions, in fact, although indispensable for calibration of next cyclic tests, are not to be considered representative of real behaviour of floors at work, being samples with dimensions in plan comparable to those components that make it up. For this reason the displacements and stiffness determined in these tests are to be considered only indicative of real features.

Regarding numerical modelling the main aim was to develop a model able to faithfully simulate global behaviour of floor subject to seismic action, to offer the chance to plan reinforcement system with tie-beam, to be able to use it within more complex models of buildings, guaranteeing a simplicity of modelling and easy interpretation of results. Such a model is not meant to be and cannot be able to estimate with exactness the local stresses in the in-plane floor. Also in the modelling of building presented in Chapter 9 it is important to underline that the perimeter walls show us a heavily simplified model, function only of the elastic module and few other parameters, with the aim to highlight the influence of different techniques of floor reinforcement on global building behaviour. The shell modelling of walls is not able to simulate tension damage of masonry and the qualitative representation of the in-plane principal tension stresses has the only scope of pinpointing the horizontal loads paths and critical points in which masonry is subject to tension stresses.

Floor model is able to simulate behaviour with sufficient precision if compared with experimental tests. They confirm the comparisons presented in the preceding Chapter 10 which gives differences in terms of stiffness and maximum floor displacement lower than 10%.

It is important to underline the simplicity of model which includes use of elements of elastic-plastic behaviour, directly proportional to load-displacement curve of floor tested experimentally and at the same time able to consider presence of gravitational loads on floor bearing beams. Modelling is easily used also for other types of reinforcement, with prior determination of load-displacement curve. Also for perimeter tie-beam and for floor-wall connections were used elements of linear elastic and elastic-plastic behaviour.

From the comparisons made in Chapter 10 we note the importance of laying the tie-beam, firmly connected to perimeter walls, with the double scope of avoiding overturn outside its own plane of orthogonal walls to seismic action, to guarantee the transferral of seismic action to bracing

walls and to increase in-plane stiffness of floor in each of the reinforcement techniques considered.

As expected the model is not able to estimate with exactness the stresses of floor and of tie-beam. The differences from experimental tests are due in part to laying difficulties of strain gauges on test specimens, in fact, in some cases it was not possible to obtain measurements for the leeway of the strain gauges, but in particular for the type of modelling chosen.

Numerical analysis carried out on building type has allowed us to confirm the benefits offered by tie-beam and to deepen study about the contribution of differing techniques of reinforcement on global behaviour of a building. It was also shown the necessity of stiffening intervention in the case of floor with simple boards. In fact, not even the presence of perimeter tie-beam is able to avoid activation of local collapse kinematism. The contribution of tie-beam is important for walls orthogonally to seismic action because limited the maximum in-plane displacement of floor. This contribution is less great for bracing walls that are influenced instead by seismic weights.

11.2 Future developments

Work carried out can be completed and integrated analysing further techniques of timber floors stiffening, so as to obtain a set of experimental data useful for designing the improvement of the seismic behaviour of buildings.

Consequently, it will be possible to implement reliable numerical models for the mechanical behaviour of the whole building based on accurate description of the in-plane floor behaviour, adopting different existing models for the behaviour of masonry walls. With regard to the floor-masonry connections, further experimental tests on single and multiple

connections are required with the aim of gathering information about the real floor-wall interaction.

BIBLIOGRAPHY

Baldessari C., Piazza M., Pederzoli S., (2008), *Prove sperimentali nel piano di solai lignei diversamente rinforzati*, DIMS, Università di Trento, Technical Report n. 30

Baldessari C., Piazza M., Tomasi R., (2009), *The refurbishment of existing timber floors: characterization of the in-plane behaviour*, Prohitech International Conference, 2009, June 21-24, Roma, Elsevier Science, ISBN 978-0-415-55804-4, vol. 1: 255-260

Borri A., Corradi M., Grazini, (2004), *Rinforzo di strutture lignee con materiali compositi*, Il Manuale del Legno Strutturale, Mancosu Editore, Roma, vol. IV

Borri A., Corradi M., Grazini A., (2005), *A method for flexural reinforcement of old wood beams with CFRP materials*, J Compos Part B, 36/2:143–53

Brignola A., Lagomarsino S., Podestà S., Romano L., (2005), *Consolidamento di solai lignei – La scelta dell'intervento e le verifiche di sicurezza*, L'Edilizia, 141, 52-59

Brignola A., Pampanin S., Podestà S., (2008), *In-plane stiffness of wooden floors*, NZSEE 2008 Annual Conference, 11-13 April 2008, Wairakei Taupo, New Zealand

Cangi G., (2005), *Manuale del recupero strutturale e antisismico*, DEI Tipografia del Genio Civile, Roma

Ceccotti A., (2004), *Verifiche e consolidamenti delle strutture lignee in zona sismica*, Il Manuale del Legno Strutturale, Mancosu Editore, Roma, vol. IV

Cifani G., Lemme A., Podestà S., (2005), *Beni monumentali e terremoto. Dall'emergenza alla ricostruzione*, DEI Tipografia del Genio Civile, Roma

CNR-DT 200/2004, (2004), *Istruzioni per la Progettazione, l'Esecuzione ed il Controllo di Interventi di Consolidamento Statico mediante l'utilizzo di Compositi Fibrorinforzati – Materiali, strutture di c.a. e di c.a.p., strutture murarie*, CNR, Roma

CNR-DT 201/2005, (2005), *Studi Preliminari finalizzati alla redazione di Istruzioni per Interventi di Consolidamento Statico di Strutture Lignee mediante l'utilizzo di Compositi Fibrorinforzati*, CNR, Roma

CNR-DT 206/2007, (2007), *Istruzioni per la Progettazione, l'Esecuzione ed il Controllo delle Strutture di Legno*, CNR, Roma

Corradi M., Speranzini E., Borri A., Vignoli A., (2006), *In-plane shear reinforcement of wood beam floors with FRP*, Composites, Part B, N. 37, 310-319

D'Ayala D., Speranza E., (2002), *An integrated procedure for the assessment of seismic vulnerability of historic buildings*. 12th European Conference on Earthquake Engineering, London, Elsevier Science, paper n. 561

Doglioni F., (2000), *Codice di pratica (linee guida) per la progettazione degli interventi di riparazione, miglioramento sismico e restauro dei beni architettonici danneggiati dal terremoto umbro-marchigiano del 1997*, Bollettino Ufficiale della Regione Marche, Ancona

D.M. 14/01/2008 e s.m., (2009), *Norme Tecniche per le Costruzioni*, Ministero delle Infrastrutture e dell'Interno, Roma

EN 12512, (2006), *Timber structures – Test methods – Cyclic testing of joints made with mechanical fasteners*, UNI

EN 1992-1-1, (2005), *Eurocodice 2 – Progettazione delle strutture di calcestruzzo - Parte 1-1: Regole generali e regole per gli edifici*, UNI

EN 1993-1-1, (2005), *Eurocodice 3 – Progettazione delle strutture in acciaio – Parte 1-1: Regole generali e regole per gli edifici*, UNI

EN 1995-1-1, (2009), *Eurocodice 5 – Progettazione delle strutture di legno – Parte 1-1: Regole generali - Regole comuni e regole per gli edifici*, UNI

EN 1998-1, (2005), *Eurocodice 8 – Progettazione delle strutture per la resistenza sismica – Parte 1: Regole generali, azioni sismiche e regole per gli edifici*, UNI

FEMA 310, (1998), *Handbook for the Seismic Evaluation of Buildings*, ASCE, Washington

FEMA 356, (2000), *Prestandard and commentary for the seismic rehabilitation of buildings*, ASCE, Washington

FEMA 547, (2006), *Techniques for the Seismic Rehabilitation of Existing Buildings*, ASCE, Washington

Felicetti R., Gattesco N., Giuriani E., (1997), *Local Phenomena Around a Steel Dowel Embedded in a Stone Masonry Wall*, *Materials and Structures*, RILEM, Vol. 30, 238-246

Gattesco N., Del Piccolo M., (1997), *Shear Transfer Between Concrete Members and Stone Masonry Walls Through Driven Dowels*, *European Earthquake Engineering*, No. 3, 3-17

Gattesco N., (2001), *Experimental Study on Different Dowel Techniques for Shear Transfer in Wood-Concrete Composite Beams*, *Creative Systems in Structural and Construction Engineering*, Balkema, Rotterdam, 487-492

Gattesco N., Macorini L., (2006), *Strengthening and Stiffening Ancient Wooden Floors with Flat Steel Profiles*, *Structural Analysis of Historical Constructions*, Macmillan India Ltd., Delhi, 405-412

Gattesco N., Macorini L. & Benussi F., (2007), *Strengthening of wooden floors for seismic rehabilitation of historical buildings through high reversibility techniques*, ANIDIS 2007, XII Convegno "L'ingegneria Sismica in Italia", 10-14 June, Pisa

Giuriani E., (2002), *Solai in legno rinforzati con lastra collaborante: criteri di dimensionamento*, *L'Edilizia*, Speciale Legno Strutturale, n. 4, 32-40

Giuriani E., Marini A., Plizzari G., (2002), *Shear behavior of wooden floors strengthened by stud connected wooden planks*, Dipartimento di Ingegneria Civile, Università di Brescia, Technical Report n. 7

Giuriani E., (2004), *L'organizzazione degli impalcati per gli edifici storici*, L'Edilizia, Speciale Legno Strutturale, n. 134, 30-43

Giuriani E., (2006), *Rinforzo dei solai in legno mediante soletta collaborante di calcestruzzo*, Strutture Composte – Nuove costruzioni, recupero, ponti, International Centre for Mechanical Sciences, CISM, Udine, ISBN 88-85137-20-2, 311-322

Modena C., Tempesta F., Tempesta P., (1998), *Il recupero a secco di impalcati in legno*, L'edilizia 3/4, 38–45

Modena C., Valluzzi M.R., Garbin E., da Porto F., (2004), *A strengthening technique for timber floors using traditional materials*, Fourth International Seminar on Structural Analysis of Historical Constructions, 10-13 Nov Padova, Italy, 911-921

Piazza M., Turrini G., (1983), *Una tecnica di recupero statico dei solai in legno*, Recuperare, Milano, Vol. 5, 6, 7

Piazza M., Tomasi R., Modena R., (2005), *Strutture in Legno*, Ulrico Hoepli, Milano, Italy

Piazza M., Ballerini M., (2006), *Strutture composte legno calcestruzzo con connettori di calcestruzzo. Indagine sperimentale*, Strutture Composte – Nuove costruzioni, recupero, ponti, International Centre for Mechanical Sciences, CISM, Udine, ISBN 88-85137-20-2, 323-340

Piazza M., Baldessari C., Tomasi R., Acler E., (2008), *Behaviour of refurbished timber floors characterized by different in-plane stiffness*, Proceedings 6th International conference: "Structural Analysis of Historical Constructions", 2008, July 2-4, Bath, U.K., CRC-Press, Balkema, ISBN 978-0-415-48107-6, vol. 2: 843-850

Ronca P., Gelfi P., Giuriani E., (1991), *The Behavior of a Wood-Concrete Composite Beam under Cyclic and Long Term Loads*, Structural Repair and Maintenance of Historical Buildings, 2nd International Conference STREMAH 91, Seville, Spain, Vol. 1, 263-275

Valluzzi M.R., Garbin E., Dalla Benetta M. & Modena C., (2008), *Experimental assessment and modelling of in-plane behaviour of timber floors*, Proceedings 6th International conference: "Structural Analysis of Historical Constructions", 2008, July 2-4, Bath, U.K., CRC-Press, Balkema, vol. 2, 755-762

